The influence of aluminium and silicon on the reaction between iron and zinc


THE INFLUENCE OF
ALUMINIUM AND SILICON
ON THE REACTION BETWEEN
IRON AND ZINC
KAZIMIERZ OSINSKI

Cover: Surface of a hot-dip galvanized iron sheet - zinc flowers (magnification 1:1).

Omslag: Oppervlakte van een thermisch verzinkte ijzeren plaat - zinkbloemen (vergroting 1:1).

DISSERTATIE DRUKKERIJ
wibro
HELMOND
TELEFOON 04920-23981

THE INFLUENCE OF ALUMINIUM AND SILICON ON THE REACTION BETWEEN IRON AND ZINC

THE INFLUENCE OF ALUMINIUM AND SILICON ON THE REACTION BETWEEN IRON AND ZINC

PROEFSCHRIFT

TER VERKRIJGING VAN DE GRAAD VAN DOCTOR IN DE TECHNISCHE WETENSCHAPPEN AAN DE TECHNISCHE HOGESCHOOL EINDHOVEN, OP GEZAG VAN DE RECTOR MAGNIFICUS, PROF. DR. S. T. M. ACKERMANS, VOOR EEN COMMISSIE AANGEWEZEN DOOR HET COLLEGE VAN DEKANEN IN HET OPENBAAR TE VERDEDIGEN OP VRIJDAG 29 APRIL 1983 TE 16.00 UUR

DOOR

KAZIMIERZ OSINSKI

GEBOREN TE BUDEL-DORPLEIN

Dit proefschrift is goedgekeurd door de promotoren.

1e promotor: Prof.Dr. R. Metselaar

2e promotor: Prof.Dr. G.D. Rieck

Co-promotor: Dr.Ir. G.F. Bastin.

For the moment, we will have to content ourselves with a sense of wonder and awe, rather than with an answer. And perhaps experiencing that sense of wonder and awe is more satifying than having an answer, at least for while.

Douglas R. Hofstadter,
"Gödel, Escher, Bach: an Eternal Golden Braid".

"Holmes", I cried, "this is impossible".
"Admirable!" he said. "A most illuminating remark. It is impossible as I state it, and therefore I must in some respect have stated it wrong..."

Sir Arthur Conan Doyle,
"The Adventure of the Priory School".

CONTENTS

page

Dankwoord

Hoewel op de omslag van dit boekje alleen mijn naam staat vermeld betekent dit niet dat ik alleen aan het erin beschreven onderzoek heb gewerkt. Zonder de hulp van anderen is het waarschijnlijk zelfs niet mogelijk zoiets te doen. Dit onderzoek werd verricht in het Laboratorium voor Fysische Chemie van de Technische Hogeschool Eindhoven. Bij deze wil ik iedereen van dit laboratorium bedanken voor hun hulp en prettige samenwerking tijdens de periode dat ik er gewerkt heb. Een aantal van hen wil ik hier met name noemen.
Allereerst Giel Bastin en Frans van Loo voor hun enthousiaste begeleiding. Diverse in dit proefschrift verwerkte ideeën zijn gevormd tijdens discussies met hen.
Anton Vriend heeft me erg goed geholpen ; met hem heb ik erg fijn samengewerkt gedurende een jaar dat hij in het kader van een TAP project op het laboratorium werkte. Hij zag voor het eerst de banden die beschreven staan in hoofdstuk 5.3.
De studenten (of reeds afgestudeerden) Jaap Stijlaart, Geert Kastelijns en André Gehring dank ik voor hun bijdragen die zij geleverd hebben gedurende practica of afstudeerperiode.
Goede ideeën hebben is een eerste, ze uitvoeren een tweede. Goede technische assistentie is hiervoor onontbeerlijk. Jo van der Ham heeft me hiermee altijd enthousiast geholpen.
Behalve de inhoud van dit proefschrift vind ik ook belangrijk dat het er mooi uitziet. Dit aspect is voornamelijk het werk van:
Charlotte Ruisendaal, die het typewerk zeer snel en fraai verzorgde,
Gerard Schepens, die de meeste tekeningen en figuren maakte, en
de heer Horbach, die de foto's en omslag van dit proefschrift haarscherp maakte en afdrukte.

Naast deze mensen die min of meer direct bij de verwezenlijking van dit proefschrift waren betrokken wil ik een paar mensen noemen die meer een rol op de achtergrond hebben gespeeld.
Allereerst mijn ouders, zij lieten mij studeren en hebben mij steeds daarin aangemoedigd.
Betsy, tenslotte, kan ik het beste bedanken door de (enigzins aangepaste) woorden van Thomas Kuhn uit zijn boek "De Structuur van Wetenschappelijke Revoluties" aan te halen: "Zij heeft mij namelijk mijn

gang laten gaan(....). Iedereen die heeft geworsteld met een project als dit zal inzien wat het haar heeft gekost. Ik weet niet hoe ik haar moet bedanken". Aan haar draag ik dit proefschrift op.

De Nederlandse Organisatie voor Zuiver Wetenschappelijk Onderzoek (Z.W.O.) ben ik erkentelijk voor de verleende materiële steun.

CHAPTER I.

INTRODUCTION.

1.1 General

Chemical reactions occurring in and between solids are of great practical interest and are encountered in several processes such as cladding, carburizing, oxidation, galvanizing and so forth. During all these processes diffusion of one or more components occurs and reaction layers may develop. The study of these reaction layers is an important field of research for materials engineers.

The simplest approximation of these complex processes is a binary system in which only two components are involved. A lot of research has been done on diffusion in binary systems such as Ti-Ni[1], Ti-Al[2], Ni-Al[3], Fe-Sn[4], Fe-Zn[5], Ag-Zn[6] etc. and this has yielded a multitude of information concerning amongst other diffusion coefficients and phase diagrams. A somewhat more realistic approximation to reality is a ternary system in which the behaviour of three components is studied. The study of ternary systems is more complicated as compared to binary systems, especially from a theoretical point of view, because the introduction of a third element is attended with an extra degree of freedom for the system. This is probably the reason that it is only during the last 20-30 years that research on ternary systems comes up. It concerns both theoretical and practical investigations and there will be recalled here for example the investigations of Dayananda et al. on the systems Fe-Ni-Al[7,8] and Cu-Ni-Zn[9], Roper and Whittle on the system Co-Cr-Al[10], Kirkaldy and Brown on the system Cu-Zn-Sn[11], Laheij and van Loo on the system Fe-Cr-O[12] and van Loo et al. on the systems Ti-Ni-Cu[13], Fe-Ni-Mo and related systems[14] and Ti-Ni-Fe[15].

The investigation described in this thesis deals with the study of ternary diffusion phenomena in the systems Fe-Zn-Si and Fe-Zn-Al. The background of this investigation lies in the process of hot-dip galvanizing of steel and iron in which as we will see aluminium and silicon play an important role.

1.2 Diffusion in metals

An important tool for studying diffusion phenomena is a so called diffusion couple, in which two different starting materials are brought into contact with each other and annealed for appropriate times at a chosen temperature. Owing to a chemical potential gradient diffusion will occur.
According to the number of components we distinguish binary, ternary, etc. diffusion couples. In view of the nature of this investigation we will limit ourselves to diffusion phenomena in binary and ternary metal systems.

The relation between the concentration profile in a binary diffusion couple and its corresponding binary phase diagram may be best demonstrated with the help of fig. 1.1.

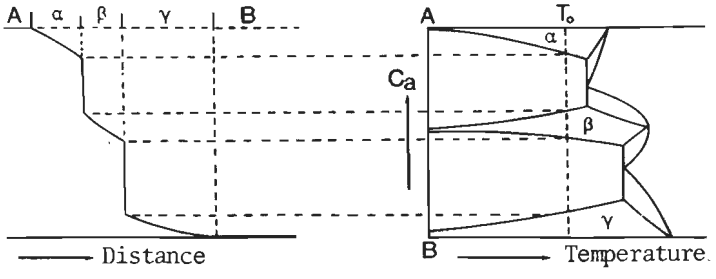

Fig. 1.1. Relation between the hypothetical phase diagram (fig. b) of two metals A and B and the concentration profile (fig. a) in a binary diffusion couple A-B annealed at T_o.

Fig. 1.1 shows a hypothetical phase diagram for two metals A and B with solid solutions α and γ and with an intermetallic compound β. When the two metals A and B form the starting materials of a diffusion couple which is annealed at a temperature T_o, then in principle we will find, going from metal A to B in the couple, subsequently the solid solution α, the intermetallic compound γ and the solid solution β, all lying in layers parallel to the

original contact surface. The penetration curve shows a number of concentration jumps corresponding to the phase boundaries. In a state of equilibrium the concentrations at these boundaries correspond with those of the phase diagram.

With ternary diffusion couples the situation is more complicated because it is not a priori possible to predict the phase sequence in the couple from its ternary phase diagram. Let us take as an example the system A-B-C with an isothermal section of the phase diagram as drawn in fig. 1.2.

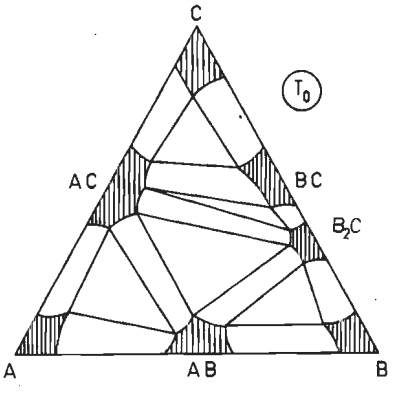

Fig. 1.2. Hypothetical isotherm of the ternary system A-B-C.

In the diffusion couple AB-C several phase sequences may develop, for example:
AB/B_2C/AC/C, AB/B_2C/BC/AC/C or AB/AC/BC/C.
The only condition which has to be fullfilled is the mass balance. This means that if a phase develops which is relatively rich in component B this has to be compensated by the development of a phase poor in B. It is also possible that the phases in a ternary diffusion couple do not develop in layers parallel to the original contact surface but in interwoven layers. In chapter II we will go further into this matter.

1.3 Hot-dip galvanizing of steel and iron

The protection of steel and iron against corrosion by coating

the surface by means of a zinc layer is already an old process. In practice there are four different procedures to attach this zinc layer on the steel or iron surface. Here we consider only the process of hot-dip galvanizing in which a zinc layer is deposited on the surface by dipping the specimen in a bath containing a zinc melt. By dipping an iron specimen into a zinc melt we make in fact a binary diffusion couple in which the starting materials consist of solid iron and liquid zinc. The reaction products which develop during this process will consist of the phases as predicted by the Fe-Zn phase diagram (see chapter III, fig. 3.2), and will be arranged in layers parallel to the original contact surface (see fig. 1.3).

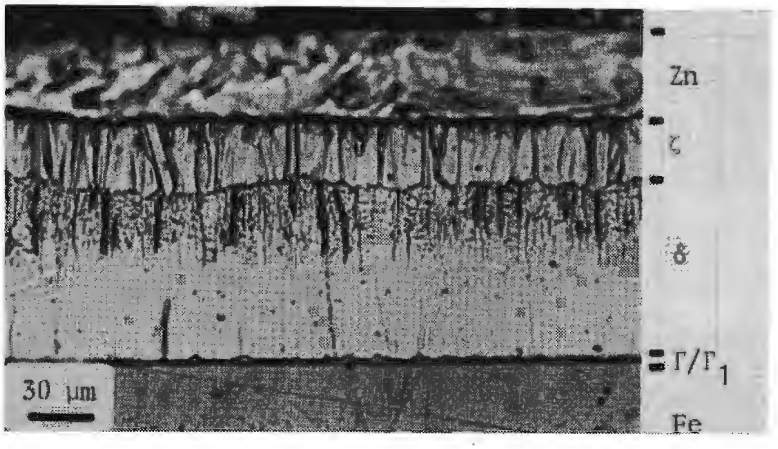

Fig. 1.3. Fe-Zn diffusion couple, dipped for 10 min at 450°C.

The reaction between iron and zinc shows some unusual kinetic features. Up to 495°C the total layer thickness follows the well-known law of parabolic growth, however at temperatures between 495 and 530°C a sudden change occurs to linear kinetics. Above 530°C the reaction shows again parabolic growth kinetics. These changes in the reaction kinetics are reflected in the morphology of the reaction layers: up to 495°C the formed $\delta + \gamma$ layers are compact and closed. In the region of linear growth the layers are broken up and consist of small δ cristallites and some loose ζ cristallites on top of them, between which zinc is found. Between 505°C and 530°C no ζ is found at all. Above 530°C a compact δ layer is again formed.

The ζ layer is not found above this temperature in accordance with the phase diagram.

The reason for this unuasual behaviour in the temperature region of 495-530°C lies clearly in the fact that no closed ζ layer is formed in this temperature region. According to Horstmann[16] the reason for this absence of a closed layer is due to nucleation difficulties of this phase. However, Allen and Mackowiak[17] showed that a closed ζ layer formed at a temperature below the region of linear growth totally disappears when dipped again at a temperature in the region of linear growth. Thus, though ζ nuclei were present, this phase was not found after dipping at a temperature in the region of linear growth. So the reason for this change in kinetics is still obscure.

The reaction layer formed at a temperature in this region of linear growth will be very thick, which means a waste of zinc, has poor mechanical qualities and a dull appearance. In practice this temperature region of linear growth with these unfavourable effects can simply be avoided by galvanizing at temperatures between 450°C and 460°C. However, the situation totally changes when the iron or steel which has to be galvanized contains some silicon. The presence of silicon causes an extension of the region of linear growth especially to lower temperatures. This feature is illustrated in fig. 1.4a[18]. This influence of silicon has been known for a long time[19], but it was R.W. Sandelin[20] who discovered in 1963 that silicon already present in the steel or iron in very small amounts (0.07-0.12 wt%) also extended the region of linear growth to lower temperatures (see fig. 1.4b). So the relation between the amount of silicon present in steel or iron and the reaction velocity shows a relative maximum at $\pm$ 0.1 wt% Si. This is known as the Sandelin effect and is illustrated in fig. 1.5.

Untill about 20 years ago all this did not cause any problems in all-day galvanizing practice because the steel produced by the steel manufacturers (via the ingot-process) contained less than 0.02 wt% Si. However, since $\pm$ 1962, owing to modified production methods (continuous casting), still more and more steel is being produced which contains silicon and it is not possible to avoid the

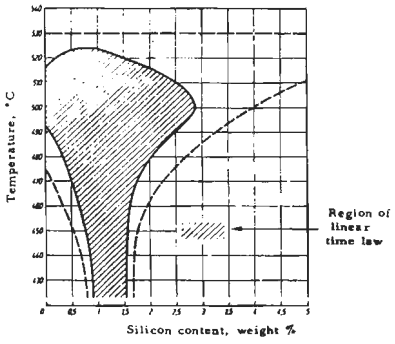

a

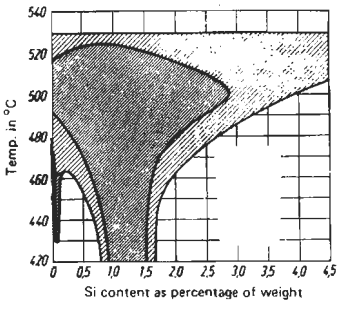

b

Fig. 1.4a en 1.4b. a) Extension of region of linear growth with increasing silicon content in iron.
b) as a) but including the effect of a small silicon content (≈0.1 wt%) in iron.
After Horstmann(18).

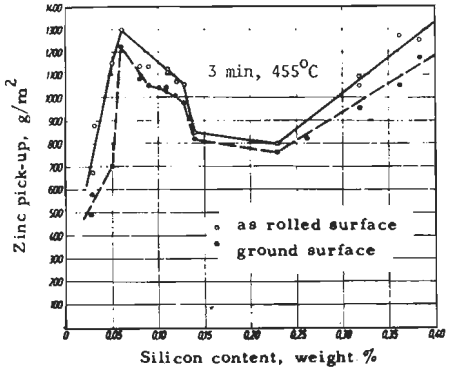

Fig. 1.5. Relation between silicon content in iron and weight of coating formed during galvanizing (after Sandelin(20)).

temperature region of linear growth during galvanizing the silicon containing steels. Because ≈ 40% of the world's yearly production of zinc is used for hot-dip galvanizing of steel and iron(21) it is clear that the galvanizing industry is confronted with big problems by this development.
A lot of research has been done in order to explain this adverse

effect of silicon, a short review of which will be given below.

- Gutmann and Niessen[22,23] investigated the reaction between liquid zinc and steel containing 0.4 wt% Si. They gave a phenomenological model of the enhanced reactivity in which they propose that due to the very small solubility of silicon in the intermetallic Fe-Zn phases, the liquid zinc (a phase with a slightly higher solubility for silicon) would remain between the crystallites of the growing layer as "liquid pockets". This presence of liquid zinc near the steel surface would lead to the enhanced reactivity. The aggregate zone consisting of zinc "liquid pockets" and δ cristallites was called by them the "Δ diffuse zone".
- Horstmann[24] discussed the influence of silicon on the nucleation of the ζ phase.
- Sørensen[25] was one of the first who regarded the problem as a ternary diffusion problem and described it that way.
- Habraken[26] proposed a model based on the work of his group during 10 years[27,28]. They refined the model of Gutmann and Niessen and investigated the "Δ diffuse zone" on the presence of silicon rich precipitates, which is essential for this model. Indeed these precipitates were found and identified by them as FeSi particles.
- Ferrier[29] studied the effect of silicon present in pure iron on the reaction between iron and zinc by using diffusion couples in which the starting materials were binary Fe(Si) alloys and pure zinc.

Aluminium additions to the zinc bath (0.1-1.0 wt%) appeared to have a beneficial effect by reducing the reactivity of silicon containing steel[30,31]. This favourable effect of aluminium probably arises from the formation of an inhibiting aluminium rich layer (Fe_2Al_5 and/or $FeAl_3$) on the iron or steel surface[32]. This protection is only temporary because after some time the aluminium rich layer is broken up because of a depletion of the bath in aluminium.

1.4 Purpose of this investigation

As we have seen in the preceding section the elements silicon and aluminium play an important role in the process of hot-dip galvanizing. The first purpose of this investigation was to gain more insight into the influence of these elements on the reaction between

iron and zinc and to introduce some refinements in the models mentioned in the preceding section. In principle it concerns an investigation on reaction diffusion in ternary systems.

This brings us to the second goal of this investigation viz. the study of reaction diffusion phenomena in ternary metal systems. Research on this subject concerns especially the development of reaction layer morphologies in ternary diffusion couples. An understanding of the mechanism for the formation of different reaction layer morphologies is very important for understanding the properties of coatings on a metal substrate. By means of this study on the systems Fe-Zn-Al and Fe-Zn-Si (and related systems) we hoped to gain more information on this subject.

CHAPTER II

THEORECTICAL BACKGROUND

2.1 Mechanisms of diffusion

Diffusion of atoms through a solid can occur in several ways. We can distinguish two types of diffusion viz.:

- Diffusion via the atomic lattice. This is called lattice- or volume diffusion.
- Diffusion via the surface or via the grain boundaries. This is called short-circuit diffusion.

It is generally observed that at low temperatures short-circuit diffusion exceeds volume diffusion. However, the relative contributions vary with temperature so that in different temperature regions different diffusion mechanisms dominate the behaviour.

In this section we will only consider lattice diffusion. On an atomic level we can distinguish in the case of lattice-diffusion a number of diffusion mechanisms. The most important of these mechanisms, which are supposed to play a role in atomic movements in metals and non-ordened alloys, will be shortly reviewed below. For an extended review see for example Adda and Philibert[33] and Shewmon[34].

In the mechanism of direct exchange and the so-called ring mechanism resp. a direct exchange of sites between two atoms or a simultaneous exchange of three or more atoms in a ring takes place. These mechanisms imply large lattice deformations and are supposed to occur only in rather open structures.

In more close-packed structures the mechanisms in which lattice defects play a role are more obvious. The presence of these lattice defects makes it possible for atoms to move without too large lattice deformations. Two types of this diffusion mechanism are the interstitial and vacancy mechanism. In the case of the interstitial mechanism an atom moves from one interstitial site to another. A variant on this mechanism is the interstitialcy mechanism in which the interstitial atom pushes a lattice atom from its site and forces it to occupy an interstitial site. In the case of the vacancy mechanism the atoms move by changing place with a neighbouring vacancy.

It has been observed that in metals diffusion generally occurs

by a vacancy mechanism. This follows both from calculations and determinations of vacancy concentrations and activation energies, and from the observation of a Kirkendall effect[35] (the phenomenon of marker displacements, see section 2.2.2) in almost all metal systems.

Normally the number of vacancies in a metal is in thermodynamic equilibrium with the lattice. However, when two atoms diffuse countercurrently and with different velocities, a vacancy flux will appear which disturbs the equilibrium. To maintain this equilibrium it is necessary to have sources and sinks for the vacancies. On the basis of observations and theoretical calculations it is accepted that in diffusion couples dislocations are the most important sources and sinks for vacancies. In regions in which the incoming flux of vacancies is greater than can be assimilated by the dislocations an oversaturation of vacancies may occur giving rise to pore formation.

2.2 The phenomenological laws of diffusion

2.2.1 General

One-dimensional diffusion in a diffusion couple is quantitatively described by Fick's first law:

$$J_i = -D_i \frac{\delta C_i}{\delta x} \qquad [2.1]$$

in which J_i = the flux of the diffusing component i $(\frac{\text{gr moles}}{\text{cm}^2\ \text{s}})$

C_i = concentration of component i $(\frac{\text{gr moles}}{\text{cm}^3})$

$\frac{\delta C_i}{\delta x}$ = concentration gradient of component i $(\frac{\text{gr moles}}{\text{cm}^4})$

D_i = a diffusion coefficient $(\frac{\text{cm}^2}{\text{s}})$

A problem, which arises when we want to describe the diffusion process is the choice of a suitable frame of reference to which the fluxes of the different diffusing components can be related. The choice of a frame of reference determines also the meaning of the diffusion coefficient, as we will see.

We will now discuss the matter of diffusion in metallic systems more deeply for binary and ternary systems. We will treat these systems seperately in order to make more clear the differences and

resemblances between both systems.

2.2.2 Diffusion in binary systems

As a frame of reference we take the volume-fixed frame of reference. In this reference system the flux of a component is measured in a plane, which is defined by the condition that the volume at both sides of this plane remains constant. This means that through this plane no net volume flux occurs, so:

$$\sum_{i=1}^{2} \bar{v}_i J_i = 0 \qquad [2.2]$$

In this equation $\bar{v}_i$ is the partial molar volume of component i. As a further condition we assume that the total volume remains constant. For each component we can now define a diffusion coefficient:

$$J_i = -\tilde{D}_i \frac{\delta C_i}{\delta x} \qquad [2.3]$$

A simple calculation, however, shows that $\tilde{D}_1 = \tilde{D}_2 = \tilde{D}$, so that in this case the diffusion coefficient for a binary system describes the behaviour of both components and is called the interdiffusion coefficient. The corresponding flux is called the interdiffusion flux and is written as $\tilde{J}_i$. The interdiffusion coefficient is a kind of measure for the rate of homogenisation of an inhomogeneous diffusion couple. This homogenisation can take place by diffusion of both or only one of the components.
A combination of Fick's first law and the law of conservation of matter yields Fick's second law:

$$\frac{\delta C_i}{\delta t} = \frac{\delta}{\delta x}\left(\tilde{D} \frac{\delta C_i}{\delta x}\right) \qquad [2.4]$$

From this equation we can solve the interdiffusion coefficient as a function of concentration by applying a Boltzmann[36] - Matano[37] analysis with the following initial and boundary conditions (see also fig. 2.1).

$$t = 0 \quad \begin{cases} x<0, & C_i = C_i^- \\ x>0, & C_i = C_i^+ \end{cases} \qquad t > 0 \quad \begin{cases} x=-\infty, & C_i = C_i^- \\ x=+\infty, & C_i = C_i^+ \end{cases}$$

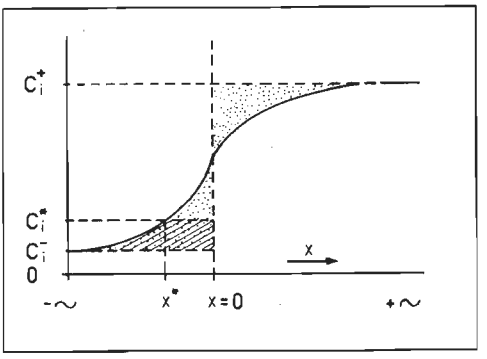

Fig. 2.1. Schematic penetration curve of component i with the Matano interface at x = 0 (the two dotted areas at both sides of this plane are equal). The integral in [2.5] equals the shaded area.

This yields: $\tilde{D}(C_i^*) = -\frac{1}{2t}(\frac{\delta x}{\delta C_i})_{C_i^*} \int_{C_i^-}^{C_i^*} x dC_i$ [2.5]

If $C_i^* = C_i^+$, equation [2.5] reduces to $\int_{C_1^-}^{C_1^+} x dC_i = 0$ [2.6]. In fact eq. [2.6] defines the plane x = 0 and is called the Matano interface. From an experimentally determined penetration curve we are now able to calculate the interdiffusion coefficient. This has been illustrated in fig. 2.1.

This general method of determination of the interdiffusion coefficient has to be applied very carefully because it is only valid in the case that the total volume remains constant. This is in general not the case especially when intermetallic compounds are formed. If volume changes occur a modified second law of Fick has to be used. This has been treated extensively by v. Loo[38] and Bastin[39].

The Boltzmann-Matano analysis implies the substitution of the function $\lambda(C_i) = \frac{x}{t^{\frac{1}{2}}}$ in eq. [2.4].

This has in fact a physical meaning because the function λ only depends on the concentration. This means that all concentrations, thus also the phase boundary concentrations, move proportionally with the square root of time. From this follows that also the layer thickness increases by the square root of time, so we obtain: $d^2 = kt$ [2.7].
This is the well-known law of parabolic growth, where d is the layer thickness, t is the annealing time and k represents the penetration coefficient with dimension $(\frac{cm^2}{s})$. In practice, the validation of this parabolic growth law is considered as a proof of an undisturbed development of the (volume)diffusion process.

As we have seen the interdiffusion coefficient describes the diffusion behaviour of both components. By using the intrinsic or Kirkendall frame of reference a diffusion coefficient can be defined which describes the diffusion behaviour of each component apart. In this frame of reference the fluxes are related to a lattice frame which has been marked with small inert particles (so called markers). These markers are placed at the original contact interface of both couple halves before interdiffusion is started.
We now obtain two equations:

$$J_1 = -D_1 \frac{\delta C_1}{\delta x} \qquad [2.8]$$

$$J_2 = -D_2 \frac{\delta C_2}{\delta x}$$

in which D_1 and D_2 are called the intrinsic diffusion coefficients. These two intrinsic diffusion coefficients are in general not alike and are a measure of the atomic mobility[40] of each component in the binary system. The relation between the interdiffusion coefficient and the intrinsic diffusion coefficients for a binary system is expressed by Darken's[41] equation:

$$\tilde{D} = C_2\bar{v}_2D_1 + C_1\bar{v}_1D_2 \qquad [2.9]$$

where $\bar{v}_1, \bar{v}_2$ are the partial molar volumes.

The general method for determination of the intrinsic diffusion coefficients is based on the measurement of the displacement of the markers which were placed on the original contact surface of the diffusion couple. For an extended treatment of this matter see v. Loo[38] and Bastin[39].

2.2.3 Diffusion in ternary systems

Consider a ternary diffusion couple with the following couple halves: Fe-C and Fe-Si-C with in both alloys the same carbon content. After annealing we observe a redistribution of carbon as illustrated in fig. 2.2. This is the famous experiment of Darken[42]. The result of this experiment is in contrast with Fick's first law because no carbon gradient was present originally and so no carbon diffusion should occur. This diffusion of a component against its own concentration gradient is called "up hill" diffusion and has been observed a number of times in other systems[43] since then. The explanation is that the driving force for diffusion is an activity or chemical potential gradient rather than a concentration gradient. The uphill diffusion effect occurs when the gradients of concentration and chemical potential are opposite in sign. In a binary system this effect can not be observed because here the chemical potential for each component increases continuously with its concentration making it impossible for the chemical potential and concentration

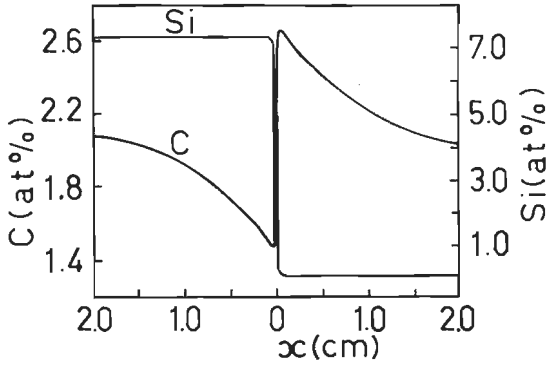

Fig. 2.2, Si-and C-concentration profile in a ternary Fe(C,Si)-Fe(C) couple, 13 days, 1050°C. Notice the "up hill" diffusion of carbon (after Darken[42]).

gradient to differ in sign. Also it is possible that a component in a ternary system diffuses not only along its own chemical potential gradient but also along the chemical potential gradients of the other components (= cross effects). These effects also have to be included when describing diffusion in ternary systems.

The theoretical basis for the description of the interactions in terms of the chemical potential of the elements is found in the phenomenological description of multicomponent diffusion. However, rather than using chemical potential gradients it is more convenient to describe the diffusion process in terms of concentration gradients because this is the experimentally measured parameter. This can be done by an extension of Fick's laws to multicomponent diffusion, as originally proposed by Onsager[44] (See also Kirkaldy[43]). We will now treat these extended Fick equations for both systems of reference as discussed in the preceding paragraph on binary diffusion.

In the volume fixed frame of reference the extended form of Fick's first law for a single-phase ternary system reads as follows:

$$\tilde{J}_1 = -\tilde{D}_{11}^{(3)} \frac{\delta C_1}{\delta x} - \tilde{D}_{12}^{(3)} \frac{\delta C_2}{\delta x} \qquad [2.10]$$

$$\tilde{J}_2 = -\tilde{D}_{21}^{(3)} \frac{\delta C_1}{\delta x} - \tilde{D}_{22}^{(3)} \frac{\delta C_2}{\delta x}$$

(component 3 has been chosen as the dependent one). We see that for the description of the diffusion process in a ternary system we need for each phase four interdiffusion coefficients. Thus beyond the direct interdiffusion coefficients $\tilde{D}_{11}^{(3)}$ and $\tilde{D}_{22}^{(3)}$, which represent the influence of the concentration gradients of components 1 and 2 on resp. the interdiffusion fluxes of the components 1 and 2, there are also two cross interdiffusion coefficients $\tilde{D}_{12}^{(3)}$ and $\tilde{D}_{21}^{(3)}$, which represent the influence of the concentration gradients of the components 1 and 2 on resp. the interdiffusion fluxes of the components 2 and 1. Fick's second law for a single-phase ternary system reads:

$$\frac{\delta C_1}{\delta t} = \frac{\delta}{\delta x} \tilde{D}_{11}^{(3)} \frac{\delta C_1}{\delta x} + \frac{\delta}{\delta x} \tilde{D}_{12}^{(3)} \frac{\delta C_2}{\delta x} \qquad [2.11]$$

$$\frac{\delta C_2}{\delta t} = \frac{\delta}{\delta x} \tilde{D}_{21}^{(3)} \frac{\delta C_1}{\delta x} + \frac{\delta}{\delta x} \tilde{D}_{22}^{(3)} \frac{\delta C_2}{\delta x}$$

To solve the interdiffusion coefficients as a function of concen-

tration from eq's [2.11] we again apply a Boltzmann-Matano analysis with suitable initial and boundary conditions. For a single-phase ternary diffusion couple of the semi-infinite or infinite type the Boltzmann-Matano solution to eq.'s [2.11] becomes[45]:

$$[\tilde{D}_{i1}^{3}\ \frac{\delta C_1}{\delta x} + \tilde{D}_{i2}^{3}\ \frac{\delta C_2}{\delta x}]_{C_i^*} = -\frac{1}{2t}\int_{C_i^-}^{C_i^*} x\,dC_i \quad (i=1,2) \qquad [2.12]$$

In order to determine experimentally the four interdiffusion coefficients from eq. [2.12] we need two independent diffusion couples with a common composition point C_i^* on their experimental penetration curves. For the composition of the intersection point eq. [2.12] can be applied for each couple. This yields for each component i two equations from which the four interdiffusion coefficients can be solved. For a recent application of this procedure see for example[8].

For the intrinsic or Kirkendall frame of reference the extended form of Fick's first law for a single-phase ternary system reads:

$$\begin{aligned} J_1 &= -D_{11}^{(3)}\frac{\delta C_1}{\delta x} - D_{12}^{(3)}\frac{\delta C_2}{\delta x} \\ J_2 &= -D_{21}^{(3)}\frac{\delta C_1}{\delta x} - D_{22}^{(3)}\frac{\delta C_2}{\delta x} \qquad [2.13] \\ J_3 &= -D_{31}^{(3)}\frac{\delta C_1}{\delta x} - D_{32}^{(3)}\frac{\delta C_2}{\delta x} \end{aligned}$$

So for each phase we need six intrinsic diffusion coefficients to describe the diffusion process. As in the binary case the method of determination of the intrinsic diffusion coefficients is based on the measurement of the marker-displacements. However, again two independent diffusion couples are needed with identical compositions of the marker interface[46]. This procedure has been applied in some ternary systems[47,48].

2.2.4 Some remarks on the experimental determination of the diffusion coefficients

The experimental determination of the diffusion coefficients in a binary system is straight-forward and can be carried out with

little difficulties. This is true for both single-phase diffusion and multi-phase diffusion. The Boltzmann-Matano procedure cannot be applied for the determination of the interdiffusion coefficient in a phase with a small homogeneity range (line compound) because the concentration gradient in this phase will almost be zero. Consequently the interdiffusion coefficient calculated from eq [2.5] will obtain an infinite value.
For these cases Wagner[49] proposed an alternative diffusion coefficient viz. an integrated diffusion coefficient:

$$\bar{D}_{int} = \int_{N_i(\gamma')}^{N_i(\gamma'')} \tilde{D}\, dN_i \qquad [2.14]$$

where $N_i(\gamma')$ and $N_i(\gamma'')$ are the mole fractions of component i at the resp. interface boundaries of the phase γ. For the special case of phase γ being grown from its adjacent saturated phases and by using the simplification $N_i(\gamma') = N_i(\gamma'') = N_i(\gamma)$ = the mole fraction of component i in the phase γ, $\bar{D}_{int}$ becomes:

$$\bar{D}_{int} = \frac{(N_i(\gamma)-N_i^-)(N_i^+-N_i(\gamma))}{N_i^+ - N_i^-} \left(\frac{d^2\gamma}{2t}\right) \qquad [2.15]$$

with Ni(γ) the mole fraction of component i in the phase γ, N_i^+ and N_i^- the mole fractions of component i in resp. the righthand and lefthand couple halves and $d\gamma$ the width of phase γ.

Another problem, concerning the calculation of the intrinsic diffusion coefficients, is the determination of the marker displacements. It appears that in some case the markers which consist of particles ($\approx$1 µm) of an inert material (for example tungsten) are torn in pieces[39]. Therefore so-called "naturel" markers like dust or grinding debris, which are always present at an interface, are often used. Often the marker position can be determined from the difference in crystal morphology of a phase which has been formed at both sides of the marker interface[4]. However, it appears in these calculations that already a small shift in the marker position has a great influence on the calculated intrinsic diffusion coefficients, so care has to be exercised in interpreting these values.

In ternary systems the determination of the diffusion coeffi-

cients becomes more complicated as we have seen in the preceding chapter. Accordingly the experimental difficulties are larger. Here too we have the problem of small concentration gradients, but this problem counts twice because we need two independent diffusion couples. The precise determination of the intersection point of the two penetration curves may also give problems, if the two penetration curves intersect at small angles. This problem of intersecting penetration curves may be overcome for the determination of interdiffusion coefficients in phases with a large existence region, because the preparation of two independent diffusion couples of which the penetration curves intersect is rather easy[8]. However, for phases with a small existence region (as in the systems studied in this investigation) it may be difficult to prepare two diffusion couples, of which the penetration curves intersect at a composition point lying in the existence region of the phase in question.

A last remark considers the concentration at which the diffusion coefficients are determined. This concentration is a priori not known. The interdiffusion coefficient is determined for a composition of the intersecting point of the two penetration curves. Before we have finished the diffusion experiment this composition is unknown. Also in the case of the determination of intrinsic diffusion coefficients we do not a priori know at which composition the markers will lay after the diffusion experiment. In any case we do not know if a marker will lay at the same composition as a marker in another diffusion couple. So, if we want to determine a diffusion coefficient for a concentration of a special interest this may not be possible or we have to apply a sort of trial and error process by preparing many diffusion couples.

2.3 Diffusion structures and diffusion paths in ternary diffusion couples

2.3.1 General

The reaction layers in a binary diffusion couple are separated from each other by planar phase boundaries. Provided that the phases at both sides of a phase boundary are in local equilibrium (this means among others that the nucleation of the phases is very fast compared to the diffusion rate), this fact can easily be seen from the phase rule:

$$F = C - P + 2 \quad [2.16]$$

in which F is the number of degrees of freedom
C is the number of components
and P is the number of phases which are allowed to be in equilibrium with each other.

Because temperature and pressure generally are fixed, it follows from this rule that, if two phases are in equilibrium with each other in a binary system, there is no degree of freedom left for the concentration to adapt itself.
As a consequence only planar phase boundaries are possible in a binary diffusion couple.

In the case of a ternary diffusion couple it follows from the phase rule that we have one degree of freedom more. If now two phases are in equilibrium there is a degree of freedom left for the concentration to adapt itself freely. This means that two phases in a ternary diffusion couple can coexist in equilibrium over a range of compositions. This again means that non-planar interfaces between two phases and/or precipitation zones can arise in a ternary diffusion couple. It will be clear that three-phase regions are not possible but only planar three-phase interfaces. Before we go further into the matter of the development of two-phase zones in ternary diffusion couples it is essential to discuss first an important tool in ternary diffusion viz. the concept of a diffusion path.

2.3.2 The diffusion path concept in ternary diffusion couples

Consider the hypothetical isothermal section of a ternary phase diagram as illustrated in fig. 2.3.
We prepare a diffusion couple with terminal alloys AB and C which is annealed for a certain time at temperature T_o. The reaction layer developed in the diffusion couple may look like drawn in fig. 2.4. Two phases AC and BC have developed, which are separated by a non-planar (wavy) interface. In this two-phase region both phases are locally in equilibrium. We measure a concentration profile in the couple parallel to the diffusion direction. The concentration is measured on a line perpendicular with the diffusion direction (line L in fig. 2.4). The measured concentrations are plotted on an

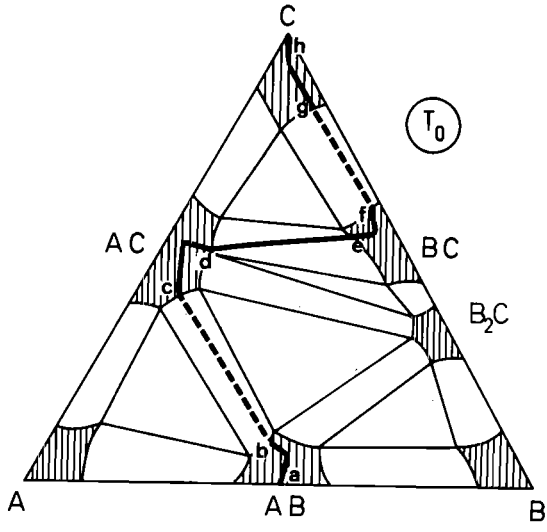

Fig. 2.3. Schematic T_o isotherm of ternary system A-B-C with plotted diffusion-path of the couple in fig. 2.4.

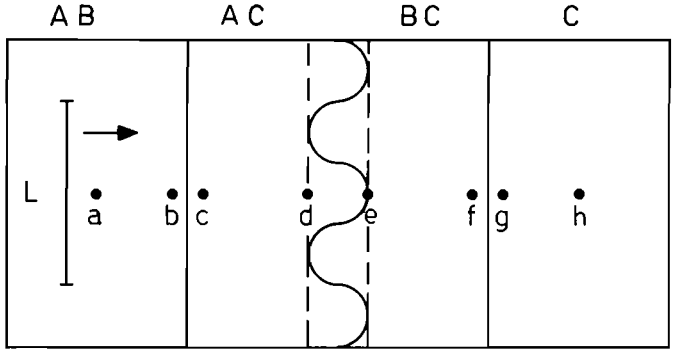

Fig. 2.4. Layer sequence in hypothetical ternary diffusion couple AB-C annealed at T_o (The isothermal section is given in fig. 2.3).

isothermal section of the ternary phase diagram (as drawn in fig. 2.3). This sequence of plotted points is called a diffusion path.

We will now follow this plotting of the diffusion path for a certain diffusion couple on the isothermal section of a phase diagram in more detail. We start with our concentration line L in the bulk of the AB compound (=a, see figures 2.3 and 2.4, the letters in both figures relate the measured compositions to the position of L in the diffusion couple). The measured compositions, going to the right from a to b, are represented by the solid line a-b in the homogeneity region of phase AB on the isothermal section. At the phase interface AB/AC (b-c) there is a concentration jump. In fig. 2.3 this is represented by a dashed line b-c parallel to a tie line in the two-phase region of the phases AB and AC. A dashed line always represents a zone of zero spatial extent in the diffusion couple. The measured compositions in the phase AC up to the beginning of the two-phase region AC-BC (c-d) are again represented by a solid line c-d in the homogeneity region of phase AC. The measured compositions in the two-phase region of AC and BC (d-e) will be between those of the pure phases AC en BC and are represented by a solid line in the two-phase region of the phases AC and BC on the isothermal section (d-e). A solid line in a two-phase region represents a zone of non-zero spatial extent in which the two phases are locally in equilibrium over a range of concentrations. This solid line cuts those tie lines which correspond to the lateral interfacial equilibria along the waved interface and should intersect the tie lines at points proportional to the weight ratio of the two phases (according to the lever rule). The further course of the diffusion path (e-f-g-h) is analogous to the first part of the diffusion path described up to now. For other principal diffusion layer configurations which are possible in ternary diffusion couples (precipitation zones, three phase interfaces) Clark[50] proposed a general convention for mapping these structures on the isothermal section of the ternary phase diagram. Fig. 2.5 gives a general outline of these conventions, which speak for themselves after the preceding example.

In principle many diffusion paths appear to be possible a priori. Fig. 2.6a-b shows two other possibilities for the couple of fig. 2.4. The only condition which has to be fullfilled is the mass balance, i.e. a diffusion path on the ternary isotherm must cross the straight

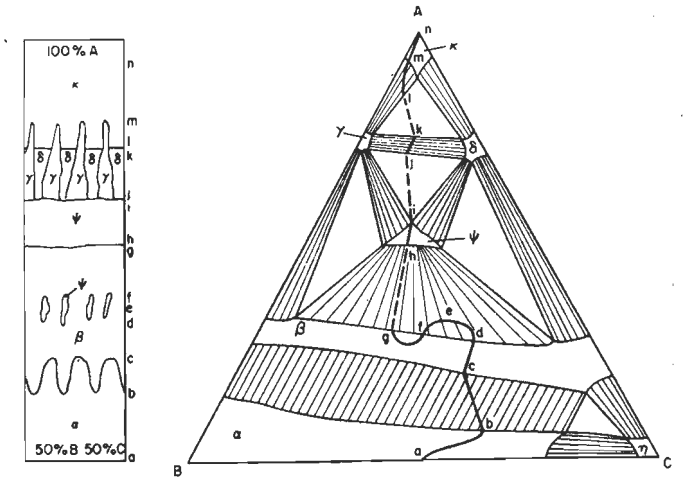

Fig. 2.5. Conventions for plotting diffusion paths on the isothermal section of a ternary phase diagram after Clark[50].

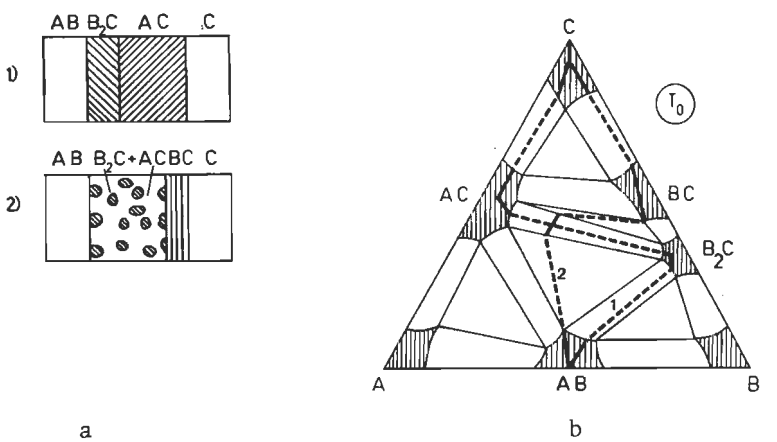

Fig. 2.6. a) Two possible layer sequences in the ternary diffusion couple AB-C.

b) Plotted diffusion paths on the isothermal section of the system A-B-C.

line joining the terminal compositions at least once. In practice, however, from the many possible diffusion paths of a given ternary diffusion couple nature selects only one. The question is, why nature chooses, from the many possible diffusion paths, just this one?

For a given ternary diffusion couple the answer of this extremely difficult question lies in the thermodynamic (i.e. the phase diagram) and kinetic (i.e. diffusion data) properties of the system. If the phase diagram is known and we can decide from the mass balance principle which phases will appear in the diffusion couple the answer to this question lies in the solution of the diffusion equations [2.11] for each phase which is involved. The analysis of these equations leads to the so-called calculated paths which we can compare with practice. We will now discuss this matter in more detail.

The solution of the diffusion equations gives us the concentration profiles of each component after a certain diffusion time. These solutions have the unique parabolic form:

$$C_1 = C_1(\lambda) \qquad C_2 = C_2(\lambda) \qquad [2.17].$$

in which $\lambda = \frac{x}{t^{\frac{1}{2}}}$ is only a function of the concentration. The solutions for both components are functions of the same parameter. By elimination of this parameter we obtain for each phase a function $C_1 = f(C_2)$, and plotted on the ternary isotherm this gives the calculated diffusion path. By making certain assumptions about the variation of diffusion coefficients with composition it is possible to calculate the diffusion path for a diffusion couple of a single-phase ternary system[51]. For a multi-phase ternary diffusion couple the situation is more complicated as we will see now. If we have the necessary diffusion data for each phase on a ternary isotherm we can calculate the path for each phase. But as we have seen it is also possible that non-planar interfaces and/or precipitation zones develop in a ternary diffusion couple. Exact calculation of the concentration profiles through such two-phase regions is not possible because in a two-phase region we have two phases in local equilibrium over a range of concentrations. This means that the concentration is not a function of one variable $\lambda = \frac{x}{t^{\frac{1}{2}}}$ but also of other dimensions y and z. It is necessary for lateral diffusion to occur, if a two-phase region

develops. A solution for this is to consider the system as pseudo-binary, that means we suppose as a trial consideration that all interfaces remain flat, and so all concentrations are a function of the variable $\lambda = \frac{x}{t^{\frac{1}{2}}}$ only. It is then possible to obtain a complete solution by matching the solutions of the diffusion equations of the phases on each side of the phase boundary by means of flux continuity relations[45]. The diffusion path determined in that way can then be mapped on the ternary isotherm. If the calculated path contains no loops into the two-phase regions, but it crosses the two-phase regions coincident with a tie line, then our assumption of planar phase boundaries has proved to be valid. The calculated path is then a stable solution and is probably the unique physical situation. If however, the calculated diffusion path loops into two-phase regions, thereby intersecting tie lines, this implies a region of supersaturation. Then the solution is an unstable one, because supersaturation is usually not tolerated in real solid systems. The relief of this predicted supersaturation leads, in practice to serrated interfaces and/or precipitation zones and our assumption of planar interfaces has not been valid. Kirkaldy[11] called such unstable calculated paths virtual paths. This concept of virtual paths, in which we calculate paths with the assumption that all interfaces remain flat is, as will be clear, very important for the prediction of two-phase regions in real systems i.e. what is the course of the actual diffusion path?

A serious difficulty concerning these diffusion path calculations is the formidable amount of diffusion data which are required for it. As we have seen four interdiffusion coefficients, which are all concentration dependent, are needed for the description of the diffusion process in only one phase. This means that for an actual diffusion couple in which, for example, two phases develop we need in total 16 interdiffusion coefficients to describe the diffusion process because 4 phases are involved. Also for more complicated systems it will not be possible anymore to decide unanimously which phases will occur in the diffusion couple because more phase configurations will be possible according to the mass balance. So many work in this field has been done for single-phase or two-phase diffusion couples. But also here complete diffusion data are generally not available for the ternary metallic system.

For diffusion in dilute ternary alloys the direct diffusion coefficients may be estimated from the measurements in binary systems, while the cross-term coefficients can be estimated from thermodynamic data[9,11], if available of course. For more concentrated alloys this is, of course, not possible. Direct measurements of the diffusion coefficients are known in literature[8,11], but it concerns here relatively simple ternary systems (i.e. with large solid solution ranges of the terminal alloys). For more complex ternary systems the determination of the diffusion data and consequently the diffusion path calculations demand a great effort.

2.3.3 Development of reaction layers in ternary diffusion-couples

Consider a binary diffusion couple A-C in which, according to the binary phase diagram A-C, two reaction layers develop, e.g. AC and A_2C. The reaction layer may look as schematically illustrated in fig. 2.7:

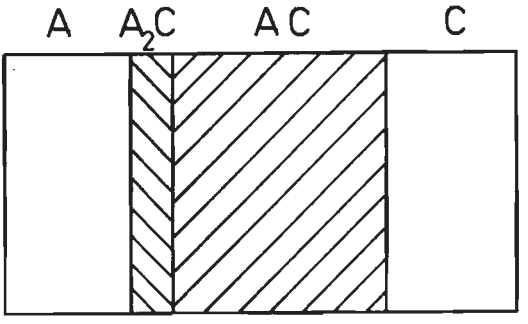

Fig. 2.7. Hypothetical binary diffusion couple A-C.

The width of both diffusion layers is determined by the magnitude of the interdiffusion coefficients in these phases. So the interdiffusion coefficient in the phase AC will be larger than the one of phase A_2C. Consider now the ternary diffusion couple AB-C in which the phases AC and BC develop. Suppose, that the interdiffusion coefficient in phase BC is small. A possible layer morphology in the diffusion couple is illustrated in fig. 2.8. We see from this figure that, though the diffusion coefficient in phase AC is high, the width of this phase is not larger than that of BC. This is a consequence of the fact

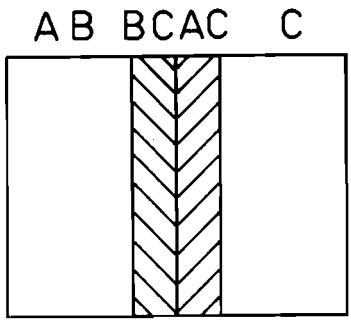

Fig. 2.8. Hypothetical ternary diffusion couple AB-C with a layered morphology.

that the amounts of both reaction products are now related to each other by a solid state reaction viz.: AB + C → BC + AC (assuming that AB and C are insoluble in each other). 1 : 1
So, the molar amounts of both phases will be equal. Consequently, in the case of equal molar volumina, the reaction layer widths will be equal. The width of phase AC now depends on the diffusion coefficients in phase BC. This example illustrates clearly how reaction layer morphologies (in this case phase widths) in ternary diffusion couples may differ from those in binary couples.

The layer morphology as drawn in fig. 2.8 is only one of the possibilities. Another possible morphology, in which the total reaction layer width is comparable to that found in the binary couple, is schematically drawn in fig. 2.9.

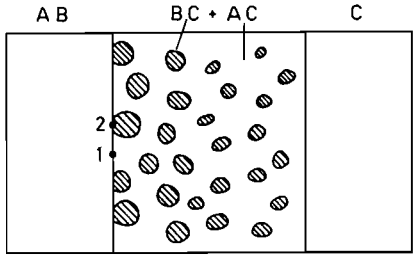

Fig. 2.9. Hypothetical ternary diffusion couple AB-C with a reaction layer of BC precipitates in a AC matrix (compare with fig. 2.8).

It concerns here BC precipitates in an AC matrix. The difference is clear: the total reaction layer width is now dependent on the diffusion through the matrix AC, which was supposed to be high, because BC precipitates rather than a closed BC layer are formed.

Which morphology will develop in a real system is not clear yet. Kirkaldy[11] says about this question: " .... discontinuous precipitates will occur when their resistance against diffusion is lower than that of the matrix, while continuous precipitates will occur when their resistance against diffusion is higher than that of the matrix". Thus, that total configuration will develop with the highest resistance against diffusion. Hence, according to Kirkaldy, in this case a layer of continuous BC precipitates (i.e. a closed BC layer as in fig. 2.8) will develop, because this configuration offers the highest resistance against diffusion. Schmalzried[52], however, takes the opposite view. According to him that layer configuration will develop which offers the least resistance to the diffusion process. For our example this means that according to Schmalzried the morphology as drawn in fig. 2.8 will develop.

As a warning we must recall the work of Laheij et al.[53]. They studied the reaction layer morphology in Cu_2O/Ni diffusion couples. Depending on the purity of Cu_2O powder used in their experiments they found a layered morphology with closed Cu and NiO reaction layers or a matrix of Cu(Ni) with NiO precipitates. The ratio between the total reaction layer widths of both reaction layer morphologies was about 100 in favour of the precipitate morphology.

The stability of a planar interface in a ternary diffusion couple was first treated by C. Wagner[54]. He developed a criterion for the stability of a planar phase boundary based on an application of perturbation methods. With the help of fig. 2.10 we will shortly outline the principles of this perturbation method. This figure represents schematically a ternary diffusion couple AB/C in which two reaction layers develop viz. BC and A_2B. A_2B is formed because B diffuses away from the terminal compound AB. A_2B will then develop because AB becomes relatively richer in A. The phase BC is formed by the reaction between B and C at the phase boundary between those two phases. C diffuses through the formed BC layer. Suppose that the diffusion rate of component B is small compared with the rate of C through phase BC. At an accidental perturbation 1-2 of the

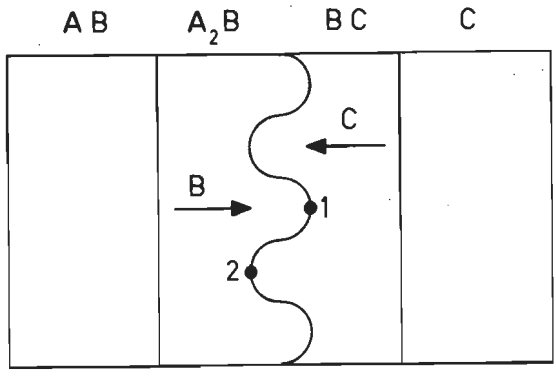

Fig. 2.10. Perturbation analysis of a phase boundary in a ternary diffusion couple (see also text).

phase boundary more B will arrive at position 2 than at position 1. Consequently more BC will be formed at position 2 compared with position 1. So the accidental perturbation will be increased and a two-phase region will develop. On the other hand if the diffusion of C through BC is rate determining, then more BC will be formed at position 1. Consequently the perturbation will be reduced and a planar interface will develop. The amount of B or C arriving at the phase boundary is not only dependent on the diffusion coefficients of these components in the reaction layer, but also on the concentration of the diffusing components in the terminal alloys. Wagner defined a quantity Q in which these factors were taken into account. Depending on the value of this factor Q (i.e.> 1 or < 1), serrated or planar boundaries will develop. This perturbation analysis was succesfully applied by Wagner and other authors[55] for the prediction of layer morphologies during solid state reactions in metal-oxide systems. Recently these analyses were applied in a semi-quantitative way by van Loo et al.[56] for the prediction of perturbations at reaction interfaces in ternary metal systems. So these analyses may have a broader field of application. However, one has to be careful using these perturbation analyses to explain two-phase regions in ternary diffusion couples, because they may not only develop as a result of a pronounced perturbation effect. Such zones may also arise during the cooling of the sample to room temperature as Van Loo et al.[15] also have shown.

As we have seen, precipitation zones also frequently occur in ternary diffusion couples. In the literature internal precipitation zones are mainly treated in relation to internal oxidation and sulfidation of metals or alloys. It concerns here precipitation from an approximately uniform solution in which diffusion occurs in only one direction. An example is the precipitation of MnS from a solid solution of Mn in Fe during the inward diffusion of S in this solution. Kirkaldy[57] describes this process quantitatively and concludes that precipitation will always occur for an alloy containing a finite amount of component 2 provided that $\tilde{D}_{11} >> \tilde{D}_{22}$ (in the case of MnS precipitation we have $\tilde{D}_{11} = \tilde{D}^{Fe}_{SS}$ and $\tilde{D}_{22} = \tilde{D}^{Fe}_{MnMn}$, Fe is the dependent component). Internal precipitation is a matter of the formation of one reaction product viz. the precipitate from an approximately uniform matrix. The situation becomes more complicated in the case of a simultaneous formation of a continuous reaction layer and precipitates of another phase in it, as for example in fig. 2.9. This case is less well understood and is difficult to describe quantitatively. Let us take as an example an AB/C ternary diffusion couple in which an AC reaction layer develops with BC precipitates (see fig. 2.9). If both reaction products are formed at the AB substrate because of the reaction of C (which diffuses through the AC matrix) with this substrate, then the formation of the precipitates can only be explained by taking into account diffusion in a lateral direction. For, at position 1, at which only AC is formed the resulting excess of component B will have to diffuse away in a lateral direction to position 2 and form there the precipitate. Of course, component A has also to diffuse in a lateral direction, but from position 2 to 1. A quantitative description of such a diffusion process, which takes into account this lateral diffusion, is a formidable task.

Finally, it should be remarked that the development of two-phase regions and/or precipitation zones is not necessarily a consequence of non-zero values of the cross-diffusion coefficients. In practice most of these instabilities are a consequence of $\tilde{D}^{(3)}_{11} >> \tilde{D}^{(3)}_{22}$, a condition which is by far the most common situation leading to diffusion instabilities[57]. An example of this we have seen in the case of MnS precipitation in Fe(Mn) alloys.

2.4 Solid-liquid diffusion couples

In the discussion of diffusion phenomena in diffusion couples we have only considered the case in which both terminal alloys are solids. In the case of hot-dipping a metal or alloy in a melt one of the terminals is a liquid, and we are dealing with solid-liquid diffusion couples. In this section we will go further into the matter of solid-liquid diffusion couples, because in the investigation described in this thesis this situation often occurred.

The reaction layers formed during hot-dipping a metal or alloy in a melt are studied after withdrawal of the metal or alloy from the bath which contains the melt. However, we must realize that we do not study the whole diffusion couple, for one of the terminal materials is the melt. This plays especially a role if flaking occurs i.e. floating of reaction products into the melt. We have to take this into account when measuring the layer widths or making a mass balance analysis.

The fact that one of the terminals is a liquid can also have an influence on the reaction layer morphology. Because of surface energy effects a melt can more easily penetrate between the crystallites of a reaction layer, giving rise to two-phase layers. However, we must distinguish these two-phase morphologies from two-phase layers as discussed in the preceding sections, because in the case of liquid penetration these morphologies do not develop as a result of diffusion instabilities. Most clearly this effect of liquid penetration is demonstrated in a binary solid-liquid diffusion couple. As we have seen only planar boundaries are in principle possible, but for example in the case of hot dipping Fe in Sn the $FeSn_2$ reaction layer which is in contact with the liquid Sn has a wavy phase boundary. The phase boundaries between the other reaction layers are planar but here we have again solid-state diffusion between the reaction layers, because they are solids at the reaction temperature[4].

Another problem is the saturation of the melt. If the melt is unsaturated with respect to a component which is being dipped, then a part of the dipped material will dissolve in the melt till it is saturated. To avoid this disturbing reaction melts saturated with the component being dipped have to be used.

2.5 The influence of growth stresses on the reaction layers

There are many factors which affect the properties of a reaction layer. The morphology of the reaction layer, whose development we have discussed in the preceding sections, is one of these factors. Another important factor, which has been overlooked up to now, will be discussed in this paragraph. It concerns here stresses generated during the layer growth. The generation of these stresses and their influence on the properties of the layer have been especially investigated for the formation of oxide scales on a metal substrate during high-temperature oxidation. Therefore the discussion of this aspect will be mainly limited to this type of reaction. Also we will only discuss the development of stresses in a reaction layer during an isothermal heat treatment. Stresses caused by differences in thermal expansion will not be considered here.

Experimental evidence for the occurrence of stresses in oxide scales is demonstrated by the way in which the scale fails: blistering, flaking or shear-cracking indicating compressive stresses in the scale (cf. fig. 2.11); tensile fractures extending as wedges from the outer surface indicating tensile stresses in the scale.

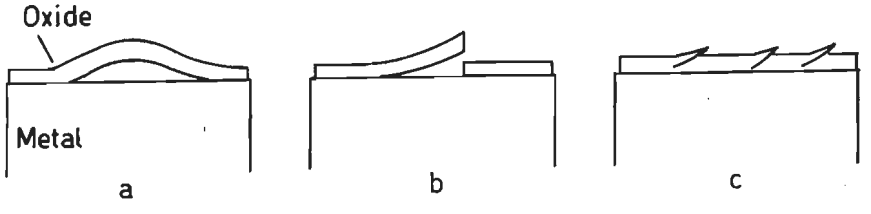

Fig. 2.11. Types of scale fracture indicating the existence of compressive growth stresses in the oxide.
a) blistering, b) flaking, c) shear cracking.

Evans[58] demonstrated the existence of stresses in thin Ni-oxide scales by removing them from the Ni substrate. Freed from the constraint of the metal wrickling and curling occurred, indicative of stresses in the film. Another demonstration of the generation of stresses is the curling of a thin strip which is allowed to oxidize at one side only[59]. The degree of bending of the strip is a measure for the magnitude of the stresses which have developed[60].

In contrast to the ease with which the presence of these stresses can be demonstrated, the explanation of the origin of the stresses is more difficult. Pilling and Bedworth[61] developed the first model dealing with this subject. In this model it is assumed that the stresses originate from volume differences between the lattices of the metal and the oxide. Further it is assumed that the transition of the metal lattice to the oxide lattice is produced by a homogeneous isotropic dilatation. The sign (a negative value points to compressive stresses) and magnitude of the stresses are related to (1-PBR), where PBR is the Pilling-Bedworth Ratio. For a Me_aO oxide formed on a metal Me the value of PBR is given by:

$$PBR = \frac{1}{a} \frac{\bar{v}_{Me_aO}}{\bar{v}_{Me}} \qquad [2.18]$$

in which the $\bar{v}$'s are the molar volumina of the compounds in question. Typical PBR values for oxides vary between 0.58 for Li_2O and 2.68 for Nb_2O_5[62]. This model is rather simple, and the processes are much more complex than this volume conservation model suggests. Nevertheless, in most cases there is a qualitative agreement between the predictions of this model and experiment, indicating that volume effects certainly play a role in the generation of stresses. The Pilling-Bedworth rule can only be applied to those metals for which the oxidation process is controlled by inward oxygen diffusion. If outward cation diffusion predominates the metal ions oxidize at the oxide/gas interface with no constraints, and the film is essentially stress-free at the outer surface. However, films which are formed by outward cation diffusion are usually under stress (for example NiO on Ni, see Evans[58]). Apparently, other sources for stresses have to be taken into account, the most important of which are:

- epitaxial constraints, due to the mismatch between the epitaxial layer and the substrate.
- oxide formation within the oxide layer,
- concentration gradients in the metal and/or oxide.

Because this would take us to far afield we will not go any further in these additional sources of stresses. For an extended review of this matter the reader is referred to Stringer[63].

Having considered the experimental evidence and origins of stresses in a reaction layer we come now to the point of the relief of

these stresses. This can occur by means of plastic deformation of either the film or the substrate. Several processes which give rise to plasticity, especially at high temperatures, can be distinguished. The most important are:

- grain boundary sliding
- creep[64][65]
- dislocation climb[66]

We will not go into a detailed treatment of these plastic deformation processes, because this falls outside the scope of this thesis. More important for us are the processes which occur at relatively low temperatures when plastic deformation of the film or substrate is not expected. The relief of the growth stresses will then occur by fracture of the reaction layer. This has a profound influence on the reaction behaviour and on the appearance of the reaction layer. In the case of compressive growth stresses and a weak adherence of the film blistering or flaking (see fig. 2.11) will occur, as has been observed during the oxidation of Fe[67]. Tylecote's[68] work on the adherence of cupric oxide film on copper showed that complete or nearly complete exfoliation of the scale occurred when the oxidation temperature was 700°C. Due to an enhanced oxide plasticity at higher temperatures no exfoliation occurred when the oxidation was accomplished at 800-900°C. The magnitude of the growth stresses depends on the thickness of the formed scale. During a continuous oxidation of a metal this may give rise to a discontinuous reaction behaviour. A well-known example is the work of Pilling and Bedworth[61] on the oxidation of copper at 500°C. They found a series of discontinuities in the weight gain - time curve (see fig. 2.12). Each time the film reaches a certain thickness fracture of the film occurs permitting a renewed direct acces of the oxygen to the substrate. At 800°C a continuous oxidation behaviour was observed, due to the enhanced plasticity at higher temperatures.

A last important aspect concerns the vacancy injection at the scale/metal interface. When an oxide scale is formed by outward diffusion of the cations this flux is accompanied by a counter flow of vacancies through the scale. The vacancies eventually coalesce to cavities at the scale/metal interface. If an oxide is plastic, it will flow over each cavity. However, at relatively low temperatures this will not be the case. It is obvious that the scale adherence will

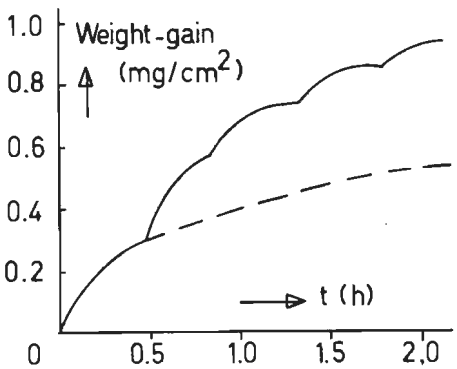

Fig. 2.12. The growth of an oxide scale on copper at 500°C (after Pilling and Bedworth[61]).

deteriorate by this effect. Dunnington et al.[69] found that cavities were formed at the scale/metal interface during oxidation of Fe. A similar observation was done by Mackenzie and Birchenall[70].

Up to now we have only discussed the influence of growth stresses on the formation of oxide scales. This is a consequence of the fact that this subject has been extensively studied for this reaction type only. This, of course, does not mean that no stress generation occurs during reactions other than oxidation. For example, Price[71] observed a curling of a Fe strip which had been galvanized at one side only. Unfortunately, he does not mention whether the reaction layer is present at the convex or concave side of the curled strips. Also observations in metal silicide films produced by interdiffusion strongly suggest the acting of stresses in these films[72][73]. However, as appears from the following example, the volume conservation model of Pilling and Bedworth is not valid in these cases. Suppose we have an Fe-Zn diffusion couple in which a δ-$FeZn_{10}$ layer is formed. Zn is practically the only diffusing component through the reaction layer[74], hence the δ-$FeZn_{10}$ layer is formed at the Fe/reaction layer interface. So far this situation is completely analogous to the formation of an oxide layer by means of inward oxygen diffusion, and the PBR value for this compound can be calculated. With a molar volume of 97.86[75] and 7.11 mol/cm^3 for the δ-$FeZn_{10}$ compound and Fe substrate respectively this gives:

$$\text{PBR } (Fe/FeZn_{10}) = \frac{1}{1}\frac{\bar{v}_{FeZn_{10}}}{\bar{v}_{Fe}} = \frac{1}{1}\frac{97.86}{7.11} = 13.76.$$

Compared with the values of the oxides as given in reference[62] this magnitude of volume change is very high; it does in fact imply that the reaction layer crumbles off the substrate. However, in practice this does not happen, suggesting that the actual stresses for these cases are much less than those predicted by the Pilling-Bedworth model.

CHAPTER III

THE PHASE DIAGRAMS

3.1 The binary phase diagrams

In this paragraph only the binary Fe-Zn phase diagram will be discussed. For the other binary phase diagrams Fe-Al [76], Fe-Si [76], Zn-Si [78] and Zn-Al [77] the reader is refered to the resp. diagrams in fig. 3.1 a-d, which are from the quoted literature.

The first systematic investigation into the Fe-Zn system was done by J. Schramm [75] [79] [80] in the years 1936-1938. Apart from some alterations in the α- and γ-Fe phase fields [81] and the discovery of the new phase Γ_1 [5], the main outlines of the diagram as given by Schramm remained unchanged. These changes are incorporated in the diagram of fig. 3.2, which is taken from O. Kubaschewski [76].

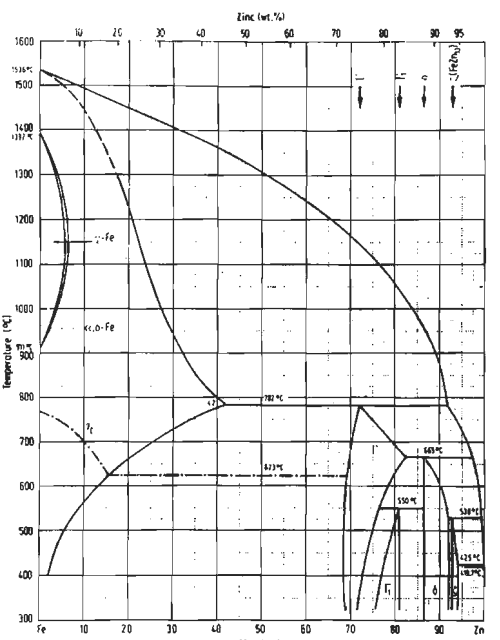

Fig. 3.2. Phase diagram of the Fe-Zn system (after O. Kubaschewski [76])

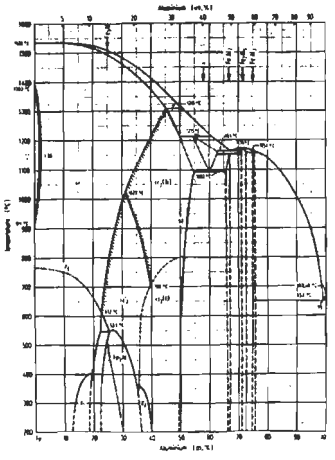

(a)

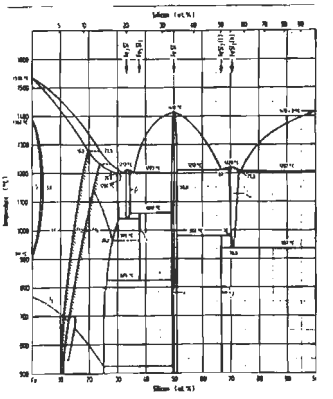

(b)

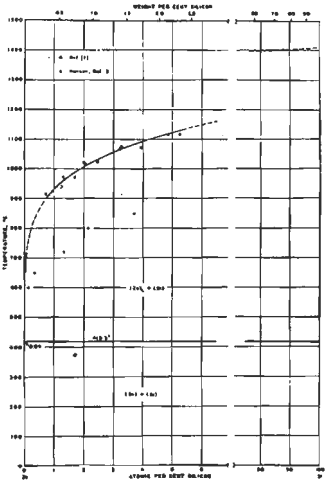

(c)

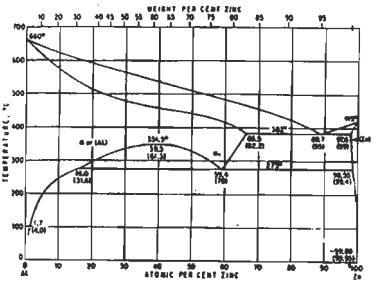

(d)

Fig. 3.1a-d, Binary phase diagrams of the systems:

a) Fe-Al (after O. Kubaschewski[76])

b) Fe-Si (after O. Kubaschewski[76])

c) Zn-Si (after R.P. Eliott[78])

d) Zn-Al (after Hansen and Anderko[77])

A few peculiarities of the various phases in this phase diagram in relation to their appearance in Fe-Zn diffusion couples will be mentioned now:

- The peritectic melting point of the ζ phase is 530°C. But, as we have seen in section 1.3, this phase does not form a closed layer in a diffusion couple above 495°C and is not observed above 505°C. The explanation of this is not clear yet.
- The solubility of zinc in iron varies between 4 and 9 at% resp. at 400°C and 500°C. Recently, however, Ferrier[82] found that this region of solid solubility is much smaller viz. $\sim$ 1 at% and 5 at% Zn at the above mentioned temperatures.
- The δ layer formed in an Fe-Zn diffusion couple consists of two parts with different morphologies. The iron-rich part (with a compact appearance) is called δ_c and the zinc-rich part (with a columnar appearance) is called δ_p. They are, however, no two distinct phases as has been reported in literature[83]. X-ray analysis on single crystals of the δ phase carried out by Bastin et al.[84] proved clearly that it is only one phase.

3.2 The ternary phase diagrams

A first systematic investigation covering the whole Fe-Zn-Al system was done by W. Köster and T. Gödecke[85] by means of metallographic observations and thermal- and X-ray analysis on alloys.

The findings of Köster and Gödecke were largely confirmed by M. Urednicek and J.S. Kirkaldy[86]. The latter authors investigated the Fe-Zn-Al system at 450°C by means of microprobe analysis and metallographic observations on alloys and solid-liquid diffusion couples of the types: FeAl, $FeAl_2$, Fe_2Al_5 and $FeAl_3$ against Zn. The diagrams in fig. 3.3a-b were composed with the help of the data, as determined by the above mentioned authors. The Fe-rich corner of the diagram has only a qualitative character since it omits the complications which arise from the order-disorder reaction in the Fe-rich phase[87].

The Fe-Zn-Si system was also investigated by W. Köster and T. Gödecke[88], again by thermal- and X-ray analysis and metallographic observations. The diagram in fig. 3.4 has been composed with the help of the data, as determined by these authors.

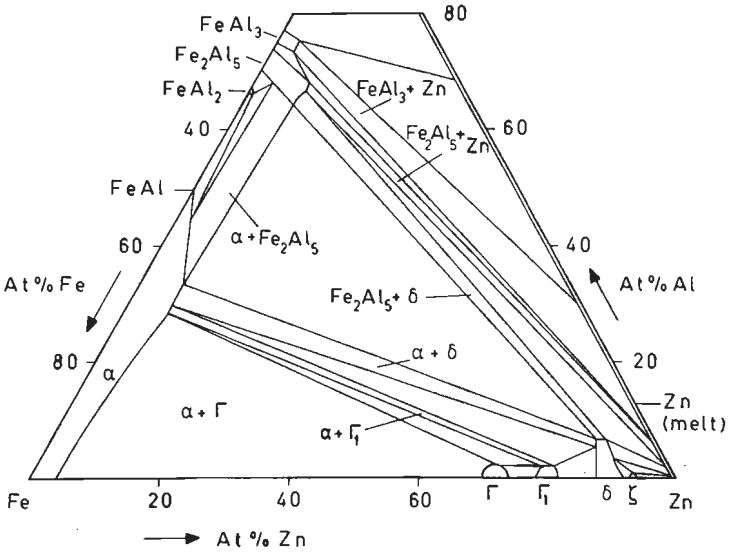

Fig. 3.3a. Isothermal section of the Fe-Zn-Al phase diagram at 450°C (after Köster et al.[85] and Urednicek et al.[86]).

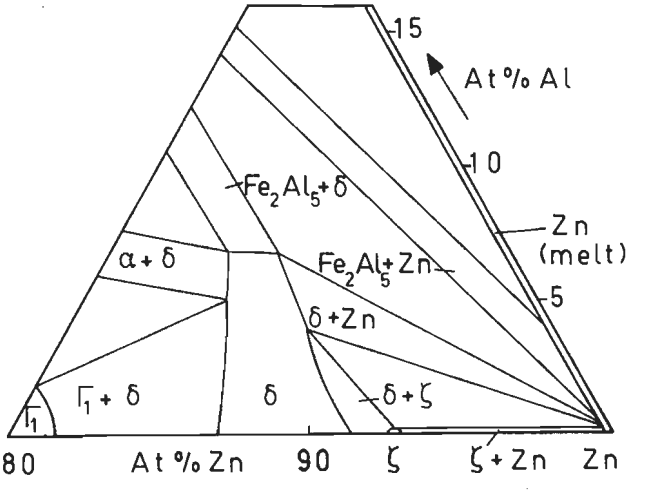

Fig. 3.3b. Zinc-rich corner of the diagram in fig. 3.3a.

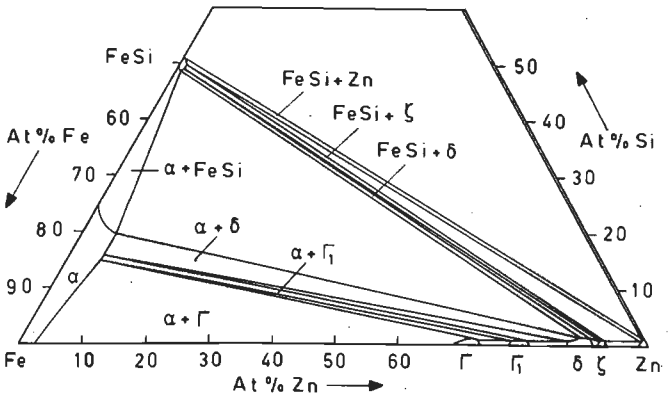

Fig. 3.4. Isothermal section of the Fe-Zn-Si phase diagram at 395°C (after Köster and Gödecke[88]).

When we compare both diagrams in figs. 3.3 and 3.4, then they seem to be very similar at first glance. But there are some striking differences, which have been pointed out in Table 3.1.

Fe-Zn-Al system	Fe-Zn-Si system
- Great solubility of Zn in the binary Fe-Al compounds Fe_2Al_5 and $FeAl_3$ viz. resp. 7.4 at% and 3.6 at%.	- Small solubility of Zn in the binary Fe-Si compound FeSi viz. < 1 at%.
- Great solubility of Al in the δ, Fe-Zn phase viz. 7 at%.	- Small solubility of Si in the δ, Fe-Zn phase viz. < 1 at%.
- No equilibrium exists between the ζ, Fe-Zn phase and the binary Fe-Al compounds (This is a consequence of the previous point, because the δ phase field acts as a "shield" for the ζ phase.	- Equilibrium between the ζ, Fe-Zn phase and FeSi.

Table 3.1. Differences between the ternary phase systems of Fe-Zn-Al and Fe-Zn-Si at 400-500°C.

CHAPTER IV

EXPERIMENTAL METHODS

4.1 The origin and purity of the used metals

In table 4.1 the different metals used during this investigation are listed according to their origin and purity.

Fe I was used in diffusion couples with pure iron as a terminal metal. A typical analysis of this metal showed that it contained less then 1 ppm Si.

Fe II together with the Al and Si were used to prepare resp. Fe-Al and Fe-Si terminal alloys for the various diffusion couples.

Zn I was used as a melt in solid-liquid diffusion couples, while Zn II was used in solid-solid diffusion couples.

Metal	Supplier	Purity (wt%)
Fe I	Goodfellow Metals (U.K.)	99.99
II	Highways International (U.K.)	99.5
Zn I	Budelco B.V. (Holland)	99.99
II	Koch Light Lab. (U.K.)	99.99
Al	Koch Light Lab. (U.K.)	99.99
Si	Hoboken (Belgium)	99.99

Table 4.1. Origin and purity of metals used in this investigation.

4.2 Preparation of the alloys and diffusion couples

Zinc-free alloys were prepared by repeated melting in an argon-arc furnace. The resulting "buttons" were remelted in the same furnace in a mould to obtain a bar of approximately 10 mm diameter. Alloys containing Zn could not be prepared in this way because of the high vapor pressure of Zn, even at low temperatures. Hence these alloys were prepared by annealing the weighed mixtures in an evacuated silica capsule. Because Al-Zn melts react with the silica, these mixtures were contained in small Al_2O_3 crucibles before sealing in the evacu-

ated silica capsules.

All alloys which were used as terminal alloys in diffusion couples were sawn in ≈ 2 mm thick slices by means of an 0.1 mm thick carborundum saw blade. Before the preparation of the diffusion couples the slices were ground and polished (see section 4.3). In the case of solid-liquid diffusion couples the slices were dry-fluxed after the grinding and polishing treatment. This dry-fluxing treatment consists of the following steps:

1) Degreasing in aceton
2) pickling in 6N HCl during 5 min. at room temperature
3) fluxing in a solution of 1M NH_4Cl and $ZnCl_2$ (1:1) at 80°C during 10 min.
4) drying in a furnace at 150°C during 15 min.

After the fluxing treatment the alloys were immediately dipped in the melt which was contained in a graphite crucible. Before dipping, the surface of the melt in the bath was cleaned by removing the slags with a spoon. The content of the bath was ≈ 100 cm^3. The zinc bath was always saturated with iron. In order to avoid contamination with Al, baths were used only once. Hence every slice was dipped in a fresh bath.

To prepare the solid-solid diffusion couples five methods were used, and these will be discussed now:

a) screw clamp

The clamp consists of two discs between which the couple halves can be pressed by means of three screws (see fig. 4.1).

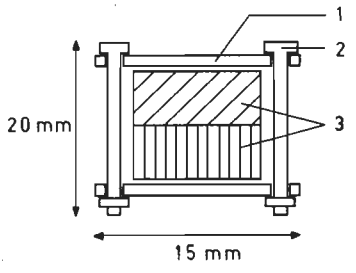

1) stainless steel discs
2) screw
3) couple halves

Fig. 4.1. Screw clamp, used for the preparation of diffusion couples.

The whole was sealed in an evacuated silica capsule and annealed. This method yielded good results, but had some disadvantages viz.:

- The load on the couple halves, which is applied by means of the screws, is not reproducible.
- The load applied with the screws may be nullified because of a relaxation process during the annealing period.
- The method is unsuitable for couples in which one of the terminal alloys is very brittle, because it will break to pieces.

b) Vacuum furnace.

By this method[39] it is possible to apply a controlled external load on the couple halves, which are annealed in vacuo. When Zn was one of the couple halves special measures had to be taken to avoid condensation of Zn vapour on the heating elements of the furnace. This was established by placing the couple in a specially designed cover (see fig. 4.2).

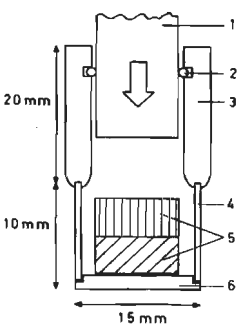

1) pressure bar
2) "O" ring
3) glass cylinder
4) molybdenum cylinder
5) couple halves
6) lid

Fig. 4.2. Cover, used in couple preparation method b), to avoid Zn condensation on heating elements of furnace.

c) This is an improved version of the screw clamp. The pressure is adjusted with a spring, which is outside the hot part of the furnace (see fig. 4.3). Advantages are:

- The pressure is controllable by means of the spring.
- No relaxation of the applied load can occur.

The tube was placed in a tube furnace and annealed under a hydrogen flow. These three methods were used throughout this investigation and no significant differences in diffusion behaviour were observed for the different methodes.

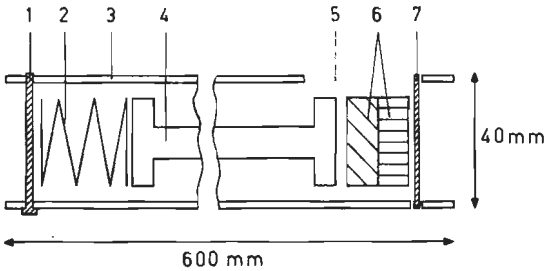

Fig. 4.3. Tube clamp, used for the preparation of diffusion couples.

For some experiments it was necessary to avoid the external load which is used in the methods mentioned above. Two methods have been applied viz.:

d) Vapour metallising.
   In this technique the couple is prepared by evaporating the Zn on the other couple halve. This was done in an evacuated chamber. The Zn which had to be evaporated was heated by means of a H.F. generator. The prepared couple was sealed in an evacuated silica capsule and annealed.

e) Welding by means of an arc furnace.
   In this technique both couple halves are welded together by means of a high electric current. This method yields problems if Zn is one of the couple halves, because of its low melting point. By applying this technique very carefully, i.e. increasing the electric current very slowly, this difficulty was overcome. Also here the couples were annealed in evacuated silica capsules.

No difference in diffusion behaviour was observed for these two other methods.

4.3 Heat treatment and metallographic preparation of the diffusion couples

The solid-solid diffusion couples were annealed in a horizontal tube furnace. The temperature was measured with a calibrated

Pt-Pt(10% Rh) thermocouple with an accuracy of $\pm$ 2°C. In the case of solid-liquid diffusion couples the bath containing the melt was heated in a vertical furnace. The temperature of the melt was continuously measured with a calibrated Pt-Pt (10% Rh) thermocouple dipped in the melt.

After the heat treatment the diffusion couples were embedded in a resin (Struers). To the resin copper powder was added in a weight ratio of 1:1 in order to make the resin conductible. The embedded couple was then ground on SiC paper up to 600 Grit and polished with 3 µm diamond paste on a nylon cloth during 5 min. Finally they were polished with 0.05 µm CeO_2 on a soft cloth during 2 min.

In most cases etching was carried out by dipping in a 3% Nital (HNO_3 in alcohol) solution for about 10s. In some couples, in which an aggregate zone of the δ- and ζ-(Fe-Zn) phases developed, etching with the Nital solution yielded no good results, because no clear distinction was visible between these two phases. In these cases a reagent developed by Schramm [79] [89] was applied successfully. The composition of this reagent is given in table 4.2. The action of this reagent is based on a preferential precipitation of Cu on the ζ crystals of the reaction layer. The colour of this precipate is reddish. To obtain a more contrast-rich image, the Cu deposit is blackened by dipping the specimen in a solution of picric acid (1 cm^3 of a 1% alcoholic picric acid solution in 100 cm^3 water). The use of this reagent yielded only good results if the couples were embedded in a pure (i.e. no copper containing) resin and the polish treatment with CeO_2 was omitted. After the metallographic treatment the couples were ready for microscopic examination.

4.4 Methods of investigation

4.4.1 Optical microscopy

With this technique information was obtained about the number of phases, morphology and layer thickness of a reaction layer. Photomicrographs were taken at appropriate magnifications.

4.4.2 Electron Probe Micro-Analysis (EPMA)

With EPMA the distribution of the elements in a reaction layer can be measured. Throughout this investigation a Jeol Superprobe 733 was used equipped with three wave-length dispersive spectrometers.

Solution I	Solution II
900 cm^3 water	1000 cm^3 water
122 g KOH	25 g kalium tartrate
60 cm^3 saturated solution of $Cu(NO_3)_2$	50 cm^3 concentrated ammonia
75 g KCN	50 g $Al(NO_3)_3$
6.5 g citric acid	

Solutions I and II are mixed in a volume ratio of 1:10.

Table 4.2. Composition of Schramm's reagent.

In most cases the operating conditions correspond with an accelerating voltage of 20 kV and an beam current of 30 nano-amperes. The used crystals in the spectrometers were:
- TAP for the Si-Kα and Al-Kα radiation
- LiF for the Fe-Kα and Zn-Kα radiation.

The pure elements were used as standard.
When measuring phase equilibrium concentrations near phase interfaces, the probe spot was always located not closer than 3 μm from the phase interface to exclude overlap.
The measured intensities were converted into concentrations with the use of an on-line ZAF correction program. The accuracy of the measurements was about 0.1-0.5 at % depending on the measured absolute concentrations. With the Jeol Superprobe 733 also secondary electron images (SEI) and backscattered electron images (BEI) of the sample surface could be obtained.

4.4.3 X-ray diffraction

This technique was used together with the EPMA analysis to identify the various phases in a diffusion couple. The phases found in a diffusion couple could be exposed by grinding the couple parallel to the contact surface. A Philips PW1010 diffractometer was used. Operating conditions were:
Co-Kα radiation with an Fe filter, accelerating voltage 36 kV and a current of 20 mA.

CHAPTER V

RESULTS

5.1 The Fe-Zn-Al system

5.1.1 Introduction

As mentioned in chapter I the addition of Al to the zinc bath during hot-dip galvanizing of Fe results in the formation of an aluminium-rich layer on the iron substrate. In the beginning of the process a closed layer will be formed. However, because the supply of Al is limited by diffusion, a depletion of this component will occur in the vicinity of the surface of the specimen. As a result the layer disintegrates and looses its inhibiting influence. For several reasons we decided to study the role of Al in the process of hot-dip galvanizing by means of dipping Fe(Al) alloys in a zinc bath (iron saturated, but without an addition of Al). These reasons are:

- It was expected that a depletion of Al in a solid Fe(Al) alloy would not occur so fast compared with a melt.
- By using solid Fe(Al) alloys the Al source is better defined.
- The phase relations of the Fe-Zn-Al system can be studied better in this way. These phase relations are crucial in studying the role of Al during hot-dip galvanizing.

All specimens were dipped at ordinary galvanizing temperatures (450°C). The Al concentration range of the investigated alloys is within the solid solubility region of Al in Fe. The reaction behaviour of three alloys, containing resp. 10.0, 22.8, 47.6 at% Al was studied. For convenience we will use the resp. notations Fe_9Al, Fe_3Al and FeAl.

5.1.2 The reaction between Fe_9Al and Zn(Fe)

Figs. 5.1a-d give a review of the observed reaction layers during dipping these alloys for various times. The total reaction layer consists in all cases of (going from the Fe_9Al alloy to Zn): Γ, Γ_1, δ and ζ; the same intermetallic compounds which appear during hot-dip galvanizing of pure Fe. The ζ layer and the (liquid) zinc, with which it is in contact, deserve special attention. At a dipping time of 30s Zn is present between the ζ grains and is also in contact with the δ phase. For longer dipping times (5 and 15 min.) the Zn is still present between the ζ grains, but it is no longer in contact

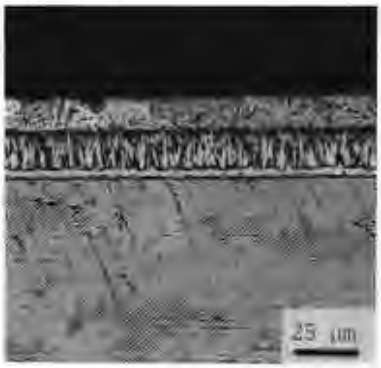

a) 30 s

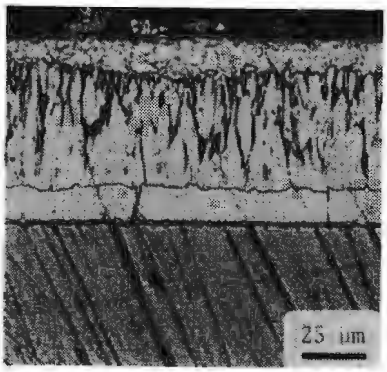

b) 5 min

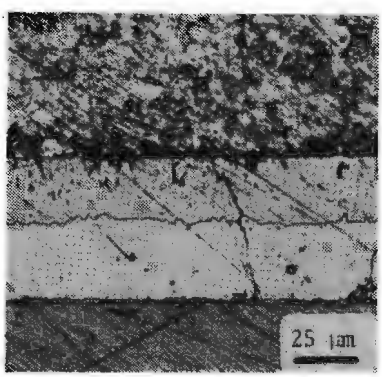

c) 15 min

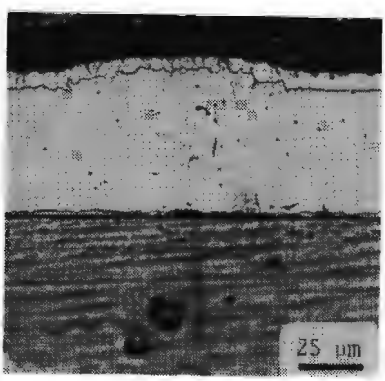

d) 1 h

Fig. 5.1a-d, Fe_9Al-Zn(Fe) couples for various dipping times. The layer sequence in the couples is (from below upwards):

a) $Fe_9Al/\Gamma/\Gamma_1/\delta/\zeta$+Zn/Zn

b,c) $Fe_9Al/\Gamma/\Gamma_1/\delta/\zeta/\zeta$+Zn/Zn

d) $Fe_9Al/\Gamma/\Gamma_1/\delta/\zeta$/Zn

with the δ phase. Finally for dipping times exceeding 1h a compact ζ layer is observed.

The ratio between the ζ and δ layer widths totally changes with increasing dipping times viz.:

$$\frac{\text{width } \zeta}{\text{width } \delta} = 9.0 \text{ at } 30s\,; \quad \frac{\text{width } \zeta}{\text{width } \delta} = 0.12 \text{ at } 1h.$$

The growth curves of the total reaction layer and ζ layer are drawn in fig. 5.2. We see that after a dipping time of 5 min. ($\sqrt{t}$=2.2) the width of the ζ layer decreases, until after 1h ($\sqrt{t}$=7.7) it starts to grow again at a very low rate. The plateau in the growth curve has also been observed for the other Fe(Al)-Zn(Fe) couples (see fig. 5.7 and 5.11) and also occurs for binary Fe-Zn couples[74].

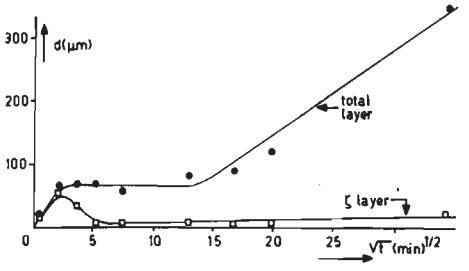

Fig. 5.2. Total layer width and width of the ζ layer vs. root of the diffusion time in Fe_9Al-Zn(Fe) couples.

Fig. 5.3 gives a measured Al concentration profile through the reaction layer of a couple dipped for 19 h. Note the difference in Al composition for the two δ sublayers δ_c and δ_p.

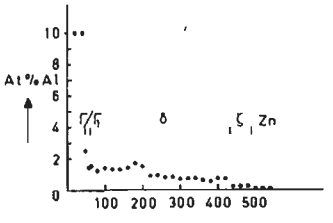

Fig. 5.3. Penetration curve for Al in an Fe_9Al-Zn diffusion couple, dipped for 19h at 450°C.

Fig. 5.4 gives the diffusion path of this couple on the zinc-rich corner of the 450°C isotherm of the Fe-Zn-Al system. The path through the Γ and Γ_1 regions has only a qualitative character. A discrepancy exists between our findings on the solubility of Zn in the Fe_9Al alloy and the values as determined by Köster and Gödecke[85]. The value of 0.5 at% measured in our diffusion couple was considerably lower than the 7.0 at% predicted by their phase diagram. This is also the case for the other Fe(Al) alloys. Though

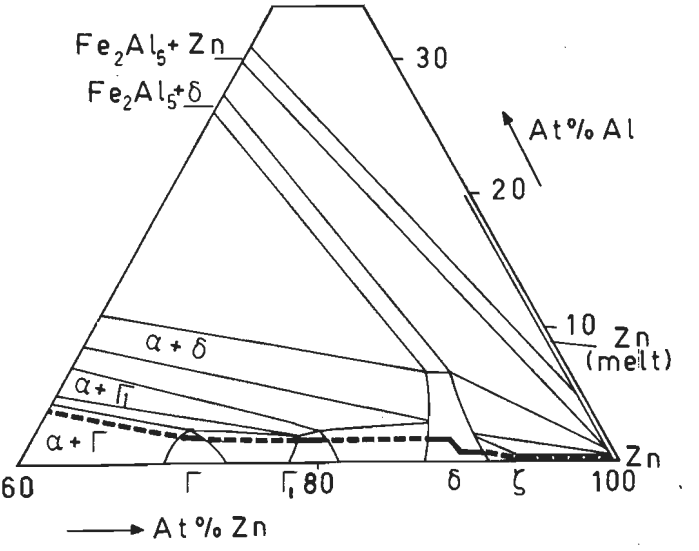

Fig. 5.4. Diffusion path of an Fe_9Al-Zn(Fe) diffusion couple, 19h, 450°C on the zinc-rich corner of the 450°C isotherm of the Fe-Zn-Al system.

the value of Köster et al. was determined at 500°C, this temperature difference can never explain the large difference in solubility. An explanation may be a very low diffusion rate of Zn in these alloys. As a consequence this high solubility of Zn is only reached in a very small region near the Fe(Al)/reaction layer phase boundary, which can not be measured by means of microprobe analysis.

5.1.3 The reaction between Fe_3Al and Zn(Fe)

Figs. 5.5a-d give a review of the observed reaction layers for these alloys at various dipping times. The Γ and Γ_1 layers are absent and only the δ and ζ phases are found. A remarkable difference in the reaction behaviour between this alloy and the Fe_9Al alloy can be seen in the morphology of the ζ phase: in this case no closed ζ layer is formed. The Zn remains between the ζ grains, but it also remains in contact with the δ phase during all dipping times. For all dipping times the ζ phase (together with the Zn) takes up the largest part of the total reaction layer.

Table 5.1 gives a summary of microprobe measurements at relevant

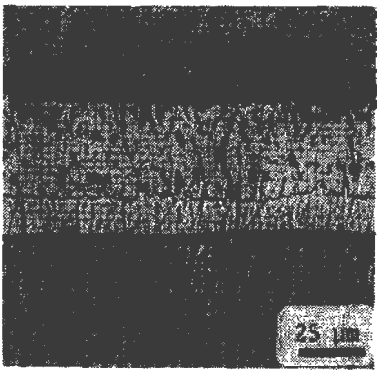

a) 5 min

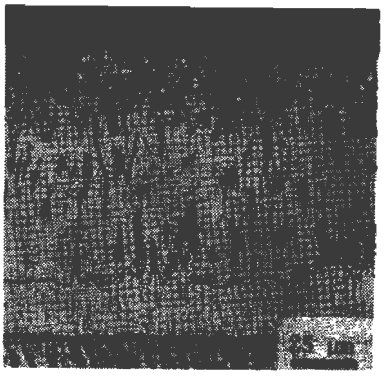

b) 15 min

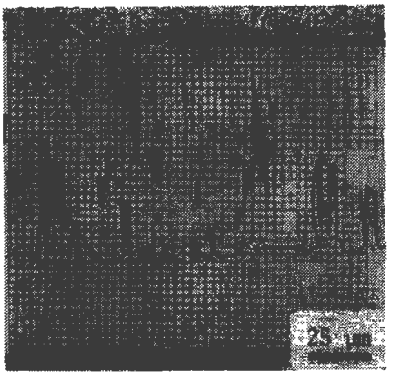

c) 1 h

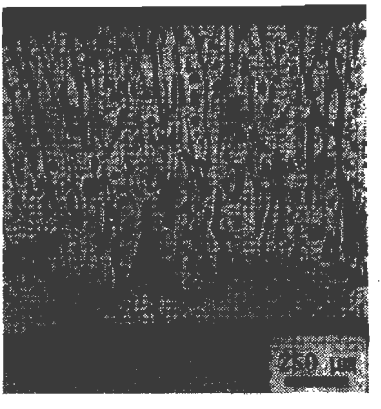

d) 21 h

Fig. 5.5a-d, Fe_3Al-Zn(Fe) couples for various dipping times.
The layer sequence in all couples is (from below upwards):
$Fe_3Al/\delta/\zeta$+Zn/Zn

No.	Phase examined	Composition (at%)		
		Al	Fe	Zn
1	Bulk Fe_3Al phase	22.8	77.2	0.0
2	Fe_3Al phase at interface with δ phase	21.7	77.8	0.5
3	δ phase at interface with Fe_3Al	3.0	10.9	86.1
4	δ phase at three-phase interface $\delta/\zeta/Zn$	2.0	8.6	89.5
5	ζ phase at three-phase interface $\delta/\zeta/Zn$	0.8	7.5	91.7
6	Zn phase at three-phase interface $\delta/\zeta/Zn$	0.0	0.8	99.2
7	ζ phase in middle two-phase ζ + Zn layer	0.5	6.9	92.5
8	Zn phase in middle two-phase ζ + Zn layer	0.1	1.1	98.9
9	ζ phase at end of two-phase ζ + Zn layer	0.0	7.0	93.0
10	Zn phase at end of two-phase ζ + Zn layer	0.0	0.4	99.6

Table 5.1. EPMA results of an Fe3Al-Zn(Fe) couple dipped for 21h.

points in the reaction layer of a couple dipped for 21h. The measured solubility of Al in the δ phase in equilibrium with the Fe_3Al alloy and the ζ phase (measurements 3 and 4 in table 5.1) are somewhat lower than predicted by the phase diagram in fig. 3.3. For the rest our measurements agree well with this diagram.
Fig. 5.6. gives the corresponding diffusion path on the zinc-rich corner of the 450°C isotherm of the Fe-Zn-Al system.

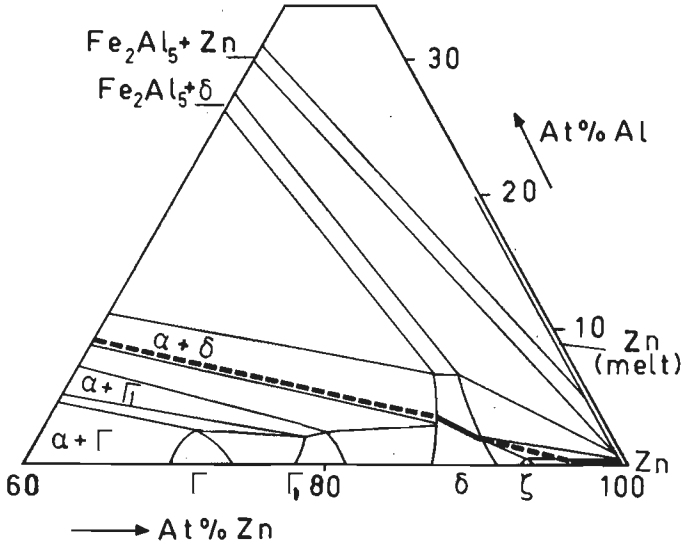

Fig. 5.6. Diffusion path of an Fe_3Al-Zn diffusion couple, 21h, 450°C on the zinc-rich corner of the 450°C isothermal section of the Fe-Zn-Al system.

The growth curve has been drawn in fig. 5.7.

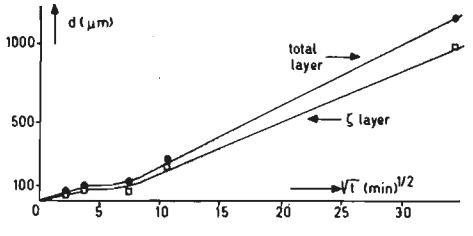

Fig. 5.7. Total layer width and width of the ζ layer vs. root of the diffusion time in Fe_3Al-Zn(Fe) couples.

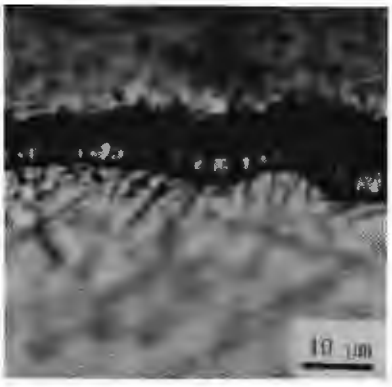

a) 30 s

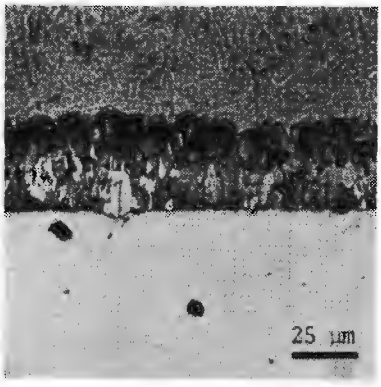

b) 5 min

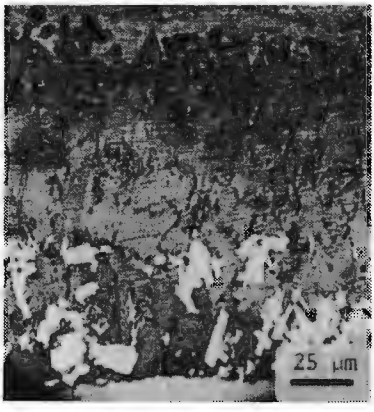

c) 1 h

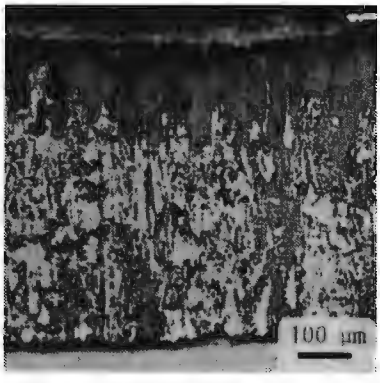

d) 19 h

Fig. 5.8a-d, FeAl-Zn(Fe) couples for various dipping times.
The layer sequence in the couples is (from below upwards):
a) FeAl/δ(white)/ζ(black)/Zn
b,c,d) FeAl/δ(white)+ζ(black)+Zn/Zn

5.1.4 The reaction between FeAl and Zn(Fe)

A review of the observed reaction layers formed at various dipping times is given in the figs. 5.8a-d. All reaction layers have been etched with Schramm's etchant. The dark and light areas correspond with the ζ and δ phases respectively. At a dipping time of 30s we can distinguish a δ layer and a layer of small ζ crystallites. For longer dipping times (≥ 5 min.) the δ layer is broken up and the whole reaction layer consists mainly of the ζ phase with some isolated δ areas. The amount of δ increases with time, but never a closed δ layer is formed. After a dipping time of 30 min. and longer an Al-rich layer is visible at the substrate. (see figs. 5.9a-b).

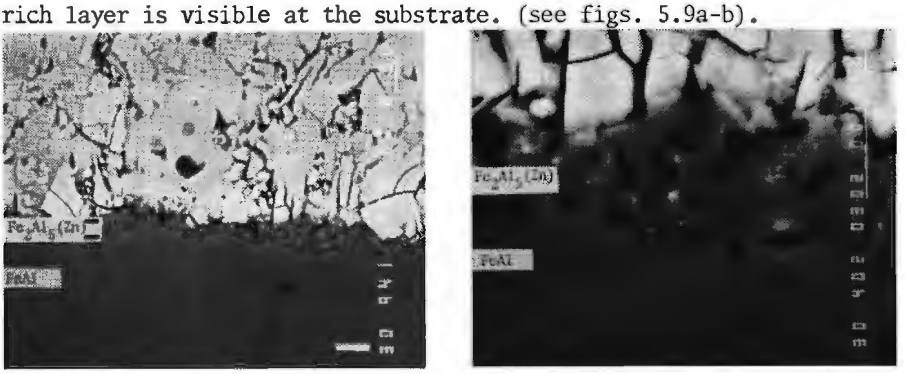

Fig. 5.9.
a. $Fe_2Al_5(Zn)$ layer formed in FeAl-Zn(Fe) diffusion couple, 5h, 450°C, (BEI).
b. idem, magnification.
The white bar indicates in both cases 10 μm.

By means of microprobe analysis we could identify this layer as $Fe_2Al_5(Zn)$ with a composition of $Fe_{27.5}Al_{59.5}Zn_{13.0}$. This value was measured in the middle of a layer developed in a couple dipped for 74h. The layer was too thin in order to measure a concentration gradient through it. The measured Zn content of the $Fe_2Al_5(Zn)$ layer is considerably higher than the values found by Urednicek et al.[86] (see also fig. 3.3). Table 5.2 gives some other measured compositions at relevant points in the reaction layer of the couple dipped for 74h. In the reaction layer of these couples three-phase zones consisting of δ, ζ and Zn can clearly be seen. In principle, the occurrence of these zones in a ternary diffusion couple is not allowed. For this reason an exact diffusion path cannot be plotted on the isothermal section. Hence the path, as has been drawn in fig. 5.10, contains only the main

No.	Phase examined	Composition (at%)		
		Al	Fe	Zn
1	Bulk FeAl phase	47.6	52.4	0.0
2	FeAl phase at interface with Al-rich phase	47.2	52.5	0.3
3	Bulk Al-rich phase	59.5	27.5	13.0
4	δ phase at interface with Al-rich phase	3.1	8.4	88.5
5	ζ phase at interface with Al-rich phase[x)]	1.4	7.9	90.7
6	δ phase in middle of reaction layer	2.4	7.5	90.2
7	ζ phase in middle of reaction layer	1.3	7.2	91.5
8	Zn phase in middle of reaction layer	0.3	0.7	99.1
9	ζ phase at end of the reaction layer	0.8	7.0	92.2
10	Zn phase at end of the reaction layer	0.3	0.6	99.1

x) Thin layer between ζ phase and Al-rich phase (see also fig. 5.12).

Table 5.2. EPMA results of an FeAl-Zn(Fe) couple, dipped for 74h.

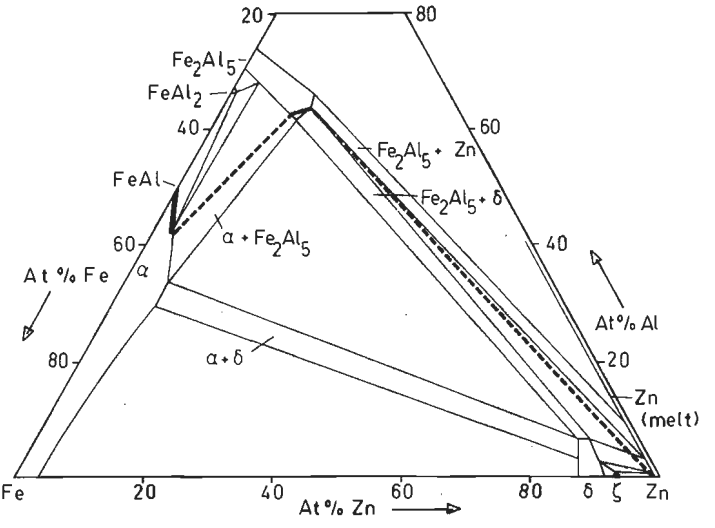

Fig. 5.10. Schematic course of the diffusion path of an FeAl-Zn(Fe) diffusion couple, dipped for 74h, on the 450°C isotherm of the Fe-Zn-Al system.

lines of the results of these couples and has only a qualitative character. The explanation for this presence of three-phase zones has to be found in a liquid penetration of the Zn between the δ and ζ grains.

Fig. 5.11 gives the growth curve of the total reaction layer formed in the FeAl-Zn(Fe) couples.

At first sight the layer sequence in these couples disagrees with the Fe-Zn-Al phase diagram because the ζ phase seems to be in equilibrium with the Fe_2Al_5(Zn). However, close examination of the ζ/Fe_2Al_5(Zn) interface reveals the occurrence of a thin layer between the ζ and the Fe_2Al_5(Zn) phase (see fig. 5.12). This thin layer is probably Zn which contains some aluminium. So the ζ and Fe_2Al_5(Zn) phases are never really in direct contact. Between the δ phase and the Fe_2Al_5(Zn) layer there always is an intimate contact as shown by the same figure.

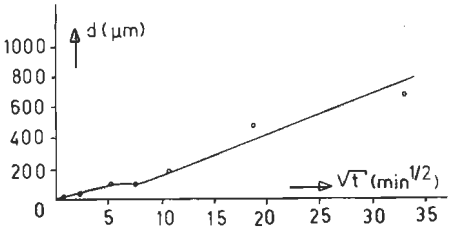

Fig. 5.11. Total layer width vs. root of the diffusion time in FeAl-Zn(Fe).

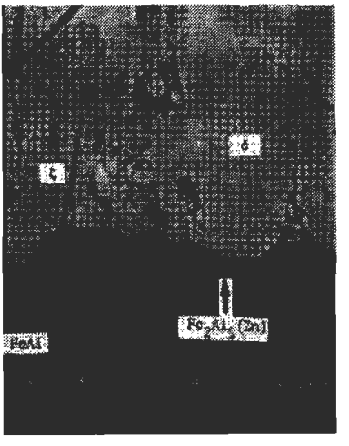

Fig. 5.12. FeAl-Zn(Fe) diffusion couple, 19h, 450°C, (BEI). Note the difference in contact between the Fe_2Al_5(Zn) layer and the δ and ζ grains respectively. (The white bar indicates 10 μm).

5.1.5 Comparison between the reaction behaviour of the different Fe(Al) alloys

In this section we will compare the reaction behaviour of the three Fe(Al) alloys. It will appear that the results of all alloys can be interpreted qualitatively on the basis of mass balance arguments.

On the 450°C isothermal section of the Fe-Zn-Al phase diagram we have drawn the straight lines connecting the Fe(Al) and the Zn(Fe) terminals (lines a, b and c resp. for the Fe_9Al, Fe_3Al and FeAl-Zn(Fe) couples, see fig. 5.13). Comparing the three lines we see that lines a and b intersect with at least one existence region of an Fe-Zn intermetallic compound, while line c does not intersect with any of these regions. This means that during the

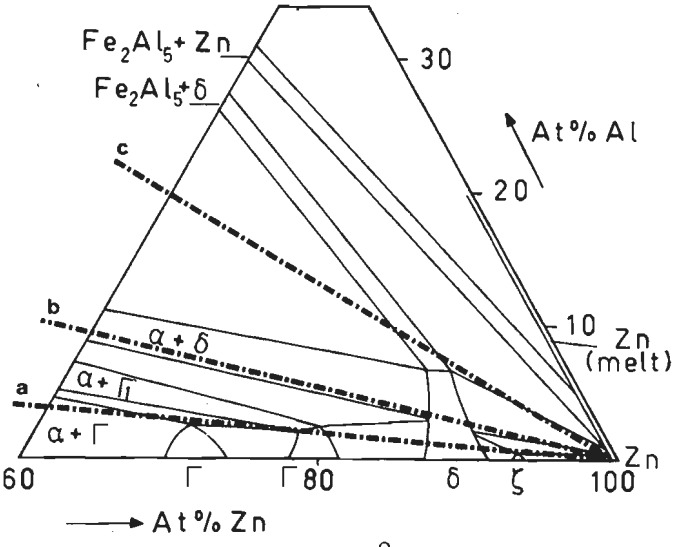

Fig. 5.13. Zinc-rich corner of the 450°C isotherm of the Fe-Zn-Al system. Lines a, b, c are the straight lines (mass balance lines) joining the terminal compositions of the Fe_9Al-, Fe_3Al- and FeAl-Zn(Fe) diffusion couples respectively.

reaction between FeAl and Zn(Fe) an Al-rich compound (i.e. a compound with more Al than the terminal FeAl alloy) must develop because of the mass balance. Also it follows from the position of line c, that besides the formation of an Al-rich compound, Fe-Zn intermetallic compounds have to develop. This indeed happens, as we have seen in the results of these couples. However, the layer morphology and sequence (i.e. the precise course of the diffusion path) cannot be predicted on the basis of these mass-balance arguments. In principle there are several possibilities. In order to predict the observed layer configuration in the FeAl-Zn(Fe) couple more diffusion and/or thermodynamic data have to be available. The formation of the Al-rich compound cannot, a priori, be excluded for the other investigated couples Fe_9Al- and Fe_3Al-Zn(Fe). However, from the positions of line a and b we can see that this does not need to happen, since an Al enrichment can now be fully accomodated by dissolving in the Fe-Zn intermetallic compounds. This possibility indeed happens as can be seen from the results of these couples.

Summarizing the results of the Fe(Al)-Zn(Fe) couples we can state the following general rule: During the reaction between Fe(Al) and Zn(Fe) Fe-Zn intermetallic compounds will develop, rather than an Al-rich compound if the liberated Al can be accomodated by dissolving in the Fe-Zn intermetallic compounds. If this is not possible an Al-rich compound will be formed during the reaction.

5.1.6 The Fe(Al)-Zn(Fe) results in relation to the inhibiting effect of Al additions to the galvanizing bath.

The purpose of the Al additions to the galvanizing bath was to inhibit the reaction between Fe and Zn by means of the formation of an Al-rich layer on the iron specimen. During the formation of this layer the attack of iron by zinc is negligible and no Fe-Zn intermetallic compounds are formed as has been shown e.g. by Urednicek et al.[32]. However, in our case of the reaction between Fe(Al) and Zn(Fe), the Fe-Zn compounds are formed immediately and no Al-rich layer, except for the case of the FeAl-Zn(Fe) couple, is observed. We will now discuss the difference between both reaction types. The diffusion path concept will be very useful in this consideration.

First let us consider the reaction between Fe and Zn(Al). Assume that the Zn is iron-saturated and that 1.2 at% Al has been added to the bath. In fig. 5.14 the composition of the melt is represented by A. (For this figure we have taken the values from Urednicek et al.[86]). When an Fe specimen is dipped into the melt with composition A, then according to the phase diagram the formation of several compounds is possible. Because the Fe_2Al_5 phase is thermodynamically more stable than the Fe-Zn intermetallic compounds[90] this phase will be formed. The Al necessary for the formation of this phase is supplied by the bath, and near the Fe substrate the bath will gradually become depleted in Al. So starting with point A the diffusion path will first go down to lower Al concentrations followed by a bend into the two-phase Fe_2Al_5-Zn region. If the supply of Al towards the Fe substrate can be maintained, then this path could be a stable one because it obeys the mass balance rule. However, in practice the supply of Al appears to be retarded after some time and a depletion in Al occurs in the melt near the dipped specimen. Hence point A will move downwards to lower Al concentrations. When the composition of the bath in the vicinity of the dipped specimen has

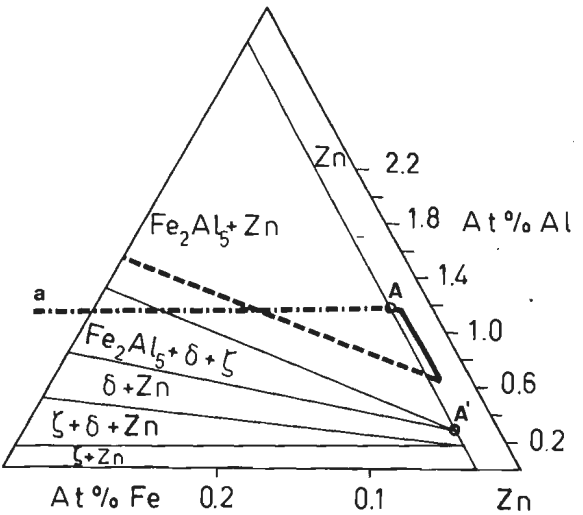

Fig. 5.14. Zn-rich corner of the 450°C isotherm of the Fe-Zn-Al system (after Urednicek et al.[86]) with schematic diffusion path and mass balance line (a) of a hypothetical diffusion couple Fe-Zn (1.2 at% Al), 450°C. (Note: the Fe and Al axes are not drawn to the same scale).

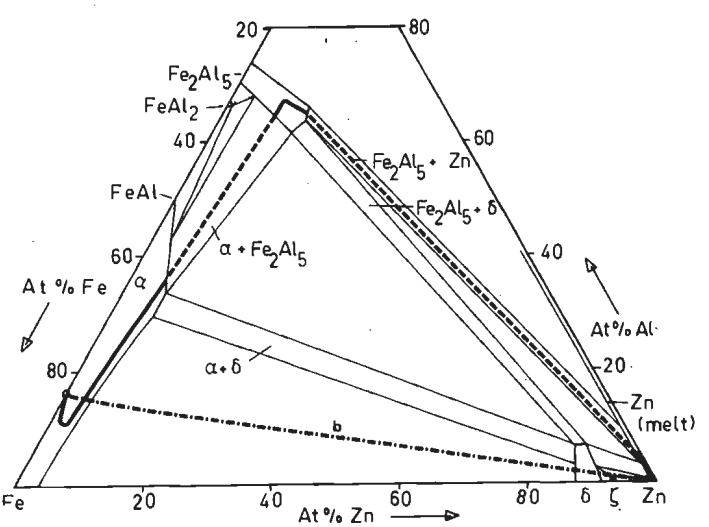

Fig. 5.15. Diffusion path of a hypothetical Fe(Al)-Zn(Fe) diffusion couple, dipped at 450°C, in which only an Fe_2Al_5(Zn) layer has developed. Line b is the mass balance line.

changed to A' the formation of the Fe-Zn intermetallic compounds cannot be avoided anymore according to the mass balance rule. The time during which the composition of the bath changes from A to A' is the incubation period, in which the formation of the Fe-Zn phases is inhibited.

Now let us consider our case viz. the dipping of a Fe(Al) alloy in an iron-saturated Zn bath. In the isothermal section of the Fe-Zn-Al system in fig. 5.15 we have plotted the diffusion path for a fictive Fe(Al)-Zn(Al) couple, in which only a Fe_2Al_5(Zn) layer is formed on the substrate. Seen from the terminal alloy which contains the Al, this path is comparable with the path of the Fe-Zn(Al) couple in fig. 5.14. Also the Fe-Zn intermetallic compounds do not need to form because this path intersects with the mass balance line (= line b in fig. 5.15).
The question is now: Why does the actual path, as determined for the Fe_9Al- and Fe_3Al-Zn couples, not follow this course. The answer to this question lies in the physical meaning of the fictive path in fig. 5.15. This path implies a large diffusion flux of Al (and Zn) through a wide region of the Fe(Al) alloy. This large Al diffusion flux is necessary to maintain the supply of Al for the formation of the Fe_2Al_5 layer. However, this large flux is not to be expected because of a low diffusion coefficient of Al in the Fe(Al) alloy at the reaction temperature. And this brings us to the ultimate difference between the Fe(Al)-Zn(Fe) and Fe-Zn(Al) reactions: In the case of the Fe-Zn(Al) reaction the mobility of Al in the Zn melt is large enough to, at least in the beginning of the reaction, maintain this necessary Al flux, while this is not possible for the Fe(Al)-Zn(Fe) reaction. If the formation of the Fe_2Al_5 layer is not to be expected on the Fe(Al) substrate in the case of the Fe(Al)-Zn(Fe) reaction, then the only possibility which remains according to the phase diagram is the formation of the Fe-Zn intermetallic compounds. This requires a large Zn diffusion flux through the formed Fe-Zn compounds, and this is certainly not an unrealistic assumption as shown by experiments in the pure Fe-Zn system. With marker experiments Onishi et al.[74] have shown that Zn was the only diffusing component in these couples. The formation of the Fe_2Al_5(Zn) layer in the FeAl-Zn(Fe) couple now simply arises from a relative Al enrichment of the FeAl substrate because the Fe of the FeAl alloy reacts with

Zn to form the Fe-Zn intermetallic compounds. So in fact the formation of the Fe_2Al_5 layer in a FeAl-Zn(Fe) and Fe-Zn(Al) couple is not directly comparable.

We may summarize the conclusions of this section as follows:

- In the case of the reaction between Fe and Zn(Al) the Fe_2Al_5 layer is formed in the beginning of the process, because this compound is thermodynamically more stable than the Fe-Zn intermetallic compounds. The necessary Al diffusion flux is possible because of the sufficiently high mobility of Al in the melt.
- In the case of the reaction between FeAl and Zn(Fe) the formation of the Fe_2Al_5 layer arises from a relative Al enrichment of the substrate.

5.2 The Fe-Zn-Si system at low Si concentrations

5.2.1 Introduction

As we have seen in the results obtained with the Fe(Al)-Zn(Fe) couples, diffusion couples in which one of the terminals is a melt may give rise to very complex reaction layer morphologies. When studying these reaction structures it is sometimes difficult to decide whether, for example, a two-phase zone is the result of a diffusion instability or of a penetration of the melt between the grains of the reaction layer. Because we wanted to study the instabilities which arise during the galvanizing of silicon-containing steel or iron from a viewpoint of solid-state ternary diffusion principles, it was necessary to avoid these confusing effects of liquid penetration. So we decided to study the influence of silicon in iron on the reaction between iron and zinc by means of solid Fe(Si) versus solid Zn diffusion couples. Of course this is a simplification of the industrial process of hot-dip galvanizing and not all aspects of this process can be studied in that way. However, because the reaction layers which develop during the galvanizing reaction are all solids at the galvanizing temperatures, diffusion through this layers occurs by solid-state diffusion. So we may expect a relationship between the results of solid-solid Fe(Si)-Zn couples and the results obtained during hot-dip galvanizing silicon-containing steel or iron.
In this part we will treat the results of the experiments with the Fe(0-6.3 at% Si)-Zn couples. The results of these experiments will be discussed in relation to the process of hot-dip galvanizing silicon-containing iron and steel. All Fe(Si)-Zn couples were annealed at 395°C, unless otherwise stated.

5.2.2 The results obtained with the Fe (0-6.3 at% Si)-Zn couples

Table 5.3 gives a review of the couples investigated with the observed layer sequences and morphologies. Photomicrographs of the reaction layers are given in fig. 5.16a-d. The layer sequence in the Fe(0.15 at% Si)-Zn and Fe(0.4 at% Si)-Zn diffusion couples is practically the same as found in binary pure Fe-Zn couples. The only difference is the little perturbation found at the δ/ζ interface. In the Fe(2.3 at% Si)-Zn couple the layer sequence has changed:

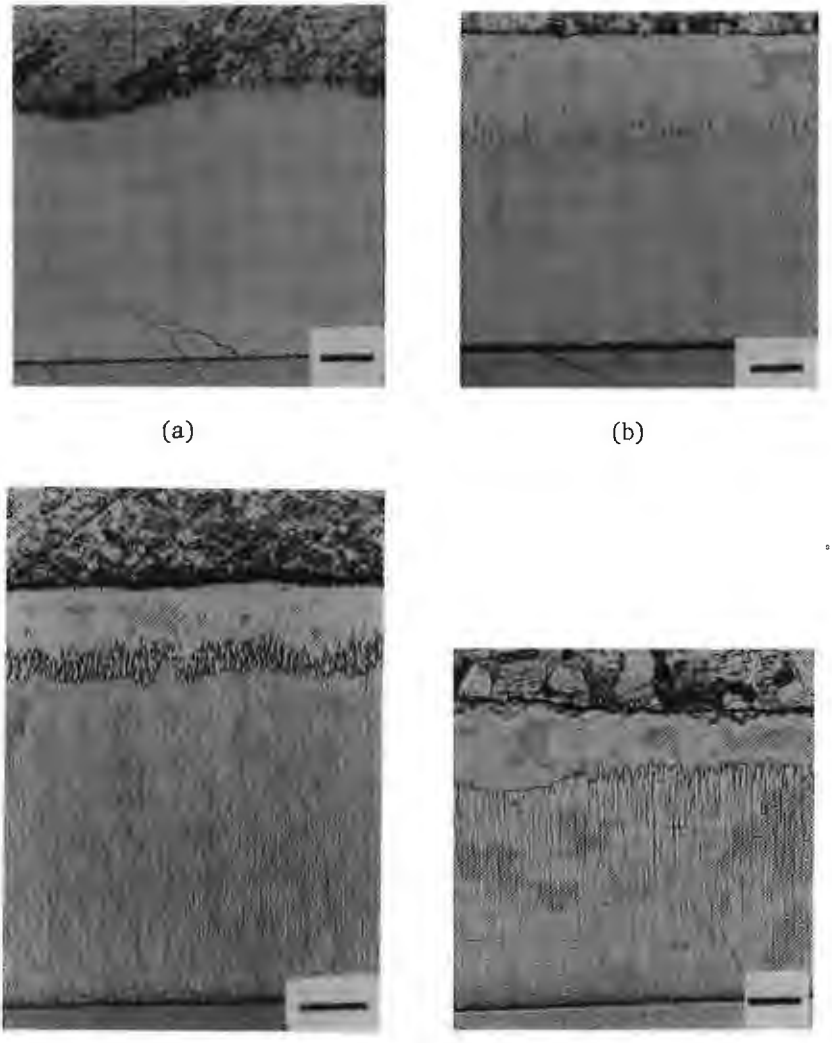

Fig. 5.16a-d, Fe(Si)-Zn diffusion couples. The layer sequences (from below upwards) and diffusion times are:

a) Fe(0.15at%Si)/Γ/Γ_1/δ/ζ/Zn, 20.5 h

b) Fe(0.4at%Si)/Γ/Γ_1/δ/ζ/Zn, 17h

c) Fe(2.3at%Si)/δ/δ+ζ/ζ/Zn, 16h

d) Fe(6.3at%Si)/δ/δ+ζ/ζ/Zn, 17h

The bar indicates in all cases 50 µm.

No.	Starting materials	Layer sequence	Morphology (mainly)
1	Fe(0.15%Si)-Zn	$\Gamma/\Gamma_1/\delta/\zeta$	planar boundaries except
2	Fe(0.4%Si)-Zn	$\Gamma/\Gamma_1/\delta/\zeta$	some perturbations at the δ/ζ boundary.
3	Fe(2.3%Si)-Zn	$\delta/\delta + \zeta/\zeta$	two phase transition
4	Fe(6.3%Si)-Zn	$\delta/\delta + \zeta/\zeta$	zone between δ and ζ.

Table 5.3. Diffusion couples investigated with observed layer sequence and morphology.

No Γ and Γ_1 layers are observed and a clear two-phase zone in which δ and ζ coexist has developed. Fig. 5.17 shows this zone at a higher magnification. The little black particles in the ζ layer were too small to be identified, but appeared to be silicon-rich. The particles were distributed randomly in the ζ layer. No preferential occurrence of the particles at, for example, grain boundaries was observed. In the δ layer of the Fe(2.3 at%Si)-Zn couple only the δp sublayer is

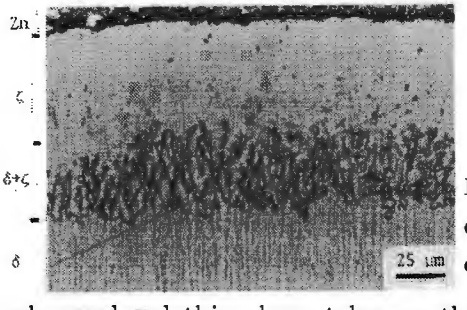

Fig. 5.17. Two-phase $\delta+\zeta$ zone observed in the Fe(2.3 at% Si)-Zn couple of fig. 5.16c.

observed and this phase takes up the main part of the total reaction layer width. The observations made in this couple are in good agreement with those of Ferrier et al.[29]. In the Fe(6.3at% Si)-Zn couple (fig. 51.6d) the results are the same as those found in the former couple, though the two-phase $\delta+\zeta$ zone is less pronounced.

Though the number of measurements is small, we can conclude from fig. 5.18 that all layers grow parabolically with time. As a reference results obtained with pure Fe-Zn couples are included in this figure. The two-phase $\delta+\zeta$ zone in the Fe(2.3at%Si)- and Fe(6.3at%Si)-Zn couples was observed at all annealing times. As fig. 5.19 indicates the width of the total reaction layers varies strongly with the

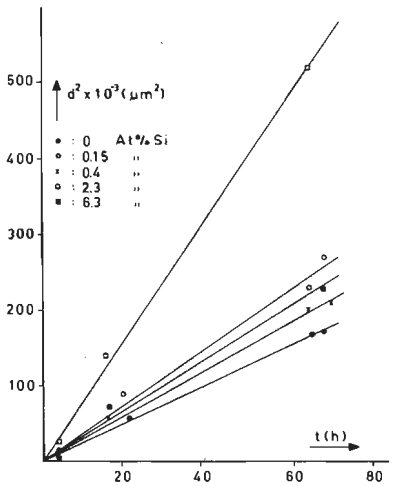

Fig. 5.18. Square of the total layer width vs. diffusion time in Fe(0-6.3at%Si)-Zn couples.

silicon content in the Fe(Si) alloys. In this figure the result of the Fe(9.0at%Si)-Zn couple is also included. This couple will be discussed in section 5.2.5. The maximum in the curve is reminiscent of the Sandelin effect (see fig. 1.5), though the peak is very widened.

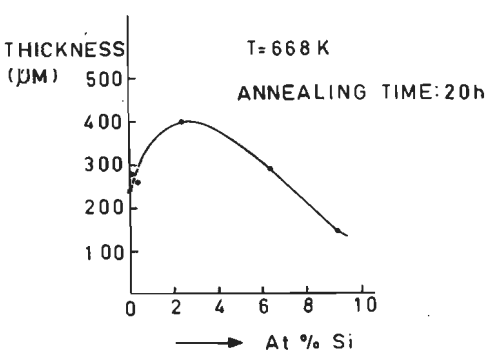

Fig. 5.19. Total reaction layer width in Fe(0.-6.3 at% Si)-Zn couples as a function of the silicon content in iron.

Because the reaction layer of the Fe(2.3at%Si)-Zn diffusion couple showed the most marked change compared with the layer found in a binary Fe-Zn couple, we concentrated the microprobe measurements on this couple. Table 5.4 gives a review of the microprobe-analyses

Phase examined	Composition (at%)		
	Fe	Zn	Si
Fe(2.3at%Si) alloy, bulk	97.7	0.0	2.3
Fe(2.3at%Si) alloy, interface with reaction layer	96.0	1.4	2.5
δ layer, interface with Fe(2.3at%Si) alloy	12.2	87.5	0.2
δ layer, middle	9.5	90.1	0.2
δ layer, in front of two-phase δ/ζ zone	8.7	91.0	0.2
δ phase of two-phase δ+ζ zone, δ side	8.8	90.1	0.4
ζ phase of two-phase δ+ζ zone, δ side	7.3	92.7	0.0
δ phase of two-phase δ+ζ zone, middle	8.7	90.2	0.6
ζ phase of two-phase δ+ζ zone, middle	7.8	92.2	0.0
δ phase of two-phase δ+ζ zone, ζ side	8.5	90.1	0.6
ζ phase of two-phase δ+ζ zone, ζ side	7.3	92.6	0.0
ζ layer, beyond of two-phase δ/ζ zone	7.3	92.6	0.0
ζ layer, middle	7.3	92.6	0.0
ζ layer, interface with Zn	7.4	92.6	0.0

Table 5.4. EPMA data of Fe(2.3 at% Si)-Zn couple, 16h, (see also fig. 5.16c).

data of this couple.
Like we experienced in the Fe(Al)-Zn(Fe) couples, the Zn solubility in the Fe(Si) alloy measured near the interface with the reaction layer does not agree with the one expected from the phase diagram in fig. 3.4. However, they fully confirm the findings of Ferrier[83] (see section 3.1). In the δ islands of the two-phase δ+ζ zone the Si content markedly increases. This effect is illustrated in fig. 5.20. The solubility of Si in the ζ phase is very small (< 0.1 at% Si) because hardly any silicon could be detected.

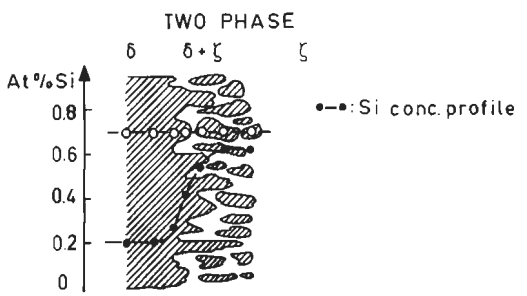

Fig. 5.20. Measured Si concentration profile through the δ phase of the two-phase δ+ζ zone of an Fe(2.3at%Si)-Zn couple (schematic drawing). The open dots represent the measured points in the two-phase zone.

5.2.3 Discussion of the results of the experiments with the Fe (0-6.3at% Si)-Zn couples on the basis of the mass balance rule

In this section we will verify whether the general rule we established for the Fe(Al)-Zn(Fe) couples in section 5.1.5 can also be applied to the reaction in the Fe(0-6.3at%Si)-Zn couples. To this end the maximum solubilities of Si in the Fe-Zn intermetallic compounds have to be known. Unfortunately these values are not exactly known. However, we can make a good estimate from the work of Köster and Gödecke[88] and our results. From the work of Köster and Gödecke we can deduce a solubility of Si in the δ phase of 0.4-1.0 at% at 395°C. This agrees very well with the value of 0.6 at% found by us in the δ islands of the two-phase δ+ζ zone in the Fe(2.3 at%Si)-Zn diffusion couple. So we can reasonably assume the solubility of Si in the δ phase to be about 0.6 at%. The maximum solubility of Si in the other Fe-Zn intermetallic compounds Γ, Γ_1,

and ζ is probably not higher than approximately 0.1 at% Si.
In fig. 5.21 we have drawn the 395°C isothermal section of the Fe-Zn-Si phase diagram in which these values have been taken into account. For clearness we have only drawn the Zn rich corner of the isothermal section in the range of 80-100 at% Zn. Line a and b are the straight lines joining the compositions of the terminal alloys with pure Zn of resp. the Fe(2.3at%Si)- and Fe(6.3at%Si)-Zn couples. (We only discuss these two couples, the other two couples are self evident). We see

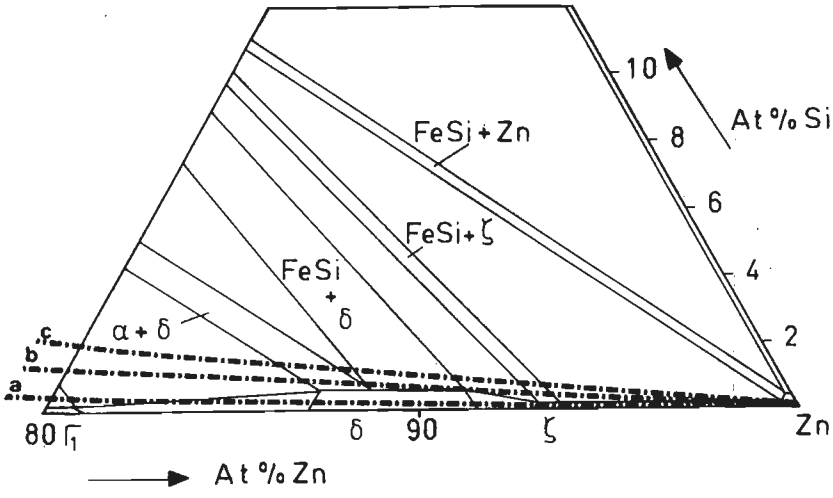

Fig. 5.21. Zinc-rich corner of the 395°C Fe-Zn-Si isothermal section with straight lines joining the terminal compositions of a) the Fe(2.3at%Si)-Zn, b) the Fe(6.3at%Si)-Zn and c) the Fe (9.0 at% Si)-Zn diffusion couples.

that in both cases the mass balance lines intersect with the δ phase field implying that, when Zn reacts with these Fe(Si) alloys, the amount of silicon eventually liberated can be accomodated by dissolving in this intermetallic compound. As we can see from the results of these couples this is indeed the case (i.e. only Fe-Zn intermetallic compounds are observed). This indicates that the general rule derived in section 5.1.5 for the Fe(Al)-Zn(Fe) couples can also be applied to this system. A strong confirmation of this was found in the results of the experiments with the Fe(9.0at%Si)-Zn diffusion couple. When we draw the straight line joining the terminal alloys of this couple (line c in fig. 5.21), it does not intersect with

the δ phase field. This indicates that, similar to the reaction between FeAl and Zn(Fe), the liberated Si cannot be accomodated by dissolving in the δ phase. As a result one would have to expect another layer sequence in this couple (i.e. not only Fe-Zn intermetallic compounds). This is indeed the case as we will see in section 5.2.5, when we will discuss the results obtained with this couple.

5.2.4 Comparison between the results obtained with the Fe(0-6.3at%Si)-Zn solid-solid couples and the process of hot-dip galvanizing of Si-containing iron or steel.

As can be derived from figs. 1.4 and 1.5, the range of concentrations, in which Si has its adverse effect on the reaction during hot-dip galvanizing can be divided into two regions. Habraken[26] called these regions resp. the first peak and second peak. The first peak arises at a concentration of about 0.2 at% Si (0.1 wt%). When galvanizing these steels at normal galvanizing temperatures, a so-called Sandelin structure is observed: a closed δ layer with a very wide ζ layer consisting of small crystallites dispersed in the zinc (see also fig. 5.22a). The second peak is situated around 0.8 at% Si (0.4 wt%). The most characteristic features of the structure found during hot-dip galvanizing of these steels are the Δ diffuse regions: an aggregated zone consisting of δ, FeSi and Zn (see fig. 5.22b).

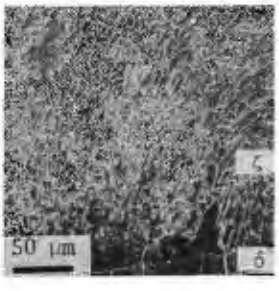

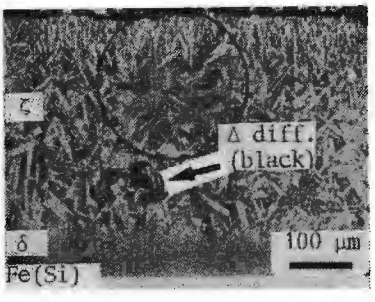

Fig. 5.22.

a) Reaction layer formed in Fe (0.2at%Si)-Zn couple, 460°C, 5 min (Sandelin structure)

b) Reaction layer formed in Fe (0.8 at% Si)-Zn couple, 460°C, 10 min.

Both figures are taken from Habraken[26].

If, with the aid of fig. 1.4b, we extrapolate these peak values, which apply to a temperature of 450-460°C, to our reaction temperature of

395°C, then we must expect these two peaks to lie resp. at ∿ 0.2 at % Si (0.1 wt%) and 2-3 at% Si (1-1.5 wt%). Indeed the reaction layer in the Fe(2.3 at% Si)-Zn couple showed a marked change in its structure compared to a binary Fe-Zn diffusion couple. So we may expect that there are parallels between the results obtained with this couple and the reaction which occurs during hot-dip galvanizing Si-containing steels with a Si content around the second peak. However, the Fe(0.15at%Si)- and Fe(0.4at%Si)-Zn diffusion couples did not show any marked changes, except for some little perturbations at the δ/ζ interface, compared with the binary reaction. Hence, there is probably no relation between the results of these couples and the reaction during hot-dip galvanizing Si "first peak" steels. This implies that the role of Si in this concentration range on the galvanizing reaction at 450-460°C cannot be exclusively explained by means of solid state diffusion aspects. Other aspects, such as surface tensions or liquid penetration have to be taken into account in order to explain the role of Si in this concentration range. So as a preliminary conclusion it appears that the results obtained with our solid-solid Fe(0-6.3 at% Si)-Zn diffusion couples (especially the Fe 2.3at%Si-Zn couple) can only be used for an explanation of the phenomena observed during hot-dip galvanizing iron or steel with a Si content lying around the second peak. We will now elaborate this relationship.

Therefore we shall go deeper into the question of the development of the two-phase δ+ζ zone and the role of Si in this respect. Before we try to give an answer to these questions we must recall the work of Onishi et al.[74]. From their marker experiments in Fe-Zn diffusion couples one can conclude that Zn is the only diffusing component in this system. So at the δ/ζ interface δ is continuously converted into ζ. When Si is present in the δ phase the Si has to be accepted by the ζ phase during the conversion reaction. From the fact that Si accumulates in the δ islands of the two-phase δ/ζ zone we can conclude that the Si present in the δ phase is not accepted easily by the ζ phase. The transition of an initially planar δ/ζ phase boundary into the two-phase δ+ζ zone can be explained by a kind of perturbation analysis. However, in this case the determining factor is not the diffusion rate of a component through the reaction layer, as in the perturbation analysis discussed in section 2.3.3, but rather

an accidental difference in dissolved Si in the δ phase along the δ/ζ phase boundary. With the help of fig. 5.23a-c this will be elucidated. In fig. 5.23a we have drawn schematically a planar phase boundary between the δ and ζ layers in an Fe(2.3 at% Si)-Zn couple. Between position 1 and 2 at this boundary there exists an accidental difference in the amount of dissolved Si in the δ layer. At position 1 the δ layer contains less Si than at position 2. At position 1 of the phase boundary the δ phase will be converted more easily into the ζ phase than at position 2, for at this position less Si has to be accepted by the ζ phase. Hence, at position 1 more ζ will be formed than at position 2 (fig. 5.23b), resulting finally in the two-phase δ+ζ zone (fig. 5.23c).

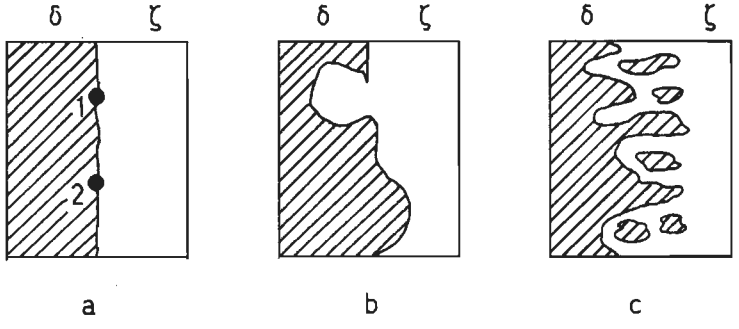

Fig. 5.23. Perturbation model explaining the development of a two-phase δ+ζ zone observed in an Fe(2.3 at% Si)-Zn couple (see also text).

As we have seen, the two-phase δ+ζ zone in the Fe(6.3 at% Si)-Zn couples was less pronounced. With the above described model we can also explain this fact. The δ layer in this couple contains ≳ 0.6 at% Si, which is the maximum solubility of Si in the δ phase. As a consequence the Si dissolved in the δ phase will be distributed more uniformly along the δ/ζ phase boundary, and accidental differences in the amount of dissolved Si in the δ layer will occur less often. The two-phase δ+ζ zone in this couple will then be less pronounced compared with the zone in the Fe(2.3 at%Si)-Zn couple.

The formation of the two-phase δ+ζ zone might well explain the observed phenomena, such as the occurrence of "liquid pockets" and the Δ diffuse regions, during galvanizing steel or iron with a Si

content around the second peak. If such a two-phase zone develops in the reaction layer of galvanized steels (in the early stages of the process) one can readily imagine that this would influence the stability of the ζ layer and especially the coherence between the grains of this layer in a negative way. For the ζ layer is not formed uniformly along the δ/ζ phase boundary, but at rather accidental places along this boundary where the δ layer contains less Si. Due to this decreased coherence the penetration of liquid zinc between the ζ grains would then be facilitated with the final result that the liquid Zn reaches the Si-containing δ phase. This situation is in fact comparable with that of the Fe_3Al-Zn(Fe) couple in fig. 5.5, in which Zn is also in contact with the δ phase. There is, however, one difference: in the case of the Fe_3Al-Zn(Fe) couple δ is permitted to be in equilibrium with the liquid Zn, whereas in the case of an Fe(Si)-Zn couple it is not possible, as we can see from the respective phase diagrams. So, a non-equilibrium situation has been created, resulting in an accelerated attack of the Si-containing δ phase by the liquid Zn. The Δ diffuse zones with the liquid pockets may be the result of the zones in which δ and Zn are in contact with each other. The FeSi particles which are found in these Δ diffuse regions are then the result of the reaction between the Si-containing δ phase and the liquid zinc.

The main points of the model outlined above correspond well with the models of Habraken[26] and Gutmann and Niessen[22][23]. Crucial in these models is the destabilisation of the ζ layer due to the Si and the non-equilibrium situation which is created when the liquid Zn comes into contact with the δ phase. Concerning the destabilisation of the ζ layer Habraken follows a different way. He assumes also that the Si present in the δ phase will not easily be accepted by the ζ phase when δ is converted in ζ. This fact has been clearly proved in our diffusion couples, and gives rise to the two-phase $\delta+\zeta$ region. Habraken, however, assumes that the Si, which hardly dissolves in the ζ phase will be segregated at the grain boundaries of this phase. At these boundaries the liquid pockets and FeSi will then develop. However, this is in contrast with our observations on the Si-rich particles in the ζ layer of the Fe(2.3 at% Si)-Zn couple. The particles were distributed randomly in the ζ layer and not preferentially at grain boundaries.

As a general conclusion of this section we may state that our results in the solid-solid Fe (0-6.3 at% Si)-Zn diffusion couples may well be used in studying the hot-dip galvanizing reaction of Si-containing steels and iron, as far as solid-state diffusion aspects are concerned. Other aspects such as liquid penetration, however, will also play a role at the hot-dip galvanizing process.

5.3 The Fe-Zn-Si system at high Si concentrations

5.3.1 Introduction

This part contains the results obtained with the Fe(Si)-Zn diffusion couples, in which the Si content of the Fe(Si) alloys is greater than or equals 9.0 at%. In the discussion of the results of these couples the accent will be laid on the development of reaction layer morphologies in ternary diffusion couples. This more general part is not specifically related to the process of hot-dip galvanizing. For comparison also other ternary systems will come to discussion. The annealing temperatures of the couples were 395°C, unless otherwise stated.

5.3.2 The results obtained with the Fe(9.0 at%Si)- and Fe_3Si-Zn couples

Fig. 5.24 gives a photomicrograph of the reaction layer in a Fe(9.0 at% Si)-Zn diffusion couple. Clear differences are seen in comparison to the Fe(0-6.3at%Si)-Zn couples. No closed δ layer is formed and the largest part of the reaction layer consists of the ζ phase. In the ζ phase near the Zn interface some small particles can be observed (see fig. 5.25), which appeared to consist of FeSi. As mentioned in section 5.23 a layer, other than an Fe-Zn intermetallic compound, develops in this couple an the Fe(9.0at%Si) substrate. Fig. 5.26 gives a photomicrograph of this thin layer. Microprobe analyses results of this couple are given in table 5.5. The microprobe analysis of the thin layer found on the Fe(9.0at%Si) substrate will

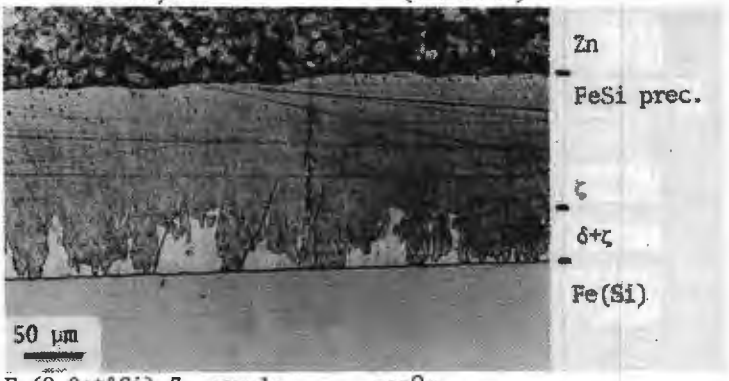

Fig. 5.24. Fe(9.0at%Si)-Zn couple, 18h, 395°C.

be treated further in the text. As table 5.5 shows the measured composition of the ζ phase near the Fe(9.0at%Si) substrate (points 3 and 8) does not agree with the value expected according to the

No.	Composition (at%)		
	Fe	Zn	Si
1	91.0	0.0	9.0
2	89.7	1.9	8.4
3	9.7	90.2	1.0
4	89.6	1.9	8.5
5	11.2	87.9	1.0
6	9.8	89.1	1.0
7	8.5	90.5	1.0
8	9.3	89.7	1.0
9	8.0	92.0	0.0
10	7.9	92.0	0.0
11	7.4	92.5	0.0
12	0.2	99.8	0.0

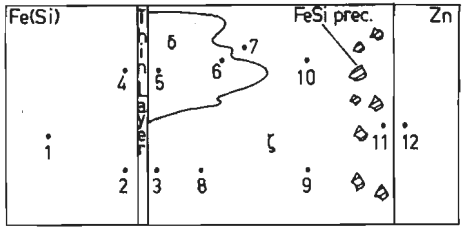

Table 5.5. EPMA data of Fe(9.0 at%Si)-Zn couple, 18h.
The numbers refer to measured spots in the couple, of which a schematic drawing is given along the table.

Fig. 5.25. FeSi precipitates observed in the ζ layer near the Zn interface of the couple in fig. 5.24.

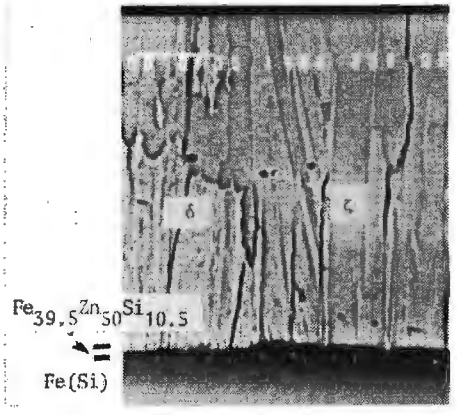

Fig. 5.26. Thin layer ($Fe_{39.5}Zn_{50}Si_{10.5}$) observed on Fe(9.0 at%Si) substrate in couple of fig. 5.24 (BEI). The white bar indicates 10 µm.

Fe-Zn-Si phase diagram in fig. 3.4: The Fe and Si concentrations are far too high. Apparently there is a non-equilibrium situation which is, however, relieved in the course of time by the formation of FeSi precipitates. These precipitates were only found near the Zn interface i.e. the oldest part of the ζ layer. The composition of the ζ phase measured in this part of the layer showed again the values according to the phase diagram. For longer annealing times the whole situation stabilises in the sense that the δ phase closes up and no meta-stable ζ is found near the Fe(9.0at%Si) substrate. This has been illustrated in fig. 5.27.

Further research on this couple concentrated on the thin layer

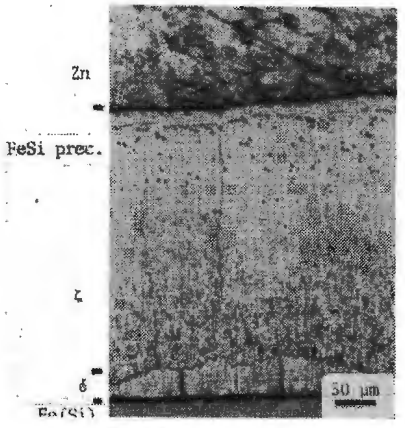

Fig. 5.27. Fe(9.0at%Si)-Zn couple, 96h, 395°C, with closed δ layer.

found on the Fe(9.0at%Si) substrate. The layer grew very slowly with time and its small width precluded accurate microprobe measurements. However, by dipping the Fe(9.0at%Si) alloy in an Fe-saturated Zn melt at 450°C during 50h we were able to produce a sufficiently thick layer (≈ 6 µm). We noticed a remarkable influence of the etching procedure on the measured composition of the layer. For an etched specimen we found a composition of $Fe_{36}Zn_{50}Si_{14}$, whereas for an unetched (only polished) specimen we found $Fe_{39.5}Zn_{50}Si_{10.5}$. The latter composition is the most reliable, because this difference is probably due to a prefered withdrawal of especially Fe from this layer by the etchant. Fig. 5.28 gives a measured Si concentration profile across this layer. The measured composition lies in the two-phase region of the α-Fe(Si)

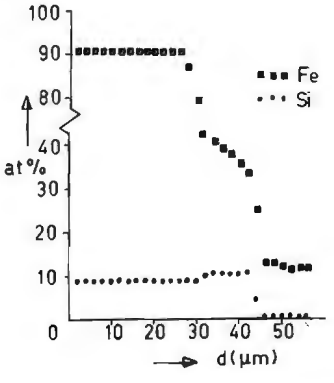

Fig. 5.28. Si- and Fe-concentration profiles across $Fe_{39.5}Zn_{50}Si_{10.5}$ layer of an Fe(9.0at%Si)-Zn couple, 50h, 450°C.

and δ phase of the Fe-Zn-Si phase diagram and does not correspond to a single phase in this system. So the idea came up that we were not

dealing with a new phase, but in fact with a two-phase layer consisting of δ and α-Fe(Si), the latter phase being the saturated solid solution of Si in Fe with the chemical formula of Fe_3Si (Fe_3Si is an ordered phase of Si and Fe). This suspicion was confirmed by the following observations:

- all efforts to detect such a phase in ternary alloys failed.
- the phase boundary between the Fe(9.0at%Si) alloy and the thin layer is not sharp but rather vague. See fig. 5.29.

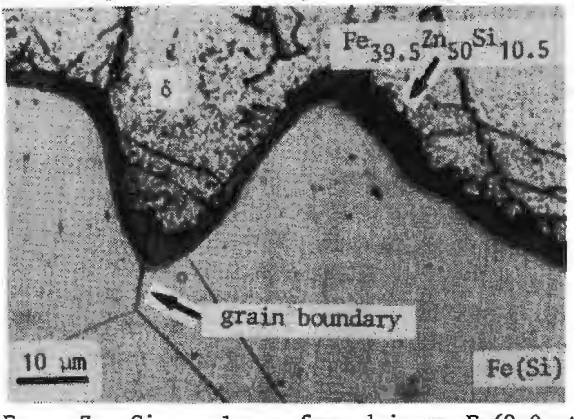

Fig. 5.29. $Fe_{39.5}Zn_{50}Si_{10.5}$ layer formed in an Fe(9.0 at%Si)-Zn couple, 50h, 450°C.

Notice 1) the vagueness of the phase boundary between this layer and the substrate.

2) the grain boundary in the substrate which continues without any deviation in this layer.

- Fig. 5.29 also shows that grain boundaries of the Fe(9.0at%Si) alloy continue in the thin layer without any deviation. This is a strong indication that the Fe(9.0at%Si) substrate and the matrix of the formed layer are the same. So no new phase has been formed.

Summarizing these results on the thin layer in the Fe(9.0at%Si)-Zn couples we can say that: - the total composition of this layer is $Fe_{39.5}Zn_{50}Si_{10.5}$. - the layer is a two-phase mixture of δ and α-Fe_3Si. The phases are mixed up on such a fine scale that they cannot be distinguished in the optical-or scanning-electron microscope.

We come now to the results obtained with Fe_3Si-Zn diffusion couple. The composition of the Fe_3Si alloy corresponds with the maximum solubility of Si in Fe at 395°C. In an Fe_3Si-Zn diffusion couple

we would expect, therefore, on the basis of the mass balance, besides the formation of Fe-Zn intermetallic compounds also the formation of FeSi. Fig. 5.30 gives a photomicrograph of the reaction layer developed in such a couple. As expected we see, besides the Fe-Zn intermetallic compound layer, another layer at the Fe_3Si substrate. As in the former case of the Fe(9.0at%Si)-Zn couples this layer was found to be a two-phase layer, but now consisting of FeSi particles and Fe-Zn intermetallic compound, as will be demonstrated in section 5.3.4. The overall composition of this layer was $Fe_8Si_7Zn_{10}$. We will discuss the reliability of these measurements in section 5.3.5.

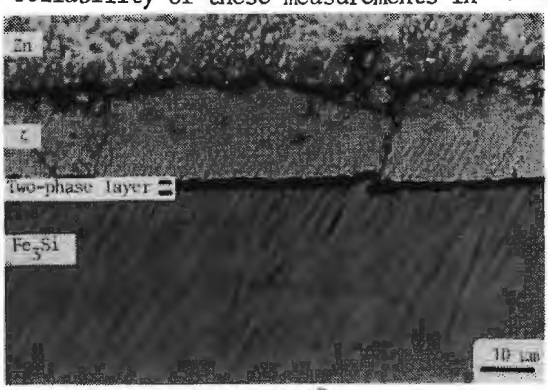

Fig. 5.30. Fe_3Si-Zn couple, 1h, 395°C.

5.3.3 The diffusion paths of the Fe_3Si-Zn (annealing time $\leq$ 1h) and Fe(9.0at%Si)-Zn diffusion couples

In this section we will go further into the matter of the formation of the two-phase layers in the Fe_3Si-Zn (annealing time $\leq$ 1h) and Fe(9.0at%Si)-Zn couples. We will do this with the help of the diffusion paths of the respective couples. In fig. 5.31 we have plotted these diffusion paths on the 395°C isothermal section of the Fe-Zn-Si system. The path of the Fe(9.0at%Si)-Zn couple is that of a couple with a closed δ layer, as shown in fig. 5.27. The first part of each diffusion path, which represents the transition from the bulk of the Fe(Si) alloy to the two-phase layer, is very schematic: we have just drawn a straight line from the terminal Fe(Si) alloy to the measured composition of the two-phase layer.

The question of why the two-phase layers develop at the substrate is the same as asking why nature has chosen this particular diffusion path. We could rephrase this question in a negative way: Why does

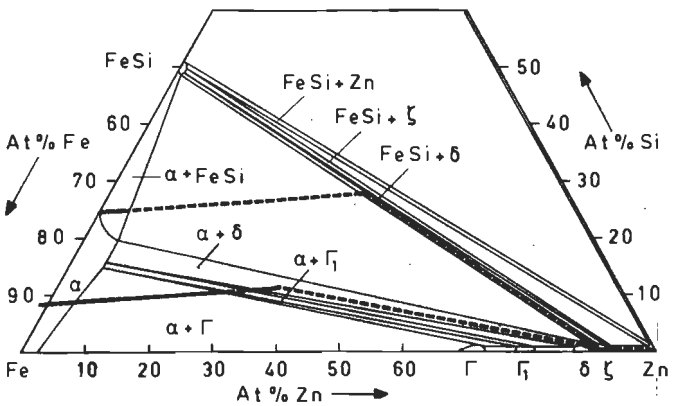

Fig. 5.31. Diffusion paths of Fe(9.0at%Si)-Zn and Fe_3Si-Zn (annealing time $\leq$ 1h) couples on the 395°C isotherm of the Fe-Zn-Si system.

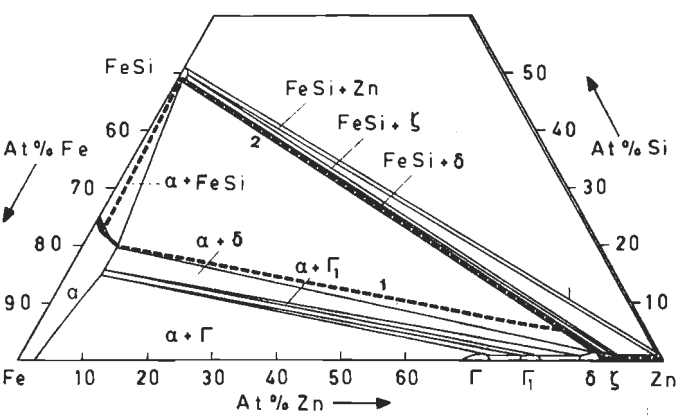

Fig. 5.32. Two fictive diffusion paths of an Fe_3Si-Zn couple on the 395°C isotherm of the Fe-Zn-Si system.

nature not choose some other possible paths? We will treat this problem for the Fe_3Si-Zn couples, but the results may also be applied to the Fe(9.0at%Si)-Zn diffusion couples. Two other possible paths for the Fe_3Si-Zn couple are drawn in fig. 5.32. Path 1 corresponds with the following layer morphology: a δ layer, with FeSi precipitates throughout it, and a ζ layer. Fig. 2.8 represents well this morphology (except for the ζ layer), if one reads instead of AC and BC resp. δ and FeSi. As we have already mentioned during the discussion of this morphology in section 2.3.3, this path implies a strong lateral diffusion of, in our case, Fe and Si. Path 2 corresponds with a closed FeSi layer at the substrate followed by the δ and ζ layers. This path implies a diffusion of Fe through the FeSi layer. This Fe reacts at the FeSi/δ interface with Zn and forms δ. FeSi particles are formed because, due to the withdrawal of Fe by Zn, the Fe_3Si substrate becomes relatively Si- richer:

$$Fe_3Si \longrightarrow FeSi + 2Fe \qquad [5.1]$$

$$(\bar{v}_{Fe_3Si} = 27.95 \frac{mol}{cm^3}) \qquad (\bar{v}_{FeSi} = 13.76 \frac{mol}{cm^3})$$

In order to form a compact FeSi layer a coarse-ripening process [91] of the FeSi particles has to occur. For this to occur a Si diffusion flux, especially in the lateral direction, is necessary.

It appears that for both paths 1 and 2 a considerable diffusion flux of both Fe and Si is necessary through either the Fe(Si) substrate or the Fe-Zn intermetallic compound. Exact data on the diffusion rates of both components through these alloys or compounds are not known, but they are expected to be very low at the reaction temperature we used. See for example Adda and Philibert [92], who give some values on the diffusion coefficients of Fe and Si through Fe(Si) alloys at 800°C and the work of Onishi et al. [74], from which it appears that Fe has a very low diffusion rate through the Fe-Zn intermetallic compounds at 395°C. These low diffusion rates of Fe and Si may provide the most likely explanation for the fact that both paths 1 and 2 do not occur in an actual diffusion couple, and that the actual path, as drawn in fig. 5.31, is prefered over path 1 and 2 in fig. 5.32. The low diffusion rates of Fe and especially Si are indeed evident from the course of the first part of the actual path, which represents the transition from the Fe_3Si alloy to the two-phase FeSi and δ layer. This part is almost parallel to the Fe-Zn axis of the phase diagram. This means

that hardly any Si concentration gradient exists across this interface and we may assume that practically no Si diffuses. In other words the Si is almost immobile. The FeSi of the two-phase layer is now formed according to reaction equation [5.1], but no closed FeSi layer will be formed because the necessary lateral diffusion of Si will not happen (the FeSi particles resist coarsening[92]). The space which is left between the FeSi particles is "filled up" with the other reaction product δ, resulting in a two-phase layer. Together with the measured overall composition of the two-phase layer $Fe_8Si_7Zn_{10}$ we can now write down the reaction equations for the reactions occurring in an Fe_3Si-Zn couple (see also fig. 5.33). At the substrate/two-phase layer interface the following reaction will happen:

I. $7Fe_3Si + 10Zn \rightarrow Fe_8Si_7Zn_{10} + 13Fe$ [5.2a]

The iron will react at the two-phase layer/δ interface with Zn and forms δ:

II. $13Fe + 130Zn \rightarrow 13FeZn_{10}$ [5.2b]

We see that some diffusion of Fe is necessary through the two-phase layer. In this way also the two-phase layer in the Fe(9.0at%Si)-Zn couple may be explained, but now Fe_3Si particles are formed.

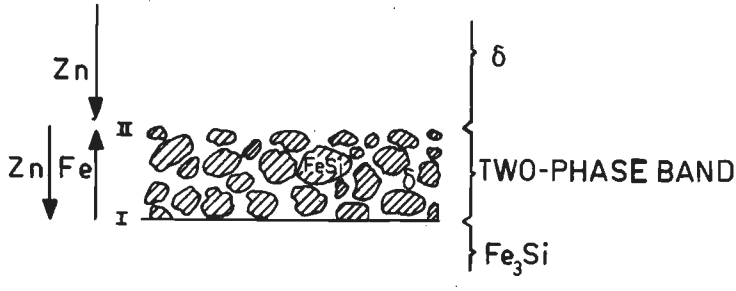

Fig. 5.33. Formation of a two-phase δ + FeSi layer on the Fe_3Si substrate in an Fe_3Si-Zn couple. (see also text).

In section 5.3.5 we will discuss the Fe_5Si_3-Zn diffusion couple. This couple showed the same behaviour as the other Fe(Si)-Zn couples: a two-phase layer was formed at the substrate. The overall composition of this layer lies in the δ-FeSi two-phase region. The average Si content of this two-phase layer was again only slightly higher than in the Fe_5Si_3 terminal alloy, indicating a very low mobility of Si.

Summarizing the results we can say that, for the investigated range of Si concentrations (9.0-37.5at%Si), during the reaction in an Fe(Si)-Zn diffusion couple always a two-phase layer is formed at the Fe(Si) substrate. For low Si concentrations ($\lesssim$ 9.0at%) this layer consists of Fe_3Si particles and δ. For higher Si concentrations this layer consists of FeSi particles and δ. The average Si composition in this layer is always only slightly higher than in the terminal Fe(Si) alloy. The very low mobility of Si is the reason that these two-phase layers form, rather than a compact layer.

5.3.4 Reaction layers formed in Fe_3Si-Zn diffusion couples at longer annealing times.

The results obtained with the Fe_3Si-Zn couple, which we discussed in the preceding section, concerned a couple which was annealed for only 1h. In the couples annealed for longer times we observed an unusual and very curious phenomenon, viz. the formation of a reaction layer with a periodic structure. Fig. 5.34 gives a photomicrograph of the reaction layer found in an Fe_3Si-Zn couple annealed for 24h. What strikes immediately is the periodic arrangement of thin bands throughout the reaction layer. The reaction layer itself consists of two main layers, which appeared to be the usual δ and ζ phases. The width of the bands is about 1.5-2 μm; The distance between them varies between approximately 20 μm for bands at the iron-side of the couple to about 16 μm for bands at the zinc-side of the couple. Fig. 5.35 gives a magnification of a single band from which it can be clearly seen that the bands consist of little particles lying in the Fe-Zn intermetallic compound matrix. By means of X-ray diffraction we were able to identify these particles as FeSi. The overall composition of a band lies for all bands around the value of $Fe_8Si_7Zn_{10}$ ($\pm$ 2.0at%). This is the same composition as observed in the reaction layer of a couple annealed for 1h (cf. section 5.3.3). We will postpone a further discussion of the composition of the bands to section 5.3.5.

Results of layer growth measurements are plotted in fig. 5.36. Though the measurements are scarce we may conclude that the total layer grows parabolically with time, indicating a diffusion controlled reaction. Compared to the binary Fe-Zn reaction at this temperature (see fig. 5.18) the reaction rate is about a factor 2 lower. Fig. 5.37 shows an Fe-concentration profile across the total layer of a

Fig. 5.34. Fe_3Si-Zn couple, 24h, 395°C. Notice the periodic arrangement of thin bands throughout the δ and ζ reaction layers. The holes between the grains of the δ layer are due to a prolonged etching (BEI). The white bar indicates 100 μm.

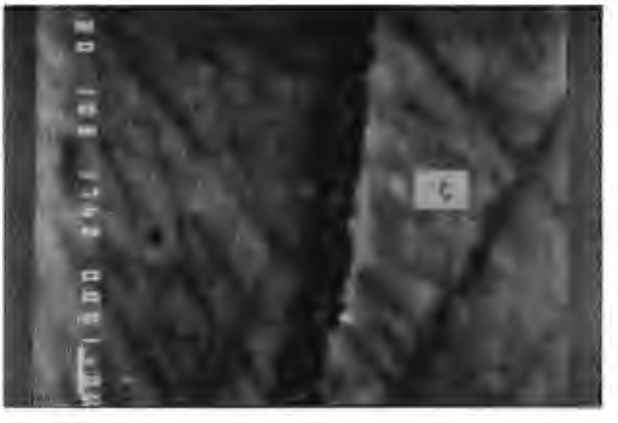

Fig. 5.35. Magnification of a thin band observed in the couple of fig. 5.34 (BEI). The white bar indicates 1.0 μm.

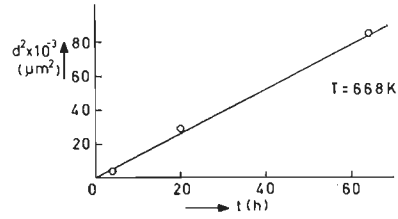

Fig. 5.36. Square root of total layer width vs. diffusion time for Fe_3Si-Zn couples annealed at 395°C.

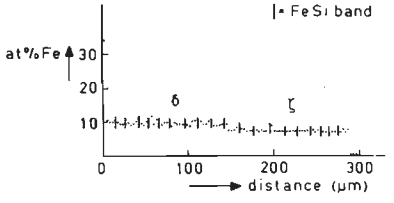

Fig. 5.37. Fe-concentration profile through reaction layer of an Fe_3Si-Zn couple, 64h, 395°C.

couple annealed for 64h. The composition of the Fe-Zn intermetallic compound layers is not influenced by the presence of the bands and shows the normal Fe composition range as found in the binary case (except for the δ layer, in which we do not find the δ_c composition). The formation of bands in the Fe_3Si-Zn diffusion couples was also investigated at other annealing temperatures. At a temperature of 450°C (solid-liquid diffusion couple) the band spacing and thickness was about the same as at 395°C. At a temperature of 350°C the layer grew very irregularly. Bands were observed, but it was difficult to determine a uniform band spacing and thickness, because the layers were broken up.

A last remark on this couple concerns its diffusion path. The first part of the path, starting with the Fe_3Si alloy is the same as for the couple annealed for 1h (cf. fig. 5.31). The further course of the path is represented by several loops from the δ and ζ single phase regions into the δ- and ζ-FeSi two-phase regions respectively. Each loop represents a two-phase band found in the reaction layer. Peculiar about this path is the fact that it is not stationary with time. For longer annealing times more bands are formed, and hence more loops will appear in the diffusion path.

5.3.5 The influence of the Si content of the Fe(Si) substrate on the band formation

By varying the Si content of the Fe(Si) terminal alloy we investigated the influence of this factor on the band spacing, thickness and composition. We have already discussed the Fe(9.0at%Si)-Zn couple. In this case no periodic structure was found, not even after long annealing times (up to 100h). Then two couples were studied, of which the Si content of the terminal Fe(Si) alloy lies between those of the Fe(9.0at%Si) and Fe_3Si alloys, viz. 17.9 and 23.2 at% Si. Figs. 5.38a-b show the observed reaction layers in these couples. We see that bands are found in the reaction layer, although they are not continuous over such long distances as in the Fe_3Si-Zn couple. The situation in these couples may be best characterized as a kind of precursive stage of the reaction layer with

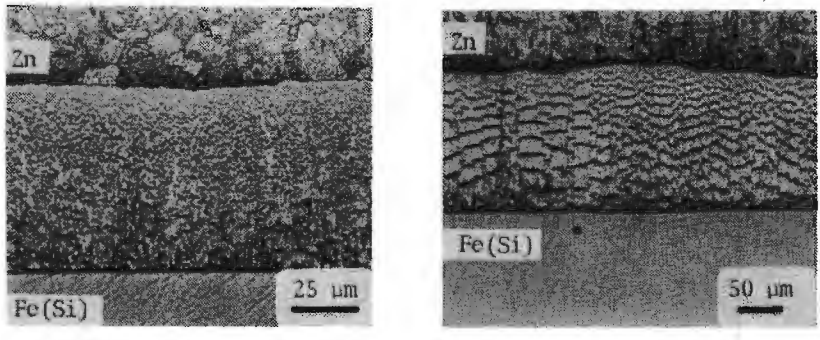

Fig. 5.38a-b.
a) Fe(17.9at%Si)-Zn couple,4h,395°C. b) Fe(23.2at%Si)-Zn couple, 22h, 395°C. The distinction between the δ and ζ layers is not visible because of a light etching.

the continuous bands found in the Fe_3Si-Zn diffusion couple. The composition of the small bands was difficult to measure, but the values lied all in the two-phase δ- or ζ-FeSi regions indicating that here too the bands consist of FeSi particles in δ or ζ.

The next couple which was studied concerned a couple with an Fe-Si compound with a higher Si content than the Fe_3Si alloy viz. Fe_5Si_3. This compound is only stable above 825°C. Below this temperature it decomposes in α-Fe(Si) and FeSi. However, this decomposition proceeds very slowly, so that it was possible to obtain this compound

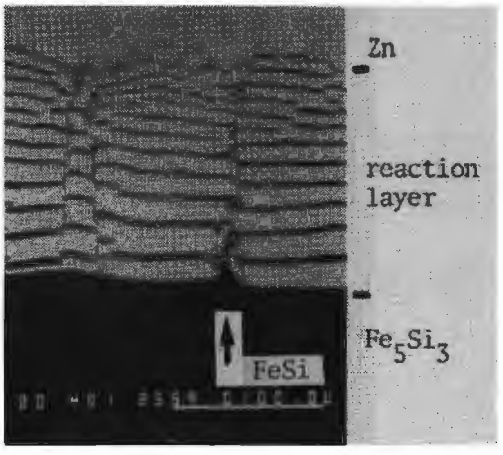

Fig. 5.39. Fe_5Si_3-Zn couple, 18h (BEI), 395°C.
Notice the FeSi phase in the Fe_5Si_3 substrate, which has not reacted at all with the Zn. The white bar indicates 100 μm.

at room temperature. However, no completely homogeneous compound was obtained as we will see. Fig. 5.39 gives the observed reaction layer in this type of couple. A clear periodic structure with continuous bands can be seen, but there are differences with the bands observed in the Fe_3Si-Zn couples viz.:

- The band thickness is larger viz. 5 μm. In other couples band thicknesses up to 9 μm were found.
- The band spacing is also larger viz. 25 to 35 μm.
- The total composition of a band is different.

The last point will be treated in more detail. Because the bands were much thicker in this type of couple we could measure its overall composition very accurately. If this composition is known we can write down the total reaction equation of the reaction which takes place in the couple. If we assume a band to consist of $\delta(=FeZn_{10})$ and FeSi the molar ratio of both compounds in a band can be calculated. With the aid of the molar volumes of the two reaction products FeSi and $FeZn_{10}$ we can calculate the molar volume of a band corresponding with its composition. From the reaction equation it is then possible to calculate the ratio of the amount of band and the δ phase formed behind it. This calculated ratio can be compared to the ratio obtained

by measuring the widths of both phases (band and δ phase behind it) in a couple. The discrepancy between both ratios is a measure of the accuracy of the measured band composition. In table 5.6 this procedure has been applied for the Fe_5Si_3-Zn couple. We see that the discrepancy between both ratios is not very large. This indicates that the measured band composition is reliable. The same procedure has been applied to the Fe_3Si-Zn diffusion couple in table 5.6. For the calculations concerning this couple we started from the measured average band composition of $Fe_8Si_7Zn_{10}$ ($=Fe_{32}Si_{28}Zn_{40}$). We see that in this case too no large discrepancy exists between both ratios, indicating that the measured composition in the bands of the Fe_3Si-Zn couple are quite reliable, though these bands are rather thin. Also it can be seen that there is a large difference in the average band compositions of both types of couples. But just like the results in the Fe_3Si-Zn couple, the average Si content in a band of the Fe_5Si_3-Zn couple is only slightly higher than the Si content of the terminal Fe_5Si_3 compound. This means that the first part of the diffusion path of this couple, representing the transition of the bulk of the Fe_5Si_3 compound to the two-phase band, runs parallel to the corresponding part of the paths of the Fe(9.0 at% Si)- and Fe_3Si-Zn diffusion couples, as they have been plotted in fig. 5.31.

The difference between the bands in the Fe_3Si- and Fe_5Si_3-Zn couples can also be seen in the latter couple alone. As has been mentioned the Fe_5Si_3 compound was not completely homogeneous, but was found to consist of also α-Fe_3Si and FeSi phases. Figs. 5.40a-b show a photomicrograph and schematic drawing of a part of the reaction layer which developed on the Fe_5Si_3 substrate, in which also the α-Fe_3Si phase was present. The difference between the bands formed on the α-Fe_3Si and Fe_5Si_3 phases can clearly be seen. The composition of the band formed at the α-Fe_3Si phase was similar to that of a band found in an Fe_3Si-Zn couple. The observation that there can be large differences in composition of bands which are lying next to each other in the same reaction layer, and which consist of the same compounds, can again be taken as an indication of the very small mobility of Si. In the Fe_5Si_3-Zn diffusion couple of fig. 5.39 also the reaction behaviour between FeSi and the Zn can be seen. It appears that the FeSi phase present in the terminal Fe_5Si_3 compound has not reacted at all with the Zn. This was confirmed by means of

	Fe_5Si_3-Zn	Fe_3Si-Zn
Measured overall composition of a band	$Fe_{43}Si_{44}Zn_{13}$	$Fe_{32}Si_{28}Zn_{40}$
Ratio of molar amounts of FeSi and $FeZn_{10}$ in a band	$42FeSi : 1FeZn_{10}$	$28FeSi : 4FeZn_{10}$
Molar volume of a band corresponding to the measured composition	$675.78 \frac{cm^3}{mol}$	$776.72 \frac{cm^3}{mol}$
Total reaction equation in couple	$\frac{44}{3}Fe_5Si_3 + \frac{949}{3}Zn \longrightarrow Fe_{43}Si_{44}Zn_{13} + \frac{91}{3}FeZn_{10}$	$28Fe_3Si + 560Zn \longrightarrow Fe_{32}Si_{28}Zn_{40} + 52FeZn_{10}$
Calculated ratio of molar volume band and $FeZn_{10}$ behind the band (from the reaction equation)	$\frac{\bar{v}_{band}}{\bar{v}_{FeZn10}} = 0.23$	$\frac{\bar{v}_{band}}{\bar{v}_{FeZn_{10}}} = 0.15$
Measured ratio of amount band and $FeZn_{10}$ behind the band (from the measured layer widths)	$\frac{\text{width band}}{\text{width } FeZn_{10}} = 0.24$	$\frac{\text{width band}}{\text{width } FeZn_{10}} = 0.16$

Table 5.6. Composition measurements and calculations concerning bands in Fe_5Si_3- and Fe_3Si-Zn couples.

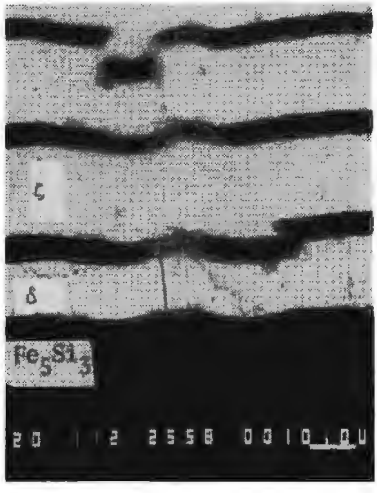

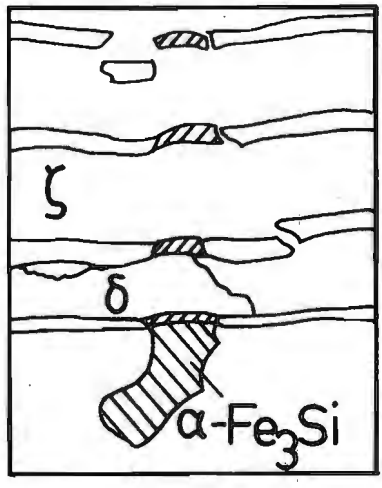

Fig. 5.40a-b.

a) Reaction layer formed on Fe_5Si_3 substrate, in which also α-Fe_3Si was present (BEI). Notice the difference between the bands formed on the Fe_5Si_3 and on the α-Fe_3Si phase. The white bar indicates 10 μm.

b) Schematic drawing of a).

an FeSi-Zn couple which did not show any reaction layer either. This is in accordance with the Fe-Zn-Si phase diagram, which says that the FeSi phase is in direct thermodynamic equilibrium with the Zn phase. The solubility of Zn in FeSi is very low.

5.3.6 Investigation on the occurrence of periodic structures in other ternary diffusion couples

Once we had investigated the Fe(Si)-Zn couples on the appearance of periodic structures, we wondered whether this phenomenon was a specific property of Fe(Si)-Zn diffusion couples or whether it was a more general phenomenon, also occurring in other ternary diffusion couples. Therefore we decided to study other ternary diffusion couples on the occurrence of such a phenomenon. The diffusion couples were selected according to a number of criteria which we derived

from general aspects, which apply to the Fe(Si)-Zn couples, in which a periodic structure was observed, viz.:

- The couple consists of the pure metal Zn and an saturated Fe(Si) alloy or an Fe-Si compound which is richer in Si.
- The solubilities of Zn and Si in respectively the Fe-Zn intermetallic compounds and FeSi are very low. The mass balance line joining the terminal compositions of an Fe(Si)-Zn couple does not intersect with the homogeneity regions of above mentioned compounds.
- The components Zn and Si are almost insoluble in each other.
- The component Si has a very low mobility. This very typical aspect was, as we have seen, expressed by the course of the diffusion path which represents the development of a two-phase band on the Fe(Si) substrate: A straight line which runs almost parallel to the Fe-Zn axis from the terminal Fe(Si) alloy to the two-phase δ-FeSi region.

For a periodic structure to be formed in an Y(Z)-X couple this means that the corresponding X-Y-Z system has to satisfy at least the following criteria (see also fig. 5.41):

- The component Y has a reasonable solubility for the component Z.
- The components X and Z are almost insoluble in each other.
- There is at least one compound Y_aX_b the phase region of which does not intersect with the mass balance line of the Y(Z)-X couple (line a in fig. 5.41).
- As the latter criterion, but now for an Y_cZ_d compound.
- The compounds Y_aX_b and Y_cZ_d can be in equilibrium with each other.

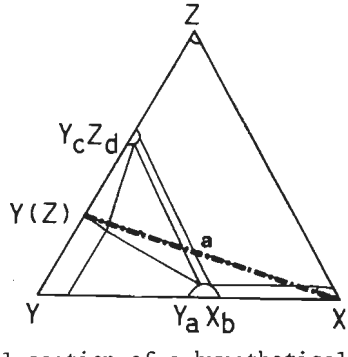

Fig. 5.41. Isothermal section of a hypothetical X-Y-Z system, which satisfies the criteria for a ternary system to be selected on the development of a periodic structure in the couple of the type Y(Z)-X. Line a is the mass balance line of this couple.

The ternary systems which were selected for a further investigation, together with the annealing time and temperature are given in table 5.7. It has to be realized that, before we started the experiments, the exact ternary phase diagrams of the selected systems were not known. The choice of these systems was based on our knowledge of the binary side-systems only. Hence important data necessary to satisfy the selection criteria (for example the appearance of ternary compounds and the solubility of the third component in a binary compound) were a priori not known.

No.	Diffusion couple Y(Z)-X	Annealing temperature (^{o}C)	Annealing time (h)
1	FeAl-Zn	450	74
2	Cu(17.8at%Al)-Si	600	24
3	Ni(9.6at%Si)-Al	650	4
4	Ti(15.2at%Fe)-Cu	850	4
5	Ti(6.7at%Cu)-Co	850	4
6	Ti(8.5at%Co)-Cu	850	4
7	Cu(9.4at%Sn)-Si	475	4
8	Ni(13.4at%Si)-Zn	395	80
9	Cu(12.4at%Si)-Zn	395	64
10	Fe(18.0at%Ge)-Zn	380	66
11	Co(11.5at%Si)-Zn	395	17
12	Co_2Si-Zn	395	44

Table 5.7. Ternary diffusion couples investigated for appearance of periodic structures.

We will now turn to the discussion of the results obtained for these systems. Periodic structures were observed only in the Fe(Ge)-Zn and Co(Si)-Zn systems. These systems will be extensively treated further in the text. First we will briefly discuss the results of the other systems, in which no periodic structure was observed. In these systems we can distinguish mainly the following reaction layer morphologies:

1) a regular layer configuration i.e. only one-phase layers separated by planar boundaries.
2) as 1), but with precipitate zones in one or more of the reaction layers. These precipitate zones did not appear in the layer which

was in contact with the Y(Z) substrate.

3) a two-phase layer at the Y(Z) substrate.

ad 1) The largest part of the investigated systems falls in this category. It concerns here the systems 1 up to and inclusive 6 of table 5.7. The results of the Cu(Al)-Si and Ni(Si)-Al couples are similar to those of the FeAl-Zn couple: an Al-rich resp. Si-rich single phase layer on the substrate followed by Cu-Zn resp. Ni-Al binary intermetallic compound layers. The results of the other systems were miscellaneous and were not directly comparable with the Fe-Zn-Si system. Ternary compounds or binary intermetallic compounds with high solubilities of the third component appeared in the reaction layers of these couples.

ad 2) Two systems are concerned viz. the Cu(Sn)-Si and Ni(Si)-Zn systems. In the reaction layers of these couples precipitate zones developed, but not in the layer which was in contact with the substrate. This was always a single phase layer.

The layer sequence in the Cu(Sn)-Si couple was:

Cu(Sn) / Cu_4Sn (width 10 μm) / Cu_3Sn (15 μm) / Cu_4Sn_3(Si) (15 μm) / Cu_3Si + Cu_4Sn_3 prec. (300 μm) / Si

The Si content of the Cu_4Sn_3 layer was about 1.5at%. The Cu_4Sn_3 precipitates in the Cu_3Si layer were only found at the grain boundaries of this layer. Apparently grain boundary diffusion plays a role here. This means that the processes of precipitate formation in this couple and the Fe(Si)-Zn couple are not the same.

The layer sequence in the Ni(Sn)-Zn couple was:

Ni(Si) / Ni_5Si_2 (5 μm) / $NiZn_3$(Si) + prec. (260 μm) / Ni_5Zn_{21} + prec. (190 μm) / Zn

The Si content in the $NiZn_3$ layer was about 3at%. The precipitates in the $NiZn_3$ and Ni_5Zn_{21} layers were very small and probably consist of Ni_3Si_2 or NiSi.

ad 3) Here only one system is concerned viz. the Cu(Si)-Zn system. The layer configuration found in this couple was unlike the former systems in that a clear two-phase layer was found at the Cu(Si) substrate. Fig. 5.42 gives a schematic illustration of the total reaction layer in this couple. A photomicrograph of the two-phase layer found on the substrate is given in fig. 5.43.

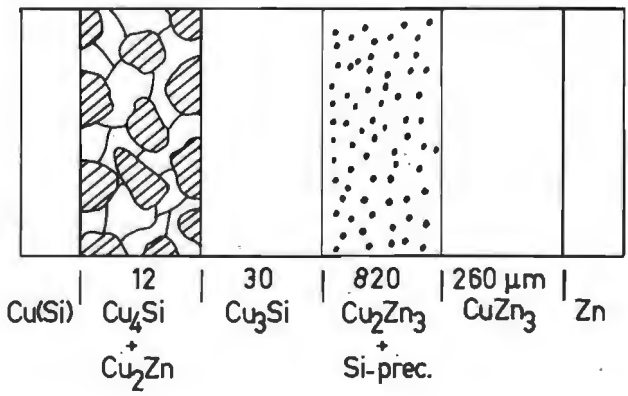

Fig. 5.42. Schematic drawing of the total reaction layer observed in a Cu(12.4at%Si)-Zn couple, 65 h, 395°C.
The layer widths are not drawn to scale.

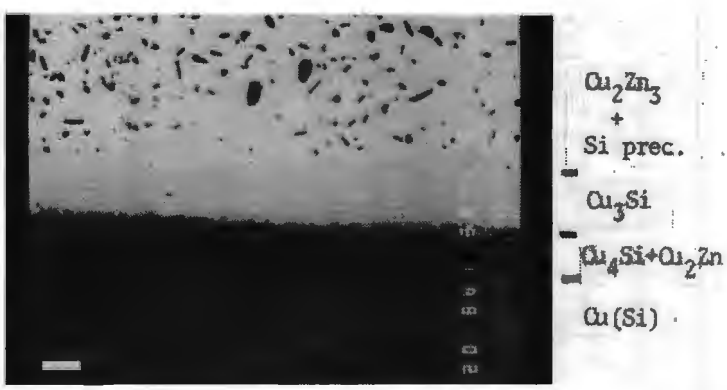

Fig. 5.43. Part of the reaction layer observed in a Cu(12.4at%Si)-Zn couple, 65 h, 395°C (BEI).
The white bar indicates 10 µm.

This two-phase layer consists probably of $Cu_4Si(Zn)$ and $Cu_2Zn(Si)$. So far the situation is similar to an Fe(Si)-Zn couple. But then, instead of finding a Cu_2Zn layer behind this layer, which would be comparable to an Fe(Si)-Zn couple, a Si-rich layer develops, viz. Cu_3Si. This difference in reaction behaviour between both systems is also clearly demonstrated with the help of the schematic diffusion path of the Cu(Si)-Zn couple in fig. 5.44.
Indeed, as for the Fe(Si)-Zn couple, the diffusion path of the couple enters a two-phase region, via a three-phase triangle, but it continues its way upwards to the Cu_3Si phase region, after which it enters the single phase regions of the Cu-Zn intermetallic compounds.

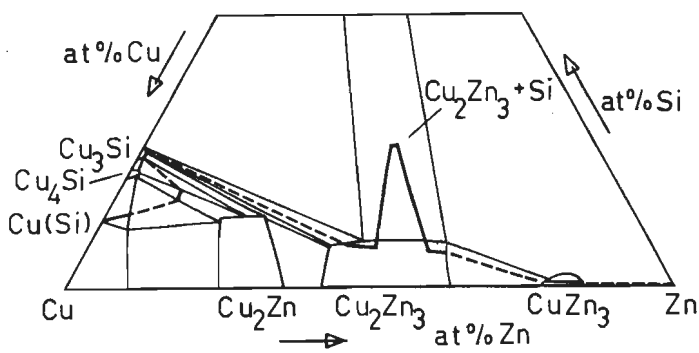

Fig. 5.44. Diffusion path of a Cu(12.4at%Si)-Zn couple on the 395°C isotherm of the Cu-Zn-Si system. The diffusion path and isotherm are schematic drawings and are based on EPMA measurements in the Cu (12.4at%Si)-Zn couple.

We come now to the discussion of the systems in which periodic structures were observed, viz. the Fe(Ge)-Zn and Co(Si)-Zn systems. The periodic structures found in these systems closely resemble those of the Fe-Zn-Si system, but there are differences as we will see. Fig. 5.45 gives a photomicrograph of the reaction layer developed in a Fe(Ge)-Zn couple. The layer sequence in this couple is as follows:
- Fe(Ge) substrate,
- band with an overall composition lying between $Fe_{37}Ge_{33}Zn_{30}$ and $Fe_{45}Ge_{32}Zn_{23}$
- dark-grey layer in which bands are visible. The composition of this layer is about $Fe_{12}Zn_{83}Ge_5$.
- needles consisting of δ-(Fe-Zn) phase.

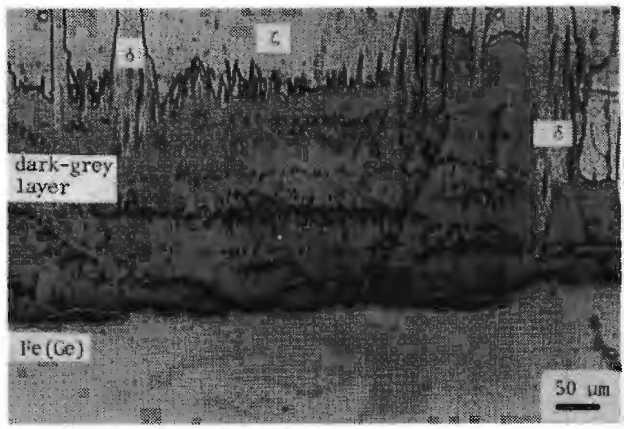

Fig. 5.45. Part of the reaction layer observed in an Fe(18.0at%Ge)-Zn couple, 66h,380°C. The dark-grey layer has a composition of about $Fe_{12}Zn_{83}Ge_5$.

- ζ-(Fe-Zn)-layer
- Zn, not visible in the photomicrograph.

The measured composition of the band at the substrate indicates that it is made up of FeGe particles lying in a matrix of the dark-grey phase. Though the situation resembles the reaction layer in an Fe(Si)-Zn couple very much, there are differences viz.: The bands are only visible in the dark grey layer, and going to interface with the δ needles they decrease in thickness. This means that the FeGe particles can not be in equilibrium with the δ phase and slowly dissolve in the dark grey layer, resulting in the decreasing width of the bands. The dark grey layer is probably made up of a ternary compound. The homogeneity range of this compound lies between those of the FeGe and δ phase regions, thus preventing the FeGe to be in equilibrium with the δ phase. Further research is necessary, especially on the phase relations in the Fe-Zn-Ge system, in order to elaborate these differences with the periodic structures found in the Fe-Zn-Si system.

The other system, in which a periodic structure was observed, was the Co(Si)-Zn system. First a diffusion couple was studied in which the Si content of the terminal Co(Si) alloy equaled the maximum solubility of Si in Co, viz.11.5 at%. A part of the reaction layer observed in this couple is given in fig. 5.46. A clear periodic structure can be seen, though this structure did not

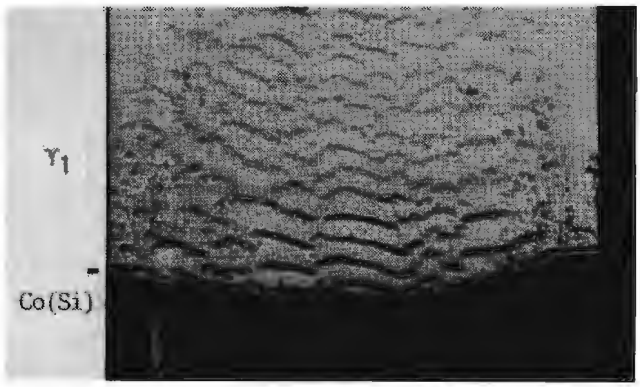

Fig. 5.46. Part of the reaction layer observed in a Co(11.5at%Si)-Zn couple, 17h, 395°C (BEI). The white bar indicates 10 μm.

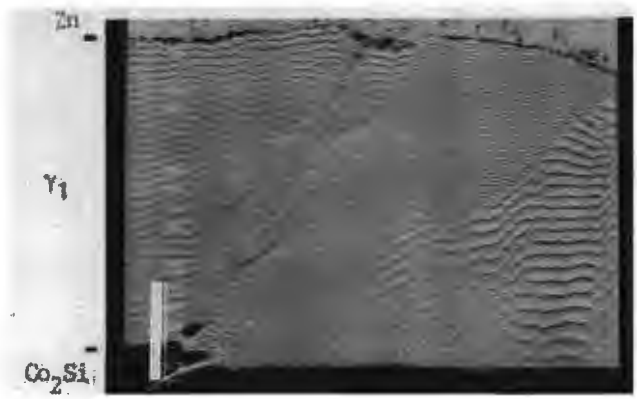

Fig. 5.47. Co_2Si-Zn couple, 44h (BEI). The white bar indicates 100 μm.

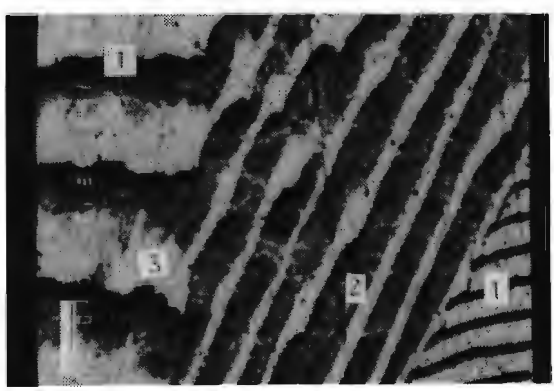

Fig. 5.48. Magnification of part of the reaction layer observed in the couple of fig. 5.47 (BEI). The white bar indicates 10 μm. 1)band(black),2)light-grey phase,3)matrix(white) (see also text)

develop over the whole length of the substrate. In the areas where the periodic structure was absent, there is always a thin layer with a composition of $Co_{40}Si_{10}Zn_{50}$ on the Co(Si) substrate. The total reaction layer for both areas is made up of two layers viz. the γ_1-$CoZn_8$ layer at the Co-side and the γ_2-$CoZn_{13}$ layer at the Zn-side of the couple. The phase boundary between these two layers is very difficult to observe optically. Further on in the text, when we discuss the results of an investigation into the phase relations of the Co-Si-Zn system, the microprobe analyses data of the bands will be treated. The band formation in this couple presents the same features as in an Fe(Si)-Zn couple, in which the Fe is unsaturated with respect to Si. In both cases non-continuous and less well-defined bands are observed. So it appeared interesting to prepare a diffusion couple with a Si-richer terminal alloy. Hence, a Co_2Si-Zn couple was prepared; a photomicrograph of this couple is given in fig. 5.47. A clear periodic structure over the whole length of the substrate is visible. The reaction layer is made up of different "cells" with corresponding different appearances of the periodic structure. There are "cells" in which the bands are parallel to the Co_2Si substrate, but in some "cells" the bands make an angle with the substrate. The band spacing in the same "cell" is nearly constant, but for different "cells" there are large differences in the band spacings. The minimum band spacing is 3-4 μm. By means of polarized light we could establish that the different "cells" correspond with different grains in the Co_2Si substrate. This points to a crystallographic relation between the observed periodicity and the orientation of the Co_2Si grains. Co_2Si has a hexagonal structure. In the Fe_3Si-Zn couples such a relation is not to be expected because Fe_3Si is cubic. Fig. 5.48 shows a magnification of a part of the reaction layer. We see that in some "cells" there is a light-grey phase between the band (black) and the matrix phase (white). For the whole reaction layer the matrix phase consists of γ_2-$CoZn_{13}$. The composition of the light-grey phase lies between that of the matrix phase and the bands. An explanation of the different morphologies of the different "cells" may be as follows: the bands in one "cell" have the same orientation with respect to the polished surface. For different "cells" the bands have a different orientation with regard to this surface. For example, when a series of bands is

orientated perpendicular to the polished surface, then the real band spacing is measured. However, when the bands in a "cell" intersect with the polished surface at an angle different from 90^{o}, then a larger band spacing and a broader band is measured. The light-grey phase which appears in some "cells" (fig. 5.48) is then in fact a continuation under the surface of the (black) band at the surface.

For a better interpretation of the results of the Co(Si)- and Co_2Si-Zn diffusion couples it was necessary to start an investigation into the phase diagram of the Co-Si-Zn system at $395^{o}C$. This was done mainly with the help of ternary alloys with the exception of the Co-Zn axis of the diagram, which was determined by means of Co-Zn diffusion couples. The results of this investigation are summarized in the tentative phase diagram of fig. 5.49. The Co-rich corner of the diagram is still obscure because alloys with a composition lying in this region gave non-equilibrium results despite a 3-5 days annealing. The results of the Co-Zn diffusion couples differ from what might be expected from the known Co-Zn phase diagram[93]. According to our measurements the homogeneity region of the γ-$CoZn_4$ phase is divided up in two phases with a composition of $Co_{19-20}Zn_{81-80}$ and $Co_{24-27}Zn_{76-73}$ (resp. called γ' and γ''). Also the measured composition of the β phase ($Co_{43-47}Zn_{57-53}$) differs from the value of the Co-Zn phase diagram ($Co_{46-48}Zn_{54-52}$). The measured solubilities of Si in the Co-Zn intermetallic compounds were always found to be less than 1at%.

Letter	Diffusion couple	Remarks
A	Co(11.5at%Si)-Zn	Average composition of thin layer between substrate and reaction layer of which the latter showed no periodic structure
B	Co(11.5at%Si)-Zn	Average composition of band in γ_1 matrix
C	Co(11.5at%Si)-Zn	Average composition of band in γ_2 matrix
D	Co_2Si-Zn	Average composition of band
E	Co_2Si-Zn	Composition of light-grey phase in fig. 5.48.

Table 5.8. Measured compositions of bands in Co(Si)-Zn diffusion couples (see also fig. 5.49)

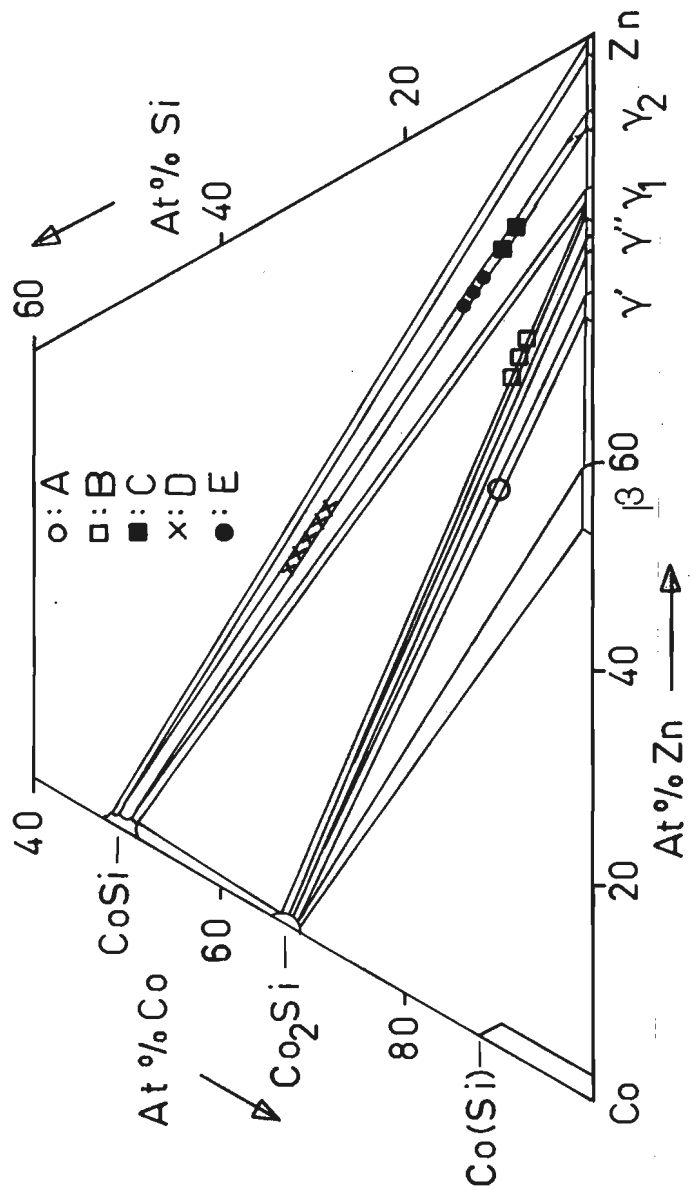

Fig. 5.49. Tentative 395°C isotherm of the Co-Zn-Si system. The letters A-E refer to measured compositions of bands in various Co(Si)-Zn couples, see table 5.8.

The letters A-E in this diagram represent the measured compositions of the various bands which appear in the reaction layers of the Co(Si)- and Co_2Si-Zn diffusion couples. In table 5.8 this has been further elaborated. For the Co_2Si-Zn diffusion couples all band compositions lie in the CoSi-$\gamma_2(CoZn_{13})$ two-phase regions, indicating that the bands are made up of CoSi particles in a γ-$CoZn_{13}$ matrix. For the Co(Si)-Zn couple two band compositions were measured: Bands at the Co-side of the reaction layer have a composition which lies in the Co_2Si-$\gamma_1(CoZn_8)$ two-phase region, whereas bands at the Zn side of the couple have a composition lying in the CoSi-$\gamma_2(CoZn_{13})$ two-phase region. Hence, these bands are made up of Co_2Si and CoSi particles in a γ_1 and γ_2 matrix respectively. As in the Fe(Si)-Zn couples the mean Si content of a band differs only slightly from the Si content of the terminal alloy. Hence, the diffusion path which represents the transition of the Co(Si) terminal alloy or compound to the band at the substrate will also run almost parallel to the Co-Zn axis. This again points to a very low mobility of Si in these couples and the same mechanism probably applies to the formation of a band at the substrate, as discussed in section 5.3.3.

Summarizing we can draw the following conclusions:

- The formation of periodic structures is not restricted to the Fe(Si)-Zn system, but has also been observed in other systems viz. the Fe(Ge)-Zn and Co(Si)-Zn systems.
- These systems all show the same characteristics, i.e. a periodic arrangement of two-phase bands; periodic structures in which the bands consist of single phase layers are not observed.
- The average Si content of the bands in the Fe(Si)- and Co(Si)-Zn couples differs only slightly from the Si content of the substrate, which indicates an immobility of Si during the formation of the band at the substrate. For the Fe(Ge)-Zn couples the difference between the average Ge content of a band and the Ge content of the Fe(Ge) substrate is larger; hence, the mobility of Ge will be larger, but probably not large enough in order to form a one-phase layer. Probably the band formation in the Fe(Ge)-Zn couples can be regarded as an intermediate case between the formation of a single phase layer (as for example in the Ni(Si)-Zn and FeAl-Zn couples) and the formation of the two-phase bands in the Co(Si)- and Fe(Si)-Zn diffusion couples.

- The immobility of Si also explains the fact that the absolute Si content rather than the relative Si content (with respect to saturation) of the substrate determines whether the bands are continuous or not. Due to the immobility of Si the amount of silicides in the band at the substrate is determined by the absolute amount of Si in the substrate. Then, the amount of intermetallic compound which is formed between the silicide particles is also fixed. When the substrate contains less Si this implies that the amount of intermetallic compound will be larger. The coherence between the silicides in a band will be smaller, which results in the non-continuous bands.

5.3.7 Discussion of the phenomenon of periodic structures

In this section we will submit the phenomenon of the formation of periodic structures in ternary diffusion couples to a critical argumentation in order to find an explanation for it. We will do this especially with the help of the Fe(Si)-Zn couples. The question is: why does the reaction in an Fe_3Si-Zn diffusion couple not proceed by a continuous, stationary growth of the different reaction layers (two-phase band and Fe-Zn intermetallic compounds), but in an apparently discontinuous way? This problem has been schematically visualized in fig. 5.50.

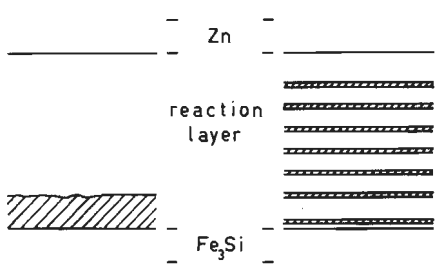

Fig. 5.50. Schematic visualization of the question why periodic structures develop. Left-hand and right-hand figures respectively show the expected and observed morphology in an Fe_3Si-Zn couple.

Let us assume for simplicity that only two reaction layers are formed in a diffusion couple viz. band and δ. Then, from the start it is essential to realize that the process is not characterized by an alternated formation (δ, band, δ, band, δ,....) of these two reaction

layers on the substrate. This can be clearly seen in fig. 5.51. We see that a new band is formed immediately on the substrate after the previous one has been released. This in fact means that an explanation of the phenomenon in terms of a Liesegang [94] [95] [96] mechanism can be excluded. The Liesegang mechanism implies that a new band is not produced until a critical supersaturation has been built up. This is obviously not the case. Hence, the process is rather characterized by a repeated formation of both reaction layers (band + δ, band + δ, band + δ,....). The periodic nature of the process is then reflected in the constant thickness of the layers.

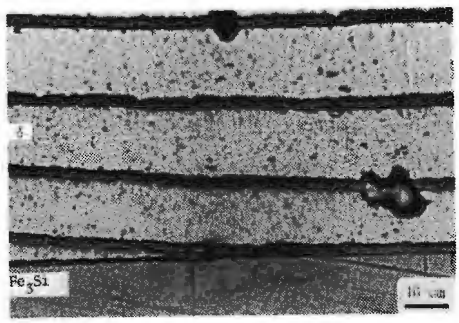

Fig. 5.51. Part of the reaction layer in an Fe_3Si-Zn couple. Notice that a band is formed immediately on the substrate after the previous one has been released.

In trying to find an explanation for this repeated formation of the reaction layers we were struck by the close resemblance with the behaviour of oxide scales under stress, as has been discussed in section 2.5, especially the repeated formation of cupric oxide films on copper at 500°C (fig. 2.12) strikes. Hence an investigation was set up in order to establish whether stresses could be responsible for the observed phenomena. Therefore, first an experiment was executed in which the generation of growth stresses was studied during the reaction in a pure Fe-Zn solid-solid diffusion couple. In order to guarantee a free development of the growth stresses in the couple, no external load was applied on the couple halves. Instead the couple was prepared by method e), as described in section 4.2. The thickness of the Fe substrate was about 200 µm. For the other dimensions of the couple see fig. 5.52a. The couple was annealed for 24h at 395°C. After the annealing treatment the couple was slowly cooled in the furnace.

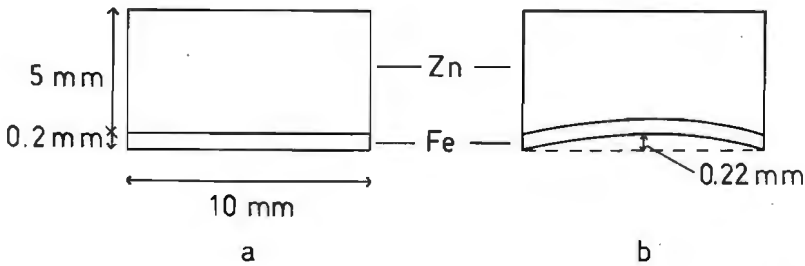

Fig. 5.52a-b. Dimensions of thin substrate Fe-Zn couple, used for the study of stress generation during the reaction in the couple.
a) before and b) after annealing, 24h, 395°C.

Together with the couple an Fe foil with the same dimensions as the foil used in the couple was annealed. This was done in order to check whether possible generated stresses were the result of, for example, recrystallisation processes in the foil. After the annealing treatment a clear bending of the couple was observed, indicating the generation of stresses. These stresses solely develop as a result of the growth of the reaction layer in the couple because the pure uncoated Fe foil remained flat. The dimensions of the couple after the annealing period are given in fig. 5.52-b. Fig. 5.53 gives a photomicrograph of the reaction layer. We see that over a large distance along the length of the reaction layer no cracks are observed.

Fig. 5.53. Thin substrate Fe-Zn couple, 24h, 395°C. Notice the absence of cracks in the reaction layer.

This clearly indicates that the growth stresses in the couple are not relieved by fracture of the layer, but by means of plastic deformation of the thin Fe substrate. From the shape of the bending (reaction layer at the convex side of the Fe substrate), and the fact that the reaction takes place at the substrate/layer interface (Zn is practically the only diffusingcomponent) we can conclude that the reaction layer is under a compressive stress.

When we neglect the contribution of the FeSi particles to the generation of stresses, then a two-phase (δ + FeSi) band, which is formed on the substrate of an Fe_3Si-Zn couple, will also be under a compressive stress. If we assume that these stresses are responsible for a release of a band from the substrate, we may expect that in an Fe_3Si-Zn couple with a thin Fe_3Si substrate the thickness of the bands will change. The bands will be thicker because the stresses will now be relieved by the facilitated plastic deformation of the Fe_3Si substrate. However, we must realize that the plastic deformation of the thin Fe_3Si substrate will not take place as easily as in the Fe, because of the increased brittleness of the Fe_3Si alloy. This appears from recent measurements of the elastic constants of Fe(Si) single crystals in the range 0-25 at% Si[97]. Fig. 5.54 gives a photomicrograph of the reaction layer formed on a thin substrate of an Fe_3Si-Zn diffusion couple. Preparation method and dimensions were the same as for the thin substrate Fe-Zn diffusion couple. We see, as expected, that the band in the δ layer is much thicker than the bands formed in a usual thick substrate Fe_3Si-Zn couple (about 6 µm instead of 1.5-2 µm). No bending of the substrate could be detected. A

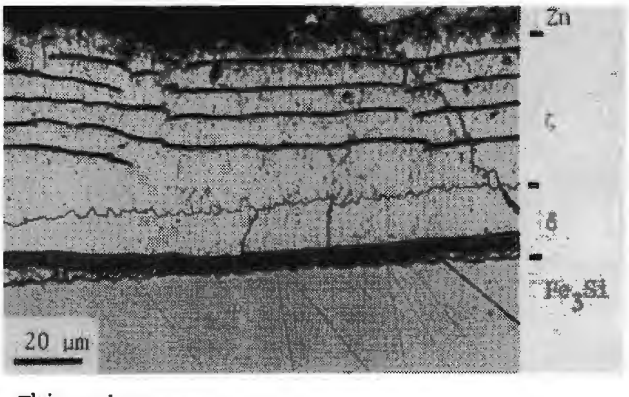

Fig. 5.54. Thin substrate Fe_3Si-Zn couple, 24h.

peculiarity can be seen for the bands lying in the ζ phase. The thickness of these bands is much smaller (< 1 μm) than of the bands observed in a thick substrate couple. We will come back to this point later on. Other experiments with thin substrate couples gave miscellaneous results. Sometimes thicker bands were observed (up to 3.5 μm), sometimes not. The difference for bands lying in the δ or ζ layer was more often observed. In none of the cases significant bending of the substrate could be noticed. These differences found in the various thin substrate Fe_3Si-Zn couples are probably due to the fact that the plastic deformation of the Fe_3Si substrate (and the corresponding stress relief) is not only determined by its thickness, but that apparently other factors play a role too. So, though there are still some obscurities, we can conclude from the thin substrate experiments, that growth stresses are very likely to play a role in the development of periodic structures.

Now that we have experimentally shown the role of stresses in the process of the formation of periodic structures we can draw up a model describing this process. In fig. 5.55 the several steps of this model have been visualized schematically. In step a) a band is formed at the substrate. The band will be under a compressive stress, which is indicated by the arrows. The stress will be maximal at the Fe_3Si substrate/band interface. When the band grows and becomes thicker these stresses will increase. When the band has reached a critical thickness (step b), the stresses will have become so large that they cause a blistering of the band (step c). In the void thus created, the reaction can start afresh by the formation of δ and another band (step d). Eventually, by a lateral growth of the δ phase or by the formation of more voids the whole band is lifted off and at the substrate the initial situation of step a) is obtained. The process of stress build-up and relief in a band started again, resulting in a periodic structure. Some remarks on some of the steps in particular are:

- the blistering of a band in step c) implies a bad adherence of the band on the substrate. As we have seen in section 2.5 the adherence of a reaction layer is decreased by the coalescence of vacancies. This may also play a role here. As has been mentioned in section 5.3.3 (fig. 5.34) the formation of a band is accompanied by an Fe diffusion flux through the band. This flux will be accompanied by a flux of vacancies which will coalesce at the band/substrate

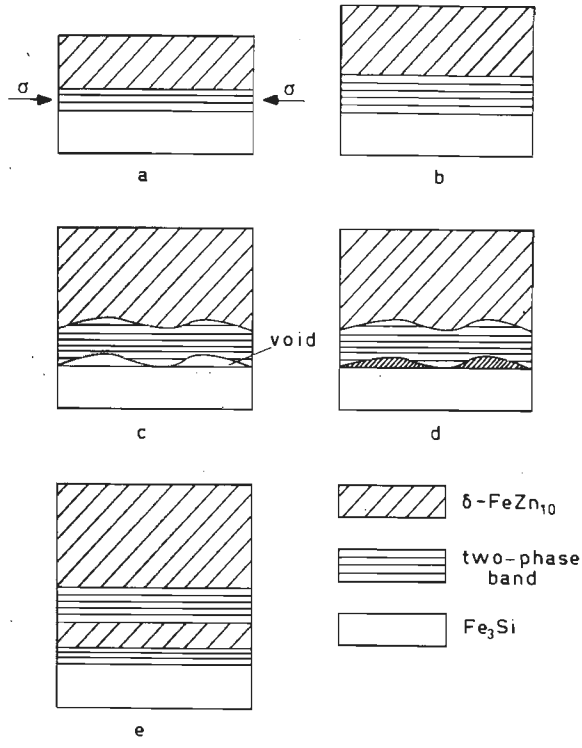

Fig. 5.55. Model explaining the development of a periodic structure in Fe(Si)-Zn diffusion couples (see also text).

interface, causing a deterioration of the band adherence.

- For clarity steps c) and d) are drawn as two separate steps. The transition between these two steps will be very fast and, in fact, occurs almost simultaneously.
- The restart of the reaction in step d) occurs by a process of surface diffusion of the Zn. Because of the high vapour pressure of the Zn at the used reaction temperature (25°C below the melting point of Zn) this is certainly not an unrealistic assumption. The ability of Zn to diffuse via the surface is also evident from an observation often made in the diffusion couples viz. the formation of reaction products at places on the substrate which were initially not in contact with the Zn (for example around edges or even at the back side of the substrate).

With this model in mind some features of the phenomenon of

periodic structures, as they appeared from the results in the preceding sections can now be further elucidated. As has been mentioned before, the generation of stresses in a band arises from volume constraints of the metal-zinc intermetallic compound in the band. This assumption is supported by the observation that all periodic structures found up to now consist of two-phase bands. This also means that, though our model is in essence a stress model, the diffusion mechanism at the substrate is also important.
For as we have seen in section 5.3.3 the development of a two-phase band at the substrate is a result of diffusion properties of the various components. Especially the low mobility of Si seems to be important because this prevents the layer to close up and enables δ to be formed between the silicide particles.

As we have seen, the bands formed in an Fe_5Si_3-Zn couple are thicker then those formed in an Fe_3Si-Zn couple. This can be explained from the fact that these bands contain less δ. Consequently, the stresses which develop in the band will be smaller, and the bands will be able to grow thicker before the critical stress is reached at which blistering occurs.

We must be careful in comparing the results of the Fe_3Si- and Fe_5Si_3-Zn couples solely from a viewpoint of the δ content in the alloys, for we neglect eventual changes in the plastic properties of the substrate. However, both Fe_3Si and Fe_5Si_3 alloys will be very brittle, so no contribution to the relief of the stresses is expected from these alloys. However, in the case of the Fe(9.0at%Si)-Zn couple the neglect of plastic flow probably is not allowed. Büchner and Kemnitz[97], who measured the elastic constants of Fe(Si) single crystals in dependence of composition, noticed an increase in the measured elastic constants above 11at%Si. Though we do not deal with single crystals, we may assume that there is a considerable difference in the plastic properties of both alloys: the Fe(9.0at%Si) alloy will have a greater plasticity compared to the Fe_3Si alloy. And this is, probably, the reason that in the Fe(9.0at%Si)-Zn couples no lifting-off of the formed band is observed. Because of the greater plasticity of the Fe(9at%Si) alloy the growth stresses which are generated in the band at the substrate, can more easily be relieved by plastic deformation of the substrate.

If the band formation is influenced by the underlying substrate,

then one can expect also an influence from the layer lying behind the band. The difference in band spacing for bands in the ζ layer of fig. 5.54 points in this direction. When these bands were formed intitially at the substrate probably no δ layer (as usual), but the ζ layer was formed behind the band. (This retarded δ formation has also been observed in pure Fe-Zn couples[74]). Differences in plastic properties of the δ and ζ phases cause then the difference in band spacing. Unfortunately this cannot be verified, because data on the plastic properties of these phases are not available. A crucial step in our model is the restart of the reaction in the void resulting from the blistering of the band (step d). For this a component with a high tendency for surface diffusion is needed. Zn, with its high vapour pressure certainly satisfies this condition. Because the formation of periodic structures was only observed in couples with Zn as a starting material, it appears even that this is a necessary condition for the formation of a periodic structure in a couple.

Having discussed this model for the Fe(Si)-Zn couples, one can wonder whether it also applies to the Co_2Si-Zn couples. As we have seen the reaction layer of these couples consists of "cells" with different morphologies of the periodic structure. This was explained by a difference in orientation, with respect to the polished surface, for bands in various "cells". If we assume that the same model, as described in this section, can be applied to these couples, then this means that for "cells" in which the bands are not orientated perpendicular to the polished surface, these bands are lifted off from the Co_2Si substrate at an angle. In order to elaborate this view, further research is necessary. Especially the study of Co_2Si-Zn couples in which the Co_2Si substrate consists of a single crystal would be of great value.

As a summary of this section we will postulate some necessary conditions which have to be satisfied for a periodic structure to develop in a diffusion couple. We will do this with the help of a hypothetical diffusion couple Y(Z)-X:

- When X reacts with the Z(Y) substrate a two-phase band consisting of Y_cZ_d particles (richer in Y than the substrate) and Y_aX_b intermetallic compound is formed on the substrate. This condition is closely related to the diffusion properties of the component Y,

which has to have a low mobility.

- The Y_aZ_b intermetallic compound, formed between the Y_cZ_d particles, causes generation of a compressive stress in the band.
- No relief of the stresses occurs by plastic deformation of the Y(Z) substrate.
- The adherence of the two-phase band on the substrate is bad, resulting in a blistering of the band.
- In order to restart the reaction at the substrate after the blistering of the band, component X must have a high tendency for surface diffusion.

Further research is needed to establish whether these conditions are both necessary and sufficient.

REFERENCES

1. G.F. Bastin and G. D. Rieck, Met. Trans. 5 (1974) 1817.
2. F.J.J. van Loo and G.D. Rieck, Acta Metall. 21 (1973) 73.
3. M.M.P. Janssen, Met. Trans. 4 (1973) 1623.
4. J.A. van Beek, S.A. Stolk and F.J.J. van Loo, Z. Metallkde. 73 (1982) 439.
5. G.F. Bastin, F.J.J. van Loo and G.D. Rieck, ibid. 65 (1974) 656.
6. D.S. Williams, R.A. Rapp and J.P. Hirth, Met. Trans. A 12 (1981) 639.
7. G.H. Cheng and M.A. Dayananda, ibid. 10 (1979) 1407.
8. G.H. Cheng and M.A. Dayananda, ibid. 10 (1979) 1415.
9. R.D. Sisson and M.A. Dayananda, ibid. 8 (1977) 1849.
10. G.W. Roper and D.P. Whittle, Met. Sci. 14 (1980) 21.
11. J.S. Kirkaldy and L.C. Brown, Can. Met. Quart. 2 (1963) 89.
12. M.A.J.Th. Laheij, F.J.J. van Loo and R. Metselaar, Ox. Met. 14 (1980) 207.
13. F.J.J. van Loo, G.F. Bastin and A.J.H. Leenen, J. Less Comm. Met. 57 (1978) 111.
14. F.J.J. van Loo, G.F. Bastin, J.W.G.A. Vrolijk and J.J.M. Hendriks, ibid. 72 (1980) 225.
15. F.J.J. van Loo, J.W.G.A. Vrolijk and G.F. Bastin, ibid. 77 (1981) 121.
16. D. Horstmann, Proc. Seminar on Galvanizing Silicon-Containing Steels, Liège, Belgium 1975, p. 86.
17. C. Allen and J. Mackowiak, J. Corr. Sci. 3 (1963) 87.
18. D. Horstmann, Arch. Eisenhüttenwes. 25 (1954) 527.
19. E. Scheil and H. Wurst, Z. Metallkde. 29 (1937) 224.
20. R.W. Sandelin, Am. Hot Dip Galvanizers Ass. Pittsburgh (1963).
21. N. Dreulle, Proc. Seminar on Galvanizing Silicon-Containing Steels, Liège, Belgium 1975, p. 1.
22. H. Gutmann and P. Niessen, Can. Met. Quart. 11 (1972) 609.
23. L.P. Devillers, H. Gutmann and P. Niessen, Proc. Seminar on Galvanizing Silicon-Containing Steels, Liège, Belgium 1975, p. 48.
24. D. Horstmann, Proc. 11th Int. Galvanizing Conference, Madrid 1976, p. 19.
25. O.B. Sorensen and E. Maahn, Proc. Second Int. ILZRO Galvanizing Seminar, St. Louis, Missouri 1976, p. 9.1.

26. L. Habraken, Proc. 12th Int. Galvanizing Conference Paris 1979 p. 121.
27. V. Leroy, J. Pelerin, C. Emond and L. Habraken, Second Int. ILZRO Galvanizing Seminar, St. Louis, Missouri 1976, p. 13.1.
28. V. Leroy, C. Emond, P. Cosse and L. Habraken, Proc. Seminar on Galvanizing Silicon-Containing Steels, Liège, Belgium 1975, p. 97.
29. A. Ferrier, C.R. Acad. Sci. Paris serie C 283 (1976) 659.
30. H. Gutmann and P. Niessen, Proc. Seminar on Galvanizing Silicon-Containing Steels, Liège, Belgium 1975, p. 198.
31. U. Huebner and F. Nilmen, Proc. 12th Int. Galvanizing Conference, Paris 1979, p. 156.
32. M. Ürednicêk and J.S. Kirkaldy, Z. Metallkde. 64 (1973) 899.
33. Y. Adda and J. Philibert, La Diffusion dans les Solides tome I, Presses Universitaires de France, Paris (1966).
34. P.G. Shewmon, Diffusion in Solids, Ed. Mc Graw-Hill Book Company, Inc., New York (1963).
35. A.D. Smigelskas and E.D. Kirkendall, Trans. Met. Soc. AIME 171 (1947) 130.
36. L. Boltzmann, Ann. der Physik 53 (1894) 959.
37. C. Matano, Japan. J. Physics 8 (1933) 109.
38. F.J.J. van Loo, Diffusion in the Titanium-Aluminium system, Thesis, Eindhoven University of Technology (1971).
39. G.F. Bastin, Diffusion in the Titanium-Nickel system, Thesis, Eindhoven University of Technology (1972).
40. M.A. Dayananda, Trans. TMS-AIME 242 (1968) 1369.
41. L.S. Darken, Trans. Met. Soc. AIME 175 (1948) 184.
42. L.S. Darken, ibid. 180 (1949) 430.
43. J.S. Kirkaldy, Advances in Materials Research, vol. 4, Ed. H. Herman, Wiley, New York (1970), p. 55.
44. L. Onsager, New York Ac. of Sciences, Annals 46 (1945) 241.
45. J.S. Kirkaldy, Can. J. Phys. 36 (1958) 917.
46. J. Philibert and A.G. Guy, C.R. Acad. Sci. Paris serie C, 257 (1963) 2281.
47. M.A. Dayananda and R.E. Grace, Trans. TMS-AIME 223 (1965) 1287.
48. P.T. Carlson, M.A. Dayananda and R.E. Grace, Met. Trans. 3 (1972) 819.
49. C. Wagner, Acta Met. 17 (1969) 99.

50. J.B. Clark, Trans. Met. Soc. AIME 227 (1963) 1250.
51. G.W. Roper and D.P. Whittle, Met. Sci. 14 (1980) 541.
52. H. Schmalzried, Treatise on Solid State Chemistry, vol. 4 Reactivity of solids, Ed. N.B. Hannay, Plenum Press, New York (1976), p. 273.
53. M.A.J.Th. Laheij, F.J.J. van Loo and R. Metselaar, Proc. 9th Int. Symposium on the Reactivity of Solids, Cracow, Poland 1980, p.187 .
54. C. Wagner, J. Electrochem. Soc. 103 (1956) 571.
55. G.J. Yurek, R.A. Rapp and J.P. Hirth, Met. Trans. 4 (1973) 1293.
56. F.J.J. van Loo and G.F. Bastin, Proc. of the Conference on Diffusion in Metals and Alloys, Tihany, Hungary 1982.
57. J.S. Kirkaldy, Oxidation in Metals and Alloys, Ed. D.L. Douglass, ASM, Ohio, USA (1971), p. 101.
58. A.R. Evans, Trans. Electrochem. Soc. 91 (1947) 547.
59. R.E. Pawel, J.V. Cathcart and J.J. Campbell, ibid. 110 (1963) 551.
60. W. Jaenicke and S. Leistikow, Z. Phys. Chem. 15 (1958) 175.
61. N.B. Pilling and R.E. Bedworth, J. Inst. Met. 29 (1923) 529.
62. O. Kubaschewski and B.E. Hopkins, Oxidation of Metals and Alloys (2nd edition), Ed. Butterworths, London (1965).
63. J. Stringer, Corr. Sci. 10 (1970) 513.
64. F.R.N. Nabarro, Report of a Conference on the Strength of Solids, Phys. Soc. London 75 (1948).
65. C. Herring, J. Appl. Phys. 21 (1950) 437.
66. D.L. Douglass, Oxidation of Metals and Alloys, Ed. D.L. Douglass, ASM Ohio, USA (1971), p. 137.
67. H.J. Engell and F. Wever, Acta Met. 5 (1957) 695.
68. R.F. Tylecote, J. Inst. Met. 78 (1950) 301.
69. B.W. Dunnington, F.H. Beck and M.G. Fontana, Corrosion 8 (1952) 2.
70. J.D. Mackenzie and C.E. Birchenall, Corrosion 13 (1957) 783t.
71. G.D.S. Price, The control of attack by molten zinc and zinc-containing alloys on solid metals, Thesis, University of Cambridge (1971).
72. Private communication of J.A. Bonders in ref. 73.
73. G. Dearnally and N.E.W. Hartley, Physics Letters A 46 (1974) 345.
74. M. Onishi, Y. Wakamatsu and H.Miura, Trans. Jap. Inst. Met. 15 (1974) 331.
75. J. Schramm, Z. Metallkde. 28 (1936) 203.

76. O. Kubaschewski, Iron-Binary Phase Diagrams, Springer-Verlag Berlin (1982).
77. M. Hansen and K. Anderko, Constitution of Binary Alloys, Mc Graw-Hill Book Company, Inc., New York (1958).
78. R.P. Eliott, Constitution of Binary Alloys, First Supplement, Mc Graw-Hill Book Company, Inc., New York (1965).
79. J. Schramm, Z. Metallkde. 29 (1937) 222.
80. J. Schramm, ibid. 30 (1938) 122.
81. S. Budurov, P. Kovatchev, N. Stojiev and Z. Kanrenova, ibid. 63 (1972) 348.
82. A. Ferrier, Mem. Sci. Rev. Met. 76 (1979) 777.
83. A.K. Jena and K. Löhberg, Z. Metallkde. 73 (1982) 517.
84. G.F. Bastin, F.J.J. van Loo and G.D. Rieck, ibid. 68 (1977) 359.
85. W. Köster and T. Gödecke, ibid. 61 (1970) 649.
86. M. Urednicèk and J.S. Kirkaldy, ibid. 64 (1973) 419.
87. D. Horstmann, Proc. of the 4th Int. Conference on Hot-Dip Galvanizing, London 1957, p. 29.
88. W. Köster and T. Gödecke, Z. Metallkde.59 (1968) 605.
89. J. Schramm, ibid. 28 (1936) 159.
90. D.I. Cameron and G.J. Harvey, J. Aust. Inst. Metals 14 (1969) 255.
91. J.W. Martin and R.D. Doherty, Stability of Microstructures in Metallic Systems, Cambridge University Press, Cambridge (1976).
92. Y. Adda and J. Philibert, La Diffusion dans les Solides tome II, Presses Universitaires de France, Paris (1966).
93. H.H. Stadelmaier, J.M. Brett and G. Hofer, Z. Metallkde. 59 (1968) 881.
94. R.E. Liesegang, Natur Wochenschr. 11 (1896) 353.
95. W. Ostwald, Lehrbuch der Allgemeinen Chemie, Engelman Verlag, Leipzig (1897).
96. V.A. van Rooijen, E.W. van Royen, J. Vrijen and S. Radelaar, Acta Met. 23 (1975) 987.
97. A.R. Büchner and H.D. Kemmitz, Z. Metallkde. 72 (1981) 575.

SUMMARY

This thesis deals with an investigation into the influence of the elements aluminium and silicon present in iron, on the reaction between iron and zinc. To this end Fe(0-50at%Al)-Zn(Fe), (450°C, solid-liquid) and Fe(0-37.5at%Si)-Zn, (395°C, solid-solid) diffusion couples were prepared. From the results obtained with these couples we can formulate a general rule which reads as follows: During the reaction between Fe(X) alloys (X = Al, Si) and Zn only Fe-Zn intermetallic compounds will develop, if on the basis of mass balance arguments it appears that the liberated component X can be accomodated by dissolving in an Fe-Zn intermetallic compound. If this is not possible, then besides the Fe-Zn intermetallic compounds other (X-containing) compounds are formed. In the case of the Fe(Al)-Zn(Fe) couples this has been observed in the FeAl-Zn(Fe) couple, in which a closed Fe_2Al_5(Zn) layer develops on the FeAl substrate followed by the Fe-Zn intermetallic compounds.

The results obtained with Fe(Al)-Zn(Fe) couples are discussed in relation to the inhibiting effect of Al additions to the Zn bath during the process of hot-dip galvanizing. The absence of an inhibiting effect in the Fe(Al)-Zn(Fe) couples is due to a much lower mobility of Al in the solid Fe(Al) alloy compared to a melt.

In the case of Fe(Si)-Zn couples the maximum Si content up to which only Fe-Zn intermetallic compounds are formed in the couples is 6.3 at%. In the case of the Fe(2.3at%Si)- and Fe(6.3 at% Si)-Zn couples a two-phase $\delta+\zeta$ zone develops in the reaction layer. A perturbation model, based on an local difference in dissolved Si in the δ phase along the δ/ζ phase boundary, is drawn-up in order to explain the development of this zone. The results obtained with the Fe(0-6.3 at%Si)-Zn couples are discussed in relation to the process of hot-dip galvanizing Si-containing iron. A model is set-up which explains the increased reactivity when galvanizing iron with a Si content around 0.8at%. The model is compared to other models dealing with this subject.

For higher Si contents in the terminal Fe(Si) alloy other, Si-containing, layers develop on the Fe(Si) substrate of the couple. Within the investigated Si concentration range (9.0-37.5at%) this is always a two-phase layer consisting of iron-silicide particles and δ.

For the Fe(9.0at%Si)-Zn couples the iron-silicide particles consist of Fe_3Si, while for the couples with higher Si contents in the terminal Fe(Si) alloys they always consist of FeSi. The development of this two-phase layer is closely connected with a very low mobility of Si at the reaction temperature used.

For annealing times longer than 1h a reaction layer with a periodic structure develops in the Fe_3Si- and Fe_5Si_3-Zn diffusion couples. This structure is made up of thin bands which are lying at regular distances from each other in the main reaction layer, which consists of the δ- and ζ(Fe-Zn) intermetallic compounds. These thin bands consist of small FeSi particles. The influence of the Si content in the terminal Fe(Si) alloy on the formation of the periodic structure is investigated and discussed.

Other ternary diffusion couples have been tested for the occurrence of this phenomenon. So far it has been found in the Fe(18.0at% Ge)-, Co(11.5 at%Si)-and Co_2Si-Zn couples. In the Co_2Si-Zn diffusion couples a crystallographic relationship between the periodic structure and the grains of the Co_2Si substrate has been observed. From experiments with thin-substrate diffusion couples, it appears that growth stresses, which develop in the FeSi + δ band formed on the substrate are very likely to play a role in the development of a periodic structure. A model based on the action of these stresses is drawn up in order to explain the formation of a periodic structure. A further elaboration of this model is needed in order to incorporate the results obtained with the Co_2Si-Zn diffusion couples. Finally some necessary conditions are given for a reaction layer with a periodic structure to develop in a ternary diffusion couple. Further research is necessary in order to establish whether these conditions are both necessary and sufficient.

Summarizing, in the light of our original purposes, we can say that:

- No relation has been observed between the results obtained with the Fe(Al)-Zn(Fe) couples and the inhibiting effect of aluminium additions to the zinc bath during the proces of hot-dip galvanizing.
- Silicon additions to the iron have a disturbing effect on the formation of the ζ-$FeZn_{13}$ layer during the reaction between iron and zinc. This effect explains well the observed phenomena during hot-dip galvanizing of iron with a silicon content around 0.8at%.

- From the results obtained with Fe($\geq$9.0at%Si)-Zn diffusion couples it appears that a very low mobility of one of the components and the generation of growth stresses in a reaction layer play an important role in the development of reaction layer morphologies in ternary diffusion couples.

SAMENVATTING

Het onderzoek beschreven in dit proefschrift vindt zijn oorsprong in het proces van thermisch verzinken van ijzer. Bij dit proces wordt een ijzeren voorwerp gedurende een bepaalde tijd ondergedompeld in een bad dat vloeibaar zink bevat bij een temperatuur van 450-460^{o}C. Hierbij vindt er een reactie plaats tussen het ijzer en zink en wordt er op het ijzeroppervlak een reactielaag gevormd. Deze reactielaag beschermt het onderliggende ijzer tegen roesten. Bij een dompeltijd van 5 min. en een temperatuur van het zinkbad van 450^{o}C bedraagt de dikte van deze reactielaag ongeveer 80 µm. Dit proces is reeds vrij oud (135 jaren geleden werd het voor het eerst toegepast) en wordt op grote schaal gebruikt voor het beschermen van o.a. hekwerken, containers en andere voorwerpen die aan de buitenlucht worden blootgesteld.

De laatste 10-20 jaren, echter, treden er problemen op in dit proces t.g.v. veranderde ijzerfabricage methoden. Het te verzinken ijzer bevat daardoor een weinig silicium. Dit silicium heeft een zeer nadelige invloed op de reactie tussen het ijzer en het zink, daar het de reactiviteit enorm vergroot. Onder dezelfde omstandigheden als hierboven genoemd, wordt er nu een reactielaag met een dikte van ongeveer 400 µm gevormd. Het silicium in het ijzer heeft zijn nadelige effect in twee gescheiden concentratiegebieden die rond 0.15 en 0.8 at% liggen. T.g.v. deze vergrote reactiviteit neemt niet alleen het zinkverbruik toe, maar heeft de gevormde reactielaag t.g.v. zijn veel grotere dikte slechte mechanische eigenschappen. Tevens ziet de laag er aan de buitenkant dof en zwart uit. Daar 40% van de wereldjaarproductie aan zink gebruikt wordt voor thermisch verzinken, is het duidelijk dat de verzinkerijen voor grote problemen geplaatst worden.

Aluminium toevoegingen aan het zinkbad in de grootte orde van 0.5-2 at% blijken een gunstige invloed te hebben. Door de vorming van een aluminiumrijke laag op het ijzer wordt de reactie tussen ijzer en zink in het begin geremd, waardoor de reactiviteit afneemt.

Een doel van het onderzoek was de invloed die de elementen aluminium en silicium hebben op de reactie tussen ijzer en zink nader te bestuderen.
De diffusiekoppeltechniek is hierbij een belangrijk hulpmiddel.

In deze methode klemt men twee glad gepolijste plakjes metaal of legering op elkaar die vervolgens verhit worden in een oven (zgn. vast-vast diffusiekoppel) of men dompelt een glad gepolijst plakje metaal of legering in een smelt van een ander metaal (zgn. vast-vloeibaar diffusiekoppel). Na een bepaalde stook- of dompeltijd kan dan de gevormde reactielaag bestudeerd worden.

Het blijkt dat aluminium en silicium reeds in zeer kleine hoeveelheden hun invloed op de reactie tussen ijzer en zink doen gelden. Door de gebieden van onderzochte aluminium- en silicium concentraties in de uitgangsmaterialen van de diffusiekoppels uit te breiden naar hogere concentraties wilden we een tweede doelstelling, die niet zo gericht is op het proces van thermisch verzinken van ijzer, verwezenlijken. Het betreft hier de bestudering van vaste-stof diffusie verschijnselen in metaalsystemen met drie componenten (ternaire systemen) en in het bijzonder van de morfologie van de ontstane reactielagen in ternaire diffusiekoppels. In tegenstelling tot een diffusiekoppel met twee componenten (binair diffusiekoppel), waar de gevormde reactielaag bestaat uit laagjes die van elkaar gescheiden worden door grenzen evenwijdig aan het oorspronkelijk contactoppervlak , kunnen in ternaire diffusiekoppels reactielagen ontstaan waarvan de grenzen niet evenwijdig liggen aan het oorspronkelijk contactoppervlak (zgn.twee-fase grenzen of-zones) of lagen waarbij het ene gevormde reactieproduct als uitscheidingen verspreid liggen in een andere reactielaag (zgn. precipitatie zones). Bestudering van deze morfologieën is belangrijk daar zij een van de factoren zijn die de stabiliteit van een reactielaag (bijv. een beschermende coating op een metalen ondergrond) bepalen.

Ter verwezenlijking van beide doelstellingen werden de volgende diffusiekoppels bereid en bestudeerd:
Fe (0-50 at% Al)-Zn (verzadigd met Fe), vast-vloeibaar diffusiekoppels, gedompeld bij een temperatuur van 450^{o}C,
en Fe (0-37.5 at% Si)-Zn, vast-vast diffusiekoppels, verhit bij een temperatuur van 395^{o}C.
Opgemerkt dient te worden dat de invloed van aluminium op de reactie tussen ijzer en zink bestudeerd werd door het aluminium toe te voegen aan het ijzer. Dit in tegenstelling tot de praktijk, waar zoals we gezien hebben het aluminium aan het zinkbad wordt toegevoegd. Uit de resultaten verkregen met deze koppels kunnen we voor de reactie die

optreedt in deze koppels de volgende algemene regel afleiden: Gedurende de reactie tussen een Fe(X) legering (X=Al,Si) en Zn zullen er alleen Fe-Zn intermetallische verbindingen gevormd worden, indien uit de massabalansregel blijkt dat de vrijgekomen component X volledig opgelost kan worden in de Fe-Zn intermetallische verbindingen. Is dit niet het geval dan zullen er tevens andere dan Fe-Zn intermetallische verbindingen ontstaan.
In het geval van de Fe(Al)-Zn(Fe) koppels is dit laatste waargenomen in het FeAl-Zn(Fe) koppel. In dit koppel wordt er op het FeAl substraat een gesloten Fe_2Al_5(Zn) laag gevormd gevolgd door de Fe-Zn intermetallische verbindingen. De resultaten van de Fe(Al)-Zn(Fe) koppels worden in relatie gebracht met het remmende effect van Al toevoegingen aan het zinkbad tijdens het thermisch verzinken van Fe. De afwezigheid van een remmend effect in de Fe(Al)-Zn(Fe) koppels (immers, behalve in het FeAl-Zn(Fe) koppel, worden in deze koppels alleen maar Fe-Zn intermetallische verbindingen gevormd) wordt verklaard uit de veel geringere mobiliteit van Al in de vaste Fe(Al) legering vergeleken met vloeibaar zink.

De uiterste Si concentratie waarbij uitsluitend Fe-Zn intermetallische verbindingen gevormd worden in de Fe(Si)-Zn koppels bedraagt 6.3 at% Si. Het Si blijkt een duidelijke invloed te hebben op de reactie tussen Fe en Zn: De vorming van de ζ-$FeZn_{13}$ verbindingen aan de grens met de δ-$FeZn_{10}$ laag wordt verstoord, hetgeen resulteert in een twee-fasige $\delta+\zeta$ zone in de Fe(2.3 at% Si) en Fe(6.3 at% Si)-Zn koppels. De vorming van deze twee-fase zone wordt verklaard met een perturbatie model gebaseerd op een toevallig plaatselijk verschil in opgelost Si in de δ laag langs de grens met de ζ laag. Uitgaande van deze verstoorde ζ vorming aan de δ/ζ grens wordt een model ontwikkeld ter verklaring van het effect dat Si heeft op de reactie tijdens het thermisch verzinken van ijzer met een Si gehalte van ongeveer 0.8 at%. Dit model wordt vergeleken met andere modellen betreffende dit verschijnsel.

In de Fe($\geq$9.0at%Si)-Zn koppels wordt er aan het Fe(Si) substraat een laag gevormd bestaande uit andere dan alleen maar Fe-Zn intermetallische verbindingen. Het betreft hier in alle gevallen twee-fasige lagen bestaande uit Fe_3Si deeltjes (voor de Fe(9.0at%Si)-Zn koppels) of FeSi deeltjes (voor de andere koppels) liggend in een matrix van een Fe-Zn intermetallische verbinding. Het ontstaan van deze twee-fasige lagen lijkt ten nauwst

samen te hangen met een zeer lage mobiliteit van Si bij de gebruikte reactietemperatuur.

In de Fe_3Si en Fe_5Si_3-Zn koppels treedt bij stooktijden langer dan 1 uur een zeer interessant verschijnsel op nl. de vorming van een reactielaag met een periodieke structuur. In de reactielaag, die zelf bestaat uit δ- en ζ Fe-Zn lagen, worden op regelmatige afstand van elkaar dunne banden gevonden. Deze banden bestaan uit kleine FeSi deeltjes liggend in een matrix van de Fe-Zn intermetallische verbinding. De invloed van Si in de Fe(Si) legering op de vorming van de periodieke structuur is onderzocht. Tevens zijn andere ternaire diffusiekoppels onderzocht op dit verschijnsel, waarbij het werd waargenomen in de Fe(18.0 at% Ge)-, Co(11.5 at% Si)- en Co_2Si-Zn diffusiekoppels. In het Co_2Si-Zn koppel bestaat de reactielaag uit cellen, ieder met een verschillende morfologie en periodiciteit.Dit wordt verklaard door een verschillende oriëntatie van de banden in de cellen t.o.v. het gepolijste oppervlak. Iedere cel in de reactielaag komt overeen met een andere korrel in het Co_2Si substraat. Dit wijst op een kristallografische oriëntatierelatie tussen de gevormde periodieke structuur in een cel en de korrel in het Co_2Si substraat waarop hij gevormd wordt.

Uit experimenten met dun-substraat-Fe_3Si-Zn koppels blijkt dat spanningen opgewekt in een band aan het substraat een belangrijke rol spelen bij de vorming van een reactielaag met een periodieke structuur. Een model is opgesteld ter verklaring van de vorming van deze periodieke structuur. Dit model komt op het volgende neer: Wanneer een band aan het substraat wordt gevormd, zal deze onder een drukspanning staan. Deze spanning neemt toe met de dikte van de band. Bereikt de band een bepaalde kritische dikte dan zal er een "blaarvorming" (Engels: blistering) van de band optreden waardoor hij als het ware loslaat van het substraat. T.g.v. deze "blaarvorming" wordt er een "vers" oppervlak gecreëerd waarop de reactie weer opnieuw kan plaatsvinden, resulterend in de vorming van de waargenomen periodieke structuur. Met dit model kunnen verschillende verschijnselen waargenomen in de diverse koppels met een periodieke structuur verklaard worden. Verder onderzoek is nodig om de resultaten verkregen met de Co_2Si-Zn koppels in te passen in dit model.

Tenslotte wordt een aantal noodzakelijke voorwaarden genoemd waaraan de uitgangsmaterialen van een ternair diffusiekoppel moeten voldoen,

wil er zich een periodieke structuur vormen. Verder onderzoek is nodig om uit te maken of dit behalve noodzakelijke ook voldoende voorwaarden zijn.

Resumerend kunnen we in het licht van onze oorspronkelijke doelstellingen stellen dat:

- Er geen verband is geconstateerd tussen de resultaten verkregen met de Fe(Al)-Zn(Fe) koppels en het remmende effect van Al toevoegingen aan het zinkbad tijdens het proces van thermisch verzinken van ijzer.
- Si toevoegingen aan Fe een verstorend effect hebben op de vorming van de $\zeta FeZn_{13}$ verbinding tijdens de reactie tussen Fe en Zn. Dit effect kan de waargenomen verschijnselen tijdens het thermisch verzinken van ijzer met een Si gehalte van ongeveer 0.8 at% goed verklaren.
- Uit het onderzoek met Fe($\geq$9.0at%Si)-Zn diffusiekoppels blijkt dat een geringe mobiliteit van een van de componenten en spanningen opgewekt in een gevormde reactielaag een zeer grote rol spelen bij de vorming van bepaalde reactielaagmorfologieën in ternaire diffusiekoppels.

Levensbericht.

Kazimierz (Edjoe) Osinski werd op 15 juni 1954 geboren te Budel-Dorplein. Van 1966-1971 werd de H.B.S.-B-opleiding gevolgd aan het Bisschoppelijk College te Weert.
In 1971 werd begonnen met de studie van scheikundige technologie aan de Technologische Hogeschool te Eindhoven. Zijn afstudeerwerk werd verricht bij de vakgroep Fysische Chemie en betrof een onderzoek naar de textuur van de diffusielagen die bij het thermisch verzinken van ijzer ontstaan. In 1978 werd het diploma van scheikundig ingenieur behaald. Van 1978-1982 werd als wetenschappelijk assistent in dienst van de Nederlandse Organisatie voor Zuiver Wetenschappelijk Onderzoek (Z.W.O.) gewerkt bij de vakgroep Fysische Chemie van de Technische Hogeschool te Eindhoven. De resultaten van het in die periode verrichte onderzoek staan beschreven in dit proefschrift. Vanaf 1 maart 1983 wordt gewerkt als wetenschappelijk medewerker bij het Natuurkundig Laboratorium van de Nederlandse Philips Bedrijven B.V.

Stellingen bij het proefschrift

THE INFLUENCE OF ALUMINIUM AND SILICON ON THE REACTION BETWEEN IRON AND ZINC.

I. Doordat Shatynski et al. over het hoofd zien dat een van de fasen die ontstaan in hun diffusiekoppels vloeibaar is geweest, interpreteren zij hun resultaten verkeerd.

S.R. Shatynski, J.P. Hirth and R.A. Rapp,
Met. Trans. A 10 (1979) 591.

II. De metingen van Jena et al. rechtvaardigen niet hun conclusie over het bestaan van twee δ fasen in het Fe-Zn systeem.

A.K. Jena and K. Löhberg,
Z. Metallkde 73 (1982) 517.

III. Het gebruik van termen zoals elegant, mooi, symmetrisch etc. duidt op een esthetisch aspect in de wetenschap.

On Aesthetics in Science, Ed. J. Wechsler,
MIT press, Cambridge, Massachusetts (1981).

IV. Het verdient aanbeveling voor een beter begrip van de werking van inductief gekoppelde plasmas en om een vergelijking tussen verschillende systemen mogelijk te maken, om het werkelijke, aan het plasma overgedragen vermogen als parameter op te geven in plaats van het meestal gebruikte, door de generator geleverde vermogen.

P.A.M. Ripson and L. de Galan,
Spectrochim. Acta 38b (1983), in press.

V. Het kweken van forellen die bestand zijn tegen vervuild water is een bestrijding van symptomen en draagt niet bij tot een oplossing van het probleem van de vervuiling van het oppervlaktewater; het tegendeel is zelfs waar.

De Volkskrant, 24 januari 1983.

VI. In zijn studie van de Nederlandse beweging voor sexuele hervorming wordt door Nabrink te weinig erkend dat, in de periode voor de tweede wereldoorlog, binnen deze beweging het streven naar rasverbetering een belangrijke plaats innam.

G. Nabrink, Seksuele hervorming in Nederland. Achtergronden en geschiedenis van de Nieuw-Malthusiaanse Bond (NMB) en de Nederlandse Vereniging voor Sexuele Hervorming (NVSH), 1881-1971, SUN, Nijmegen (1978).
L. Osinski and P.P.L.A. Voestermans, Sexual reform in the Netherlands before World War II, in The Birth of Sexology, Ed. E.J. Haeberle (1983), to be published.

VII. Diffusiekoppels met tweefasige legeringen als uitgangsmaterialen hebben grote voordelen boven de gebruikelijke types van diffusiekoppels met eenfasige uitgangsmaterialen.

F.J.J. van Loo, J.W.G.A. Vrolijk and G.F. Bastin, J. Less Common Met. 77 (1981) 121.

VIII. Het begrip Matano integraal wordt duidelijker als men de erop betrekking hebbende figuur (bijv. fig. 2.1 van dit proefschrift) een kwartslag draait.

IX. De kreet "van rugby wordt je man" gaat niet meer op nu deze sport ook door vrouwen wordt beoefend.

Kazimierz Osinski; Eindhoven, 29 april 1983.